

Obtaining time reduction in the movement of a clamp mechanism

Tjeerd van den Elshout

MSc Report

Supervisors:

prof.dr.ir. J. van Amerongen

dr.ir. J.F. Broenink

dr.ir. T.J.A. de Vries

ir. C. Kleijn

March 2006

Report nr. 007CE2006

Control Engineering

EE-Math-CS

University of Twente

P.O.Box 217

7500 AE Enschede

The Netherlands

Summary

The aim of this assignment was to check if time reduction of the movement of a clamp mechanism is possible. The clamp mechanism is the part of an injection molding machine, which keeps two mold halves together when the plastic is inserted. One of the mold halves is moved away with the clamp mechanism, to take the product out of the mold. Until the mold is closed, no new plastic is inserted. The faster the opening and closing movements of the mold are, the more products can be produced in the same time.

A simulation model is made in 20-Sim, to analyze the dynamic behavior of the clamp mechanism. The model is made with standard 2-dimensional rigid-body models. The model is validated using measurements from the real clamp mechanism. By changing the friction coefficients the model is fitted to multiple measurements.

The movement of the clamp mechanism depends mainly on the reference motion profile. If this profile is optimized, a faster cycle-time is achievable. With the knowledge about the clamp mechanism from the simulation model, a better controller can be realized. When feed forward is added in parallel to the PID-controller the reference profile is followed much better by the mechanism, since the required force to move the clamp mechanism can be estimated in advance. Because of that, the reference profile can be tuned for better results.

During this assignment a simulation model is made, which is validated and fitted successfully with measurement data. The control system is expanded by implementing a feed forward controller, based on a reduced model. When the points where the deceleration is started are moved to a later position, the required safe velocities are still reached in time but the average velocity can be increased.

Based on the simulation experiments, it can be assumed that the closing movement can be done 10% faster and the opening movement little more than 8%, if the feed forward controller and the cycle-to-cycle method are implemented, and when the reference profile is optimized.

It is recommended to do more tests using various mold weights, in order to validate the simulation model for more situations, which will make the model more reliable. It is suggested to implement the State Variable Filter for estimating the velocity, to obtain a more accurate derivative.

It is recommended to model and analyze the hydraulic circuit, since this circuit has a large influence on the behavior. The clamp mechanism structure is rather common, but this transformation ratio has a large influence on the required force to move the mechanism. Further analysis is recommended to determine whether the lever mechanism can be improved.

Samenvatting

Het doel van deze opdracht was om te analyseren of er tijdswinst te behalen valt op de tijdsduur van de beweging van een sluitmechanisme. Het sluitmechanisme is het gedeelte van een spuitgietmachine die er voor zorgt dat de helften van de gietvorm bij elkaar blijven wanneer er plastic in de vorm geïnjecteerd wordt. Om het product uit de gietvorm te kunnen halen moet deze geopend worden. Dit gebeurt door één van de helften naar achteren te bewegen met behulp van het sluitmechanisme. Er wordt pas nieuw plastic geïnjecteerd wanneer de gietvorm weer gesloten is. Wanneer het openen en sluiten van de gietvorm sneller gebeurt, kunnen er meer producten geproduceerd worden in dezelfde tijdsduur.

De beweging van het sluitmechanisme wordt grotendeels bepaald door de referentiebeweging. Als deze geoptimaliseerd wordt, zal automatisch een betere tijdsduur gehaald worden. Met kennis van het sluitmechanisme vanuit het simulatiemodel kan een betere regelaar gerealiseerd worden. Als een Feed-Forward regelaar parallel aan de PID regelaar wordt toegevoegd, zal de referentiebeweging beter gevolgd worden, omdat er rekening gehouden wordt met de niet-lineaire overbrengverhouding van het sluitmechanisme. Hierdoor kan de referentiebeweging beter afgesteld worden voor betere resultaten.

Gedurende deze opdracht is met behulp 20-Sim een simulatie model gemaakt, waarmee het mogelijk is het dynamische gedrag van het sluitmechanisme te analyseren. Het model is opgebouwd met standaard tweedimensionale submodellen van starre lichamen. Het model is geverifieerd met behulp van een aantal simulaties, en gevalideerd aan de hand van meetdata. Door de wrijvingscoëfficiënten aan te passen kon het model passend gemaakt worden met de meetdata.

De Feed-Forward regelaar, gebaseerd op een vereenvoudigd model van het sluitmechanisme, is toegevoegd aan het huidige regelsysteem. Door het punt waar begonnen wordt met afremmen naar een later, maar nog steeds veilig, punt te verschuiven, zal er gedurende een langere tijd een hogere snelheid kunnen worden vastgehouden. Hierdoor zal de gemiddelde snelheid over het traject toenemen. Met behulp van de iteratieve Cycle-to-Cycle control afstemmethode kan na een paar bewegingslagen de referentie beweging worden verbeterd, door de afremposities te verschuiven. Dit verschuiven is mogelijk omdat de lagere, veilige snelheid ruim voor het bewuste punt bereikt wordt, wat nadelig is voor de tijdsduur.

Op basis van de simulatie experimenten kan worden aangenomen dat de sluitbeweging 10% sneller en de openingsbeweging zo'n 8% sneller moet kunnen. Hiervoor moet de Feed-Forward regelaar geïmplementeerd worden, en moeten de afremposities in de referentie beweging afgesteld worden met de iteratieve Cycle-to-cycle Control methode.

Het advies is om meer testen te doen met het sluitmechanisme, zodat het simulatiemodel gevalideerd kan worden voor meerdere situaties. Als er meetdata beschikbaar is van verschillende gietvormgewichten, zal het simulatiemodel betrouwbaarder worden. Het advies is om een State Variable Filter te gebruiken voor het bepalen van de snelheid uit de gemeten posities, om zo een nauwkeurigere snelheid te bepalen. Het wordt aanbevolen het hydraulische circuit grondig te analyseren, omdat dit een grote invloed heeft op het totale gedrag. Alhoewel de opbouw van het sluitmechanisme standaard is, wordt het aanbevolen deze nader te onderzoeken tot mogelijke verbetering, in verband met de niet-lineaire overbrengingsverhouding hiervan.

Preface

This master's thesis is the completion of my academic study Electrical Engineering at the University of Twente. After a lot of interesting courses and a few practical assignments, this master assignment is the last part before graduation.

I enjoyed my stay in Enschede for the last three and a half years, because I became a lot wiser, I met a lot of new people and friends (including my girlfriend!) and I got acquainted with another part of The Netherlands. To experience this, I first had to move out of my familiar and safe environment, but I am glad I did! It was really worth it.

I would like to thank the following people for supporting me during this assignment:

My supervisors Theo de Vries, Job van Amerongen and especially Jan Broenink and Christian Kleijn for their support. Johan Visser and Harold de Vries of Stork Plastic Machinery for letting me do this interesting and real assignment and giving me all the information and help that was needed. The team of Controllab Products B.V., Frank Groen, Johan Hemssems, Paul Weustink and Christian Kleijn for helping me with modelling issues, simulation issues and other support. It was good to have an exchange of thoughts every now and then. The rest of the people at the Control Engineering department, for talking and enjoying the daily cup-a-soup.

Finally, I would like to thank my girlfriend, my parents, and my future parents-in-law for encouragement and listening.

Without these people I doubt whether I would have been able to complete this study.

Tjeerd van den Elshout
Enschede, March 2006

Table of contents

1	Introduction	1
1.1	Background.....	1
1.2	Problem description	2
1.3	Objectives	2
1.4	Outline	2
2	Modelling of the clamp mechanism	3
2.1	Working of the clamp mechanism	3
2.2	Movement of the clamp mechanism	4
2.2.1	Velocity profile of the crosshead	4
2.2.2	Closing the mold halves	4
2.2.3	Opening the mold halves.....	5
2.3	Overview of the clamp mechanism.....	6
2.4	Bond graph model.....	7
2.4.1	Assumptions.....	8
2.4.2	Clearance in the frame	8
2.4.3	Compliance of the frame and of the bars	8
2.4.4	Collision model	9
2.5	Actuation of the crosshead.....	9
2.5.1	Hydraulic cylinder.....	9
2.5.2	Proportional valve.....	10
2.5.3	Differential circuit.....	10
2.5.4	Simulation model of the actuator	11
2.6	I/O communication	12
2.6.1	Transmission delay	12
2.6.2	A/D- and D/A-conversion	12
2.7	Verification of the simulation model	13
2.7.1	Approach for simulation experiments.....	13
2.7.2	Body orientations	13
2.7.3	Comparison between kinematic model and 2D-model	14
2.7.4	Movement and required force	14
2.7.5	Total force on the APL.....	16
2.7.6	Effect of changing friction coefficients.....	18
2.7.7	Effect of increasing the weight of the LSP	19
2.8	Concluding remarks.....	20
3	Model validation	21
3.1	Measurement information.....	21
3.2	Validation of the model	23
3.3	Parameters of the simulation model.....	26
3.4	Conclusion	27
4	Controller design.....	29
4.1	Introduction.....	29
4.1.1	Preparation phase	29
4.1.2	Controller design phase.....	29
4.1.3	Application for time reduction	30
4.2	Model reduction.....	30
4.3	Reference profile.....	31
4.4	Velocity estimation	32
4.5	Velocity feedback control.....	32
4.6	Feed forward.....	34
4.7	Possible time reduction	38

4.7.1	Principle of cycle-to-cycle control	38
4.8	Simulation results.....	40
4.8.1	Closing movement.....	40
4.8.2	Opening movement	45
5	Conclusions and recommendations	49
5.1	Conclusions.....	49
5.1.1	Only small time reduction possible	49
5.1.2	Servo behavior better by adding feed forward	49
5.2	Recommendations.....	50
5.2.1	Implementing and testing	50
5.2.2	Improve model and software.....	50
5.2.3	Analyze clamp mechanism transfer.....	50
Appendix A	Specifications of the clamp mechanism	51
Appendix B	Mathematic models	52
B.1	Position definitions	52
B.2	Mathematical model.....	52
B.3	Elaboration of mathematical model	54
Appendix C	Modelling of 2D rigid bodies	55
C.1	A single moving body	55
C.2	Connecting multiple bodies.....	59
Appendix D	Clamp mechanism transfer	60
Appendix E	Description of bond graph elements.....	61
Appendix F	State Variable Filter.....	62
F.1	First order SVF.....	62
F.2	Second order SVF	63
F.3	Software differentiation	66
F.4	Comparison between methods	66
References	69

1 Introduction

This project is about the redesign of a controller of a part of an industrial machine, the clamp mechanism of an injection molding machine. Since the industrial revolution mankind tries to invent tools that make life easier and optimize the time duration of actions. To gain precision and speed, a controller is necessary. With a better controller, a mechanism can perform faster. The faster this industrial machine is, the more products can be manufactured and the more cost effective the machine is.

1.1 Background

This MSc project is done at the laboratory of Control Engineering at the University of Twente. The main goal of this department is to investigate the applicability of modelling techniques and control methods to practical situations, mainly in the field of mechatronics. Technical problems from industrial partners can be the start of a project, where methods taught at the department can be utilized to find a proper solution. Mechatronics involves the modelling of a mechanical system and its control system. More about this can be found in literature, e.g. (van Amerongen and Breedveld, 2002).

Stork Plastics Machinery designs and produces injection molding machines, which are used for creating plastic products (like buckets) from small plastic granular material. The injection molding machine consists of two parts: an injection part and a clamping part. The injection part heats the plastic and takes care of the injection into the mold. The clamping part keeps the two mold-halves together when the plastic is injected under high pressure. Depending on the size of the products that need to be manufactured, a different injection molding machine with a certain maximum clamping forces is needed. The available clamping force varies between 150 kN and 12000 kN for the different types of the machine.

In figure 1-1 a picture of the injection molding machine is shown. The left half is the clamp mechanism and the right half is the injection part. The picture below is only for illustration of the complete injection molding machine, to show the role of the clamp mechanism and where it is located.

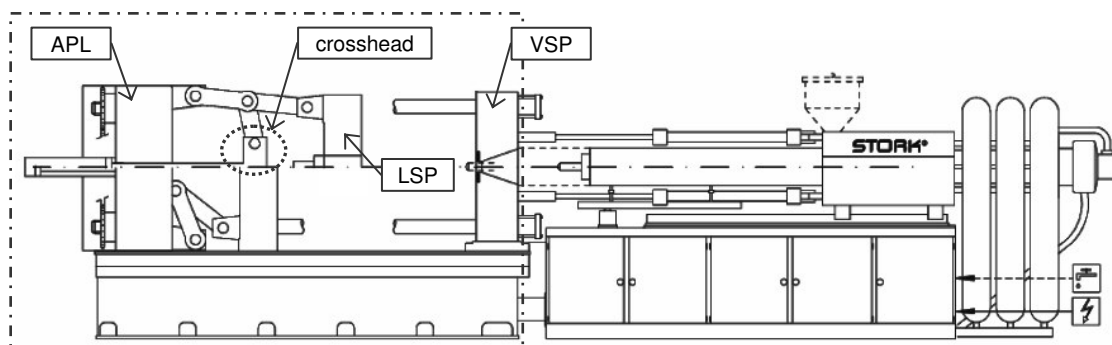


Figure 1-1 Injection molding machine exists of two parts, the injection part (right) and the clamping mechanism (left). The backside of the mechanism is called APL, the movable plate is called the LSP and the fixed plate connected to the injection part is called the VSP.

Depending on the product to make, a different mold will be attached to the heavy movable plate, called LSP. The weight of this mold half is maximal $\frac{2}{3}$ of the allowed maximum total mold weight. For the larger machines, this weight can be between a few tons and 15 tons. This weight deviation is a problem for configuring the movement of the clamp mechanism with the current controller.

1.2 Problem description

Because the dynamics of the clamp mechanism are mostly unknown and change when the weight of the mold changes, the controller can not be configured as good and as fast as possible. The dynamic behavior depends on the mass of the mold that is attached to the heavy movable plate (LSP). The clamp mechanism has to function properly in all cases, with a lightweight mold but also with the mold of the maximum allowed weight.

In the old situation, the controller is tuned such that the clamp mechanism will operate in all circumstances, for all mold weights. When a mold with a weight less than the maximum weight is used, the cycle time will be longer than that would be achievable.

If the dynamics and the behavior of the clamp mechanism for varying mold weights are known, Stork Plastics Machinery assumes the controller configuration can be optimized in order that the opening and closing movement can be done in less time.

After modelling the clamp mechanism and applying feed forward, the motion of the clamp mechanism can be held under control, and the cycle time can be reduced by optimizing the reference motion profile.

1.3 Objectives

This MSc project consists of three parts: The first part is to model the clamp mechanism of the Injection Molding Machine (IMM). The dynamic behavior of the mechanism can be studied from this model. The model is validated with measurement data. By changing the friction parameters, the model can be tuned to match with the measurement. The second part of the project deals with control issues. With the model, a better controller can be made. The third part is to analyze the motion profile, to check for possible cycle time reduction. The reference motion profile can be iteratively adjusted to gain a higher average velocity with the cycle-to-cycle control method, which can be implemented later on in a calibration phase.

The tasks of this project are:

1. Make a model of the 12000 *kN* version of the clamp mechanism to study the dynamic behavior.
2. Validate and fit the simulation model to the real machine by comparing the simulations with measurement data.
3. Make a simpler, reduced model to redesign the control system.
4. Optimize the motion profile with the iterative cycle-to-cycle method.

The main question to be answered: “Is it possible to reduce the duration of the closing/opening movement?”

1.4 Outline

The modelling of the clamp mechanism is described in chapter two. The theoretical background of bond graphs can be found in Appendix C. In chapter three the model is validated by using measurement data. By changing the friction coefficients, the model is fitted with the measurement. In the fourth chapter a reduced model is obtained, control issues are discussed, and simulations are shown to illustrate the possibilities for time reduction. The final chapter, chapter five, gives the conclusions and recommendations of this MSc thesis.

2 Modelling of the clamp mechanism

In this chapter the working of the clamp mechanism is described, which is part of the injection molding machine. It involves the working and the actuation of the mechanism, the I/O communication between the controller and the mechanism, and the modelling of the mechanism.

2.1 Working of the clamp mechanism

The injection-molding machine (IMM) shown in figure 1-1, consists of two parts: the injection part and the mold-clamping part. The injection part is used for mixing and heating the plastic granular material, which is injected into the mold. The injection happens under high pressure, because the liquefied material should fill the mold completely before it is congealed. The task of the clamping mechanism is to clamp the two mold halves together when the plastic is injected. Otherwise, the material will leak away between the two halves. The type of mold determines the required clamping force. After the plastic is injected, the mold is opened by the clamp mechanism and the product can be taken out of the mold. The product is pressed out of the mold by a cylinder that is mounted on the inside of the mold, or the product is taken out by a special robot. If it is done with a robot, it can take the product out of the mold once the gap between both mold halves is large enough.

The clamp mechanism is shown in figure 2-1. One of the mold halves is attached to a heavy movable plate, called *LSP*, while the other is mounted onto the fixed plate, called *VSP*.

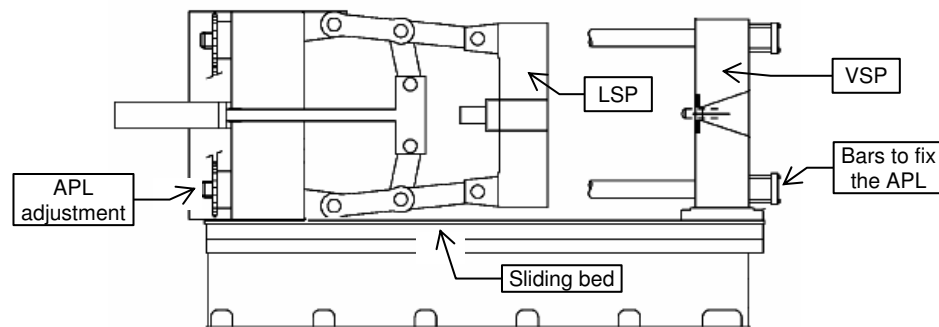


Figure 2-1 The VSP is mounted on a sliding bed. The APL and the clamp mechanism lie on this bed. The position of the APL can be adjusted to adjust clamping force. The bars keep the APL connected to the VSP.

The LSP is moved from and to the backside of the clamp mechanism (APL) via a structure of bars by a hydraulic cylinder. This bar-mechanism is called the knee-lever mechanism, which forms a nonlinear transmission from the hydraulic cylinder to the LSP. To be able to adjust the position of the moving mold half, the position of the APL can be adjusted. Therefore, a little clearance on the bars that hold the APL is necessary, so the adjustment mechanism can be moved freely.

A simplified representation of the clamp mechanism can be seen in figure 2-2. The crosshead (bar L_1) is mounted on the hydraulic cylinder. This name is due to the shape of this bar. Both knee lever mechanisms are mounted to the crosshead, at the bottom and at the top.

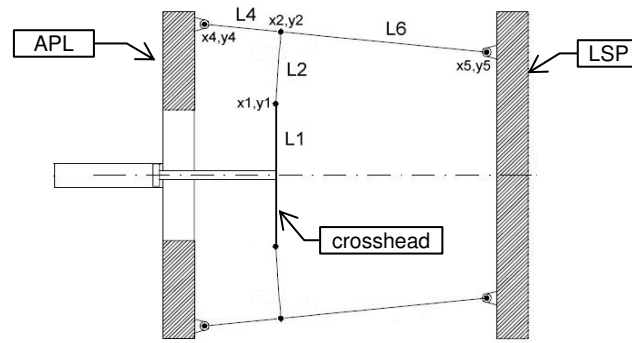


Figure 2-2 Simplified representation of the clamp mechanism, which only shows the left part of figure 2-1. The cylinder actuates the LSP via the structure of bars, called the knee-lever mechanism.

The LSP will move with a different velocity than the crosshead, due to the nonlinear and position dependent transformation ratio of the knee-lever mechanism. The nonlinear transformation ratio is described in more detail in Appendix D.

2.2 Movement of the clamp mechanism

2.2.1 Velocity profile of the crosshead

The movement of the LSP can be divided in different zones and states, including extra safety zones. Because the movement of the LSP is nonlinear, the zones are described based on the position of the crosshead. An overview of the zones and states is shown in figure 2-3. When the mechanism is open, the mechanism is in rest.

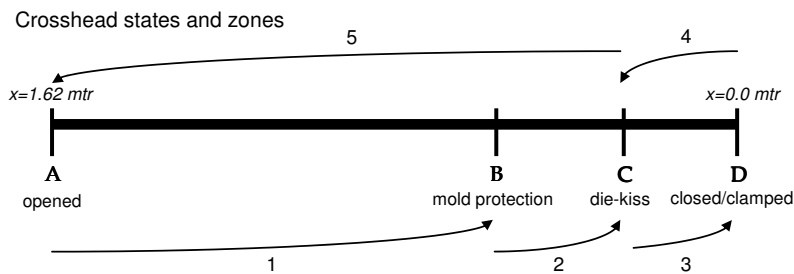


Figure 2-3 Order of opening and closing of the crosshead. The mechanism starts from rest at the open state (A). Here the LSP and the VSP are maximal apart from each other. At point C the LSP hits the VSP and a clamping force is build up between the mold halves.

The cycle is started from the open-state by moving the LSP towards the VSP. The first zone is the movement from A to B, where the LSP is accelerated. The mold protection zone is the second zone that is entered, which starts after point B. This zone is added for safety reasons. When there is an object between the mold halves, the movement will immediately halt. The third zone is the clamping zone, which starts after the die-kiss position (C). In this zone, the LSP position will barely change, and the clamping force between the mold halves is build up. When the configured force is reached, the mechanism is clamped (D) and the crosshead stops moving.

The opening movement is the opposite of the closing movement, but without the mold protection zone. The crosshead is moved slowly from point D to point C to release the clamping force, where after it is faster moved back to point A.

In the following section, the different steps of the movement are explained in more detail.

2.2.2 Closing the mold halves

Before the injection can be started, the mold halves have to be brought together. This is done by moving the LSP towards the VSP. The closing exists of multiple zones, indicated in figure 2-3 with arrow 1 and 2. These zones are used for safety reasons to protect the mold, so if exceptions occur, nothing will happen to the mold. In the next sections the different zones will be discussed.

From point A to point B

To get short production times, the LSP has to accelerate from standstill to a maximum velocity. This velocity is kept for a while. However, before zone 2 is entered, the LSP has to slow down to a lower velocity, because for zone 2 there is a maximum velocity. The first zone of the reference velocity of the crosshead exists therefore of an acceleration part and a deceleration part, as shown in figure 2-4.

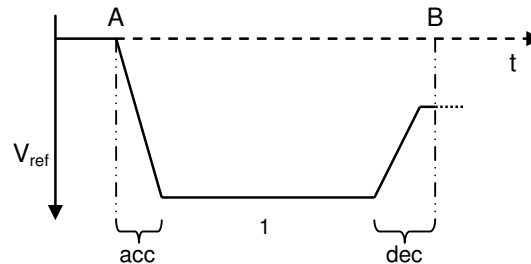


Figure 2-4 First part of the reference velocity of the crosshead for the closing movement.

From point B to point C

At a certain distance between the LSP and the VSP, zone 2 starts, just before the mold halves touch each other. This safety zone is called the mold protection, indicated with B in figure 2-4 and figure 2-5. This zone is passed with a lower velocity, as can be seen in figure 2-5. For this zone there is a pressure limitation. If there is an object between the mold halves, the LSP will hit the VSP earlier. The pressure will then rise at an earlier position. If the maximum allowed pressure limit is exceeded, the movement will halt.

This safety is used to protect the mold from damage, when objects come or remain in between the halves while closing. As an example: in case the robot does not move away, the clamp mechanism will halt so that the robot will not be crushed between the molds and the molds will not get damaged.

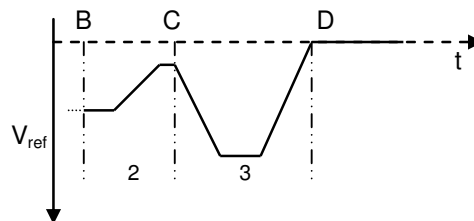


Figure 2-5 Second part of the reference velocity profile of the crosshead for the closing movement.

Before zone 3 is entered, the crosshead decelerates to a lower velocity, because zone 3 has a certain entering-velocity. This lower velocity is reached a little earlier. Zone 2 exists of a constant velocity, and of a deceleration part.

From point C to point D

At point C, called die-kiss, the mold halves (LSP and VSP) just touch each other. The LSP has almost stopped moving, but the crosshead is still moving. From point C to point D the clamping takes place and the pressure between the mold halves is build up. The velocity profile of the crosshead is shown in figure 2-5.

When the mold halves touch each other at point C, the crosshead starts accelerating. The crosshead needs a high velocity to be able to build up the force between the mold halves. When the required pressure is build up, the crosshead can slow down and will stop at position D. The deceleration has straight part for positioning the crosshead around 1 mm. Now the bars L_4 and L_6 (see figure 2-2) are in a stretched position and the physical distance between the LSP and the VSP equals zero. The mechanism is closed and clamped.

2.2.3 Opening the mold halves

When the mold is opened, the crosshead moves from point D back to point A (figure 2-3). When the crosshead is located at point D, the system is not at rest because there is a pressure build up between the mold halves to prevent that the plastic flows out of the mold.

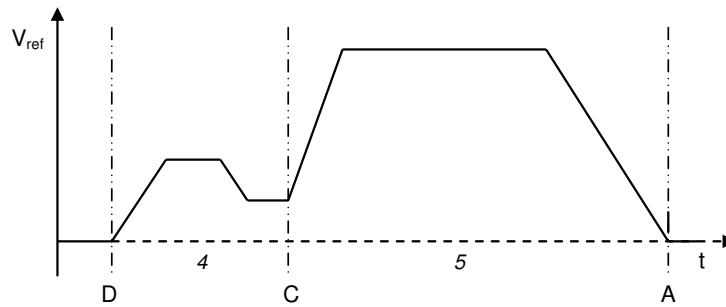


Figure 2-6 Velocity profile for the crosshead, when the mold halves are opened.

When the crosshead moves back from the closed and clamped position (D) to the open position (A), the mold-protection (B) is not used, so two zones are left. This can be seen in figure 2-6.

From point D to point C

Before the crosshead can start moving back fast, the pressure between the mold halves has to be cut back. This happens in zone 4. Once the LSP starts moving, it will be pressed very hard because of the pressure between the plates that want away. The crosshead needs to push back to prevent the LSP from clashing back too fast. The pressure on the bars is now slowly brought down. After point C both mold halves will not touch each other anymore (zone 5).

From point C to point A

The second part of the opening is bringing the LSP from touching the VSP (C) back to a maximum distance apart (A). This distance can be configured in the software as the “configured opening”. The crosshead start by accelerating to a maximum velocity, keeps this velocity for a while and then decelerates to standstill at position A. The mechanism is back in rest again.

2.3 Overview of the clamp mechanism

To understand the behavior of the clamp mechanism, it is necessary to make a simulation model of the mechanism. By doing research on this model, the dynamics can be understood and a better control system can be designed.

There are two important positions in this system: the position of the crosshead and the position of the LSP. The position of the LSP determines if the movable mold half will, or will not make contact with the fixed mold half. It is not possible to measure the position of the LSP. Therefore, the position of the crosshead is measured. In the current clamp mechanism the position of the LSP is estimated from the crosshead position by using interpolation, based on earlier measurement results stored in a lookup-table.

The clamp mechanism is a continuous system, while the reference motion profile and the controller are digital systems, implemented in software. The systems are coupled together with an I/O-block with A/D- and D/A-converters. The communication delay is added to the D/A-converter. The top-level block diagram of the complete clamp mechanism is shown in figure 2-7.

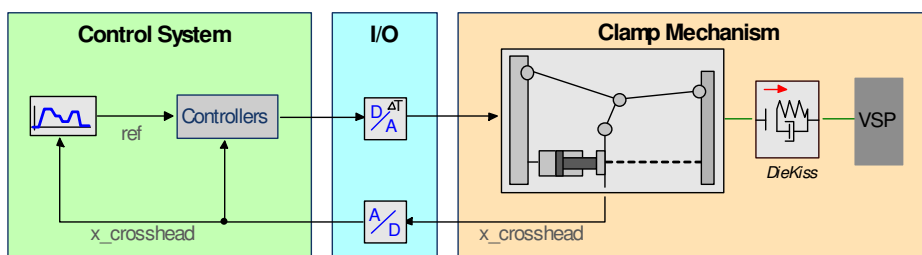


Figure 2-7 Top-level block diagram of the complete clamp mechanism.

The reference profile supplies the control system with the reference signals. The control system takes care of the signals to the hydraulic system via the I/O block, so that the crosshead will follow the

reference velocity. The three blocks are indicated with different colors. The content of the clamp mechanism model is described in the next section.

2.4 Bond graph model

To make the simulation model of the clamp mechanism, the mechanism is simplified even more. Since the knee-lever mechanism is symmetrical, the model will still be accurate if only the top half is modelled. This is shown in figure 2-8. Assumed is that moving two masses in parallel will need the same force as moving one mass with the sum of those two masses. Therefore, the bar weights need to be doubled to get the correct forces.

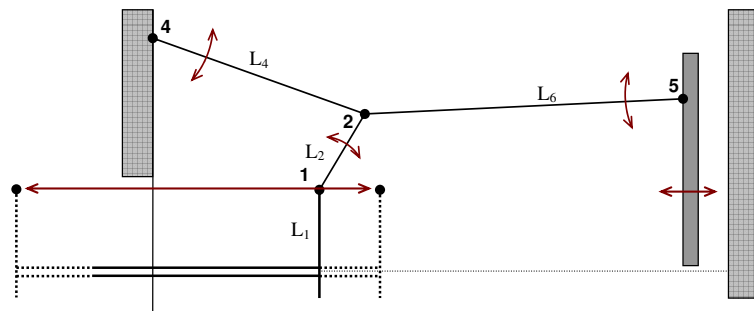


Figure 2-8 Simplified representation of the clamp mechanism. The possible movements of all the bodies are indicated with arrows. L_4 can only rotate, while L_1 can only translate. Bodies L_2 and L_6 can both rotate and translate.

Each bar can be modelled with a 2D-rigid body submodel. These bodies are described in Appendix C. The bars are connected together by means of the joints and hinges described in section Appendix C.2. The simulation model of the simplified clamp mechanism of figure 2-8 is shown in figure 2-9. Each egg-shaped body contains the content of Figure C-6 which can be found in Appendix C. Due to causality conflicts in the model, one of the two spring-dampers in y -direction is removed from each bar. The APL and the LSP submodels contain hinge connections.

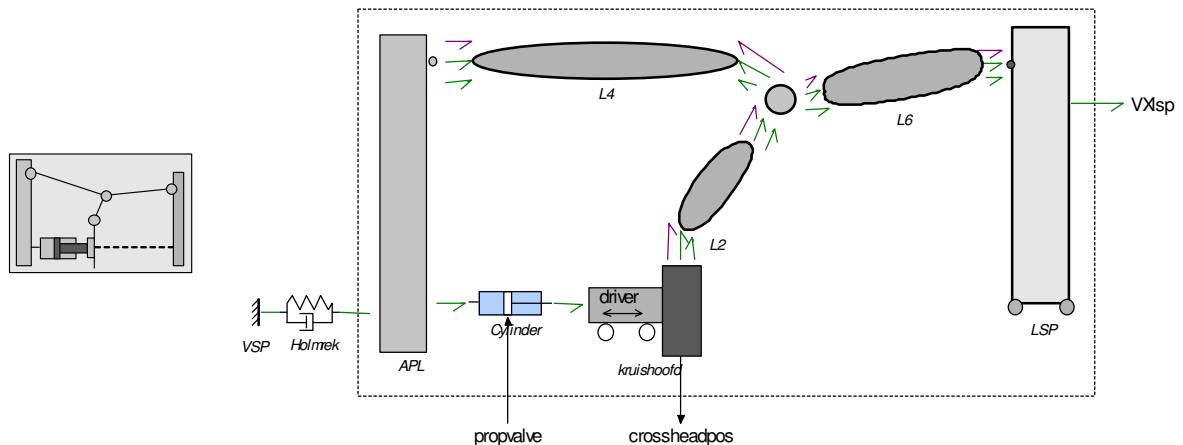


Figure 2-9 Simulation model of the clamp mechanism shown at the left. The only input to the system is the signal to the hydraulic system and the only output signal is the measured crosshead position.

The VX_{lsp} -output is connected to the collision model that represents the contact of the LSP and the VSP (*DieKiss* in figure 2-7). The *holmrek* block contains the compliance of the connection bars that keep the APL fixed to the VSP. The input to the clamp mechanism, named *propvalve*, is the signal from the control system to the proportional valve, which controls the oil flow to the hydraulic cylinder. The content of the cylinder submodel is shown in figure 2-15, which is quite ideal. The measured position of the crosshead is brought out via the *crossheadpos* signal.

The communication delay caused by the communication between the mechanism (*plant*) and the controller is included in the top layer of the model, as shown in figure 2-7. It is not included in the simulations used for verification and validation.

Each bar body in the clamp mechanism (figure 2-9) consists of two spring-dampers in the x -direction, and one or two in the y -direction, depending on the causality of the signals. When the mechanism clamps the two mold halves together, bars L_4 and L_6 are in stretched position. The springs in these two bodies are in one line between the APL and the LSP, so a force that is almost equal to the clamping force is working on the four springs in these bodies.

2.4.1 Assumptions

Because of the symmetry in the mechanism (figure 2-2), the model can be simplified by modelling only the top half. This can be seen in figure 2-8. If the mass of each bar in the model is doubled, the same behavior will be obtained.

The clearance of the adjustment mechanism of the APL is neglected in the simulations for simplicity. Some simulations have been done with the clearance included, but the assumption is made that the movement of the APL is very small and can be neglected without loss of model correctness. When something needs to be said about the accuracy of positioning the LSP and about the exact behavior when the plates hit for different LSP weights, clearance can be simply added.

2.4.2 Clearance in the frame

The backside (APL) of the mechanism is mounted to the front side (VSP) by four large bars. This is shown in figure 2-1. The APL can be moved with respect to the VSP with the adjustment mechanism. To be able to turn these adjustment screws, some clearance is necessary.

Due to this clearance the APL can move a little with respect to the VSP. When the cylinder is pushing the crosshead and thus the LSP towards the VSP, the APL is pressed backwards due to the mass and the friction of the LSP. But when the LSP is decelerated, the mass of the LSP will pull the APL towards the VSP, the force to the APL will change direction, and the APL is moved forward.

This is currently practically solved by first moving the cylinder a little towards the VSP so the APL is pressed against the adjustment screws. When the clearance is pressed out, the LSP can be accelerated. When the mechanism starts decelerating, the APL will also move back and forth because of the clearance. This has to be taken into account for the deceleration points.

2.4.3 Compliance of the frame and of the bars

The bars that keep the APL connected to the VSP are not infinitely stiff. When the mold halves are clamped together, the same force works via the APL to the bars. This can also be seen in figure 2-1. A small part of each connection bar is made a little smaller than the rest of the bar. Because of the constriction as shown in figure 2-10, this part of the bar will deform most when the mechanism is clamping the mold halves together.



Figure 2-10 Bar that keeps the APL fixed to the VSP and the rest of the injection molding machine. The constriction is used for making sure the deformation is in that part of the bar.

The assumption made is that at the maximum clamping force of 12000 kN the APL connection bars become 1.5 mm longer and the knee-lever mechanism bars become about 1.5 mm shorter.

The deformation of the connection bars is modelled by one spring (holmrek in figure 2-7). The spring stiffness is found from equation 2.1.

$$K = \frac{F_{clamp}}{\Delta x_{spring}} = \frac{1.2 \cdot 10^7}{1.5 \cdot 10^{-3}} = 8.0 \cdot 10^9 \{N/m\} \quad (2.1)$$

To realize the deformation of the bars by four springs in series (in L_4 and L_6), the spring stiffness for each spring is found from equation 2.2.

$$K_{L_4 X} = \frac{F_{clamp}}{\Delta x_{spring}} = \frac{F_{clamp}}{\frac{\Delta x_{total}}{4}} = \frac{4 \cdot 1.2 \cdot 10^7}{2 \cdot 10^{-3}} = 24 \cdot 10^9 \{N/m\} \quad (2.2)$$

The spring stiffness in the y-direction is smaller, because the bars are smaller. To prevent harmonic oscillations little damping is added.

The bearings on the APL are moved 5 mm apart. The spring stiffness for each bearing can be found from equation 2.3.

$$K_{APL-y} = \frac{\sin(\theta_4) \cdot F_{clamp}}{\Delta y_{spring}} = \frac{\sin(175) \cdot 1.2 \cdot 10^7}{2.5 \cdot 10^{-3}} = 418 \cdot 10^6 \{N/m\} \quad (2.3)$$

Both bearings move 2.5 mm apart in y-direction. The angle of bar L₄ is 175 degrees when the mold halves are clamped together at 12000 kN. The clamping force in y-direction on the APL is the sine of the angle times to the total clamping force.

2.4.4 Collision model

The model of the collision that happens at die-kiss is modelled with a simple collision model. This is the die-kiss submodel shown in figure 2-7. The die-kiss force is shown in equation 2.4.

$$F = \begin{cases} 0 & x < x_0 \\ K(x - x_0)^{0.5} & x \geq x_0 \end{cases} \quad (2.4)$$

The parameter x_0 is the position of the VSP. If the position of the LSP x equals x_0 , there is a collision between the LSP and the VSP. The stiffness of the collision is indicated by K .

2.5 Actuation of the crosshead

2.5.1 Hydraulic cylinder

Because high forces are needed to move the crosshead, it is actuated by a hydraulic cylinder. The cylinder has two hydraulic ports and one translational port. A cross-section of the cylinder is shown in figure 2-11. The diameter of the rod and the piston are chosen such that the proportion of the piston area between chamber A and B is 2:1. This means that area A_A on the left side of the piston is equal to twice the area A_B on the right side of the piston.

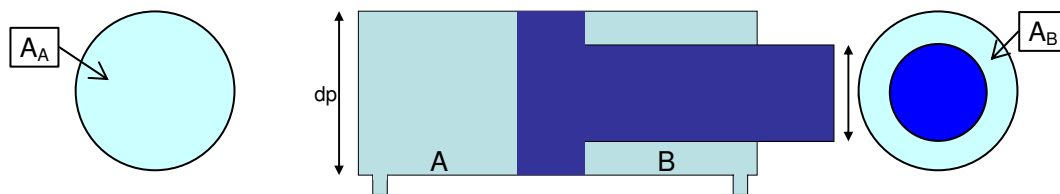


Figure 2-11 The cylinder has two hydraulic inputs. Each chamber has a certain area, in proportion of two to one. Because of the area difference and a pressure difference, the piston will move.

The force on the piston that is caused by both the pressures and areas is calculated by using equation 2.5.

$$F_{piston} = P_A \cdot A_A - P_B \cdot A_B = P_A \cdot \frac{\pi}{4} d_p^2 - P_B \cdot \frac{\pi}{4} (d_p^2 - d_r^2) \quad (2.5)$$

Depending on the pressure in chamber A and B, the diameter of the piston and the diameter of the rod, the rod will move to the left or right. When the pressure on both sides would be equal, the rod will still move to the right, because of the area proportion.

The pressure to the cylinder is adjusted by a proportional valve. In the next section, this valve will be explained in more detail.

2.5.2 Proportional valve

To control the oil flow towards and from the hydraulic cylinder a proportional valve is used, as shown in figure 2-12. The diameters of the valve openings are chosen such that they match the proportion of the area of the inside of the cylinder, A_A and A_B . The connections to cylinder chambers A and B are indicated with pa and pb . The pump connection is indicated with pp and the tank (return) connection is indicated with pt .

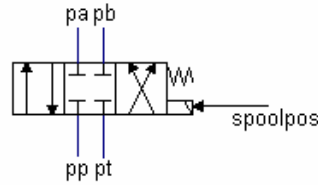


Figure 2-12 Symbol of the proportional valve that is used for moving the hydraulic cylinder. The valve switches the pump and the tank connection between the cylinder ports pa and pb , depending on the spool position.

The flow through the valve depends on the position of the spool. This is illustrated in figure 2-13. The spool will change position, depending on the reference value.

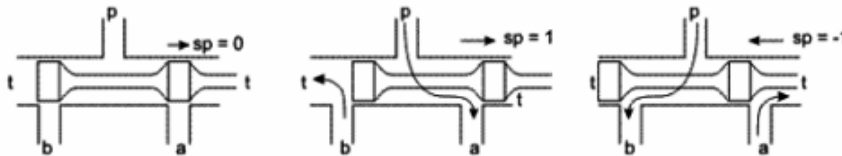


Figure 2-13 Different possible spool positions of the proportional valve. From left to right: 1) no flow between a , b , tank and pump. 2) flow goes from pump to a and from b to tank. 3) flow goes from pump to b and from a to tank

For the proportional valve of this injection molding machine, the reference value should be between -10 Volts and +10 Volts, to make the spool go from the situation of figure 2-13-2 to figure 2-13-3. If the reference value is 0.0 Volts, the spool is located in the middle and there will be no flow (figure 2-13-1). If the reference value is positive, the flow will go from the pump to cylinder chamber A and from chamber B back to the tank connection.

The opposite happens if the reference value is negative. The flow will go from the pump to cylinder chamber B, and from chamber A back to the tank connection. All possible states are given in Table 2-1.

Reference value	Action of proportional valve
- 10 Volts	Flow from pump to b and a to tank
- 10 V < ref < 0 V	Partial flow from pump to b and a to tank
0 V	No flow
0 < ref < +10 V	Partial flow from pump to a and b to tank
+10 V	Flow from pump to a and b to tank

Table 2-1 Different possible spool positions and the flow direction.

The amount of flow that goes through the valve depends on the pressure difference between both sides. This makes it harder to control the valve, because a certain valve opening doesn't always correspond to the same amount of flow. This behavior is not taken into account in the model and simulations.

2.5.3 Differential circuit

When the clamp mechanism needs to close, it should not take too much time. Because the volume of chamber A is twice the volume of chamber B, a lot of oil has to be supplied before the cylinder will move. When the pump supplies two volume parts of oil towards chamber A, one volume of oil will come out of chamber B and goes back into the tank.

This can be seen as a waste of oil. For this reason, a special valve is put in the circuit, called the differential valve. Instead of leading the oil of chamber B back into the tank, the oil is inserted into

chamber A. This way the pump can suffice by pumping halve the amount of oil, because for every volume part of oil that comes from chamber B, this part is saved and is inserted directly in chamber A. This is shown below in figure 2-14.

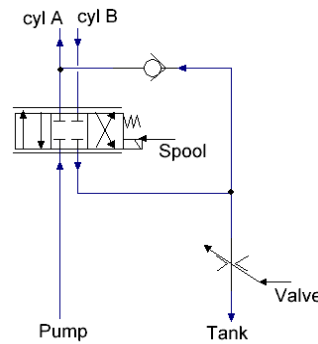


Figure 2-14 Symbolic representation of the differential circuit. The valve position will determine if the oil can go back into the tank or that it is reused.

When the valve is open, the oil coming from the proportional valve will directly go into the tank. The check valve (3) is closed because the pressure on the tank side (2) is low while the pressure on the pump side (1) is high. However, when the valve is closed, the oil cannot go into the tank and the pressure will rise at point 2. If the pressure on the right side of the check valve (3) will become higher than on the left side (point 1), the valve will open and the oil will start going back into the circuit.

A disadvantage of this technique is that the maximum available force is only half the force that would be available when this technique is not used. For the cylinder used for this clamp mechanism, the area proportion is 2:1. This results in equation 2.6.

$$\begin{aligned}
 F_{piston} &= P_A \cdot A_A - P_B \cdot \frac{1}{2} A_A = (P_A - \frac{1}{2} P_B) \cdot A_A \\
 F_{piston, large \Delta P} &\approx P \cdot A_A \\
 F_{piston, small \Delta P} &\approx \frac{1}{2} P \cdot A_A = P \cdot A_B
 \end{aligned}
 \tag{2.6}$$

For a large pressure difference between P_A and P_B , the force equals the highest pressure times the area of the piston. When the pressure for both chambers is almost equal, the force is a result of the area of the rod. The result of this can be seen in Table 2-2.

Use of differential	Available force by cylinder
Yes	F = 141 kN
No	F = 313 kN

Table 2-2 Difference in the available force delivered by the hydraulic cylinder.

Therefore, this technique is only used when closing, from acceleration until just before the mold protection zone, and cannot be used for clamping.

2.5.4 Simulation model of the actuator

The simulation model of the proportional valve and the hydraulic cylinder combined is shown in figure 2-15. The differential circuit is not modelled. The change in available force (table 2-2) can be modelled by adjusting the gain factor in the model.

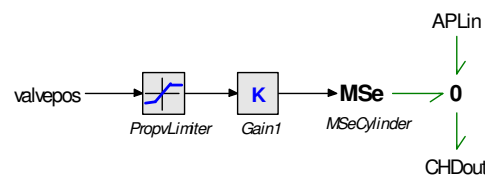


Figure 2-15 Model of hydraulic cylinder. It includes the input limitation and the gain maximal possible with the known pressure and piston area.

The only parts which are included from the hydraulic system are the input limitation of ± 10 V, the cylinder gain and the force source.

2.6 I/O communication

The communication between the clamp mechanism and the controller goes via the communication lines through the I/O rack. The controller works in the digital domain, while the plant works in the continuous domain. Conversions need to be done, which introduce errors and delay. But the transmission also will cost some time.

2.6.1 Transmission delay

This transmission takes some time. Each received data packet needs to be processed before it can be used, and a packet needs to be processed before it can be send. This processing also takes some time. If the communication order of preparing, processing and extracting is not done very smart, there is no processing time left for the controller to do all the calculations. Therefore, a communication scheme describing the order of operations is used. The timing of a communication example is shown in table 2-3 and the scheme which is used is shown in figure 2-16. The sampling frequency is 1 kHz.

Operation	Time needed for operation (μs)
Prepare data	50
Extract data	50
Process data	500
Transmission to plant	300
Transmission to controller	350

Table 2-3 Timing example of the operations needed for communication between controller and plant.

The time values shown in table 2-3 are just an example; the exact times are not known. When a telegram with new values from the controller arrives at the I/O rack, it will immediately return a telegram with the measured data. The I/O rack will communicate every millisecond. This can be seen in figure 2-16. The dashed line represents the delay in the transmission.

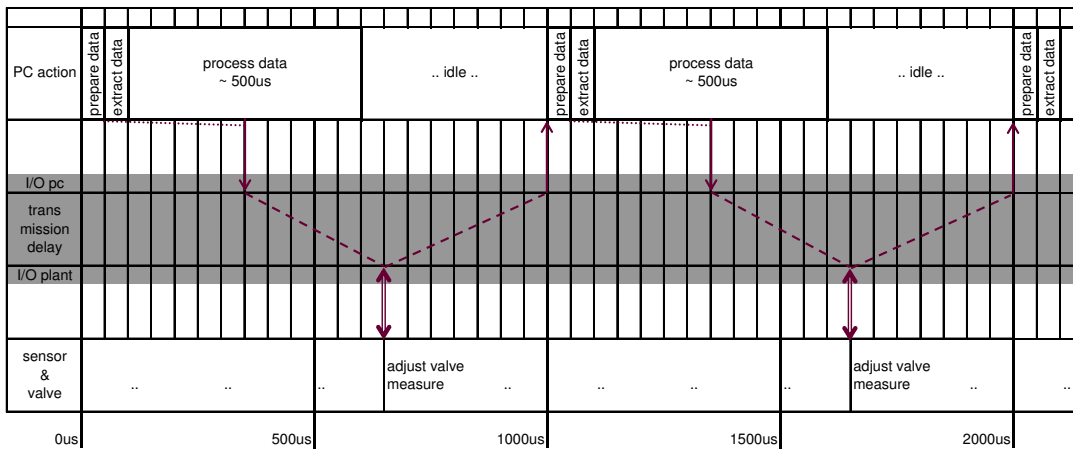


Figure 2-16 Timing scheme of a communication example. The data is sent at time T after each new period, which is determined by subtracting the total delay from the next millisecond. This way the new data will always be available at the next period, and the controller can process while the data is on its way.

The data is sent at a fixed time T after a new period is started. This way the new data will be available when the new period starts. At the start of each period, the controller starts with preparing the data to be sent that was calculated in the previous period. After the data is made ready, the telegram containing the measured values from the plant is extracted. The processing will start at a varying time, depending on the time it took for the preparation and extraction. The calculations need to be done before the new period is started, otherwise the controller can not catch up with the system.

2.6.2 A/D- and D/A-conversion

The measured position is sent to the I/O-rack. Depending on the sensor used, this value can be discrete or continuous. The voltage sent to the proportional valve is in the continuous domain. The communication between the controller and the I/O-rack is in the discrete domain. So between the plant and the controller, conversion is needed. This conversion takes place in the I/O-rack. This

process of communication between controller, I/O-rack and plant is shown in the block diagram of figure 2-17.

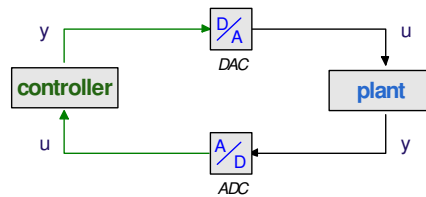


Figure 2-17 Block diagram of controller, I/O and plant. The dark lines are analog signals and the lighter lines are digital signals.

Each converter consists of some functions, which are applied to the input signal. These functions are shown in figure 2-18–a and –b.

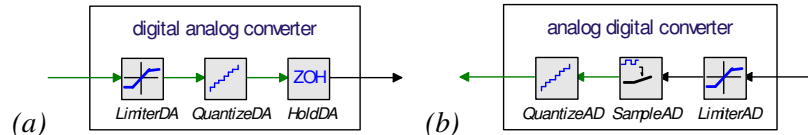


Figure 2-18 Functions implemented in the converter blocks. (a) The D/A converter consist of a signal limiter, a quantizer and signal reconstruction function. A time and amplitude discrete signal is converted to a time and amplitude continuous signal. (b) The A/D converter consist of a limiter, a sampler and a quantizer. A time continuous and amplitude continuous signal is converted to a signal with a discrete time and amplitude.

Depending on the number of bits used in the discrete domain, the signal amplitude can have a certain finite number of values. The analog amplitude is converted to integer values, from -2^{n-1} to $2^{n-1}-1$, where n is the number of bits used. The current system uses 12-bit converters. The sample frequency that is used for sampling and reconstruction is 1 kHz. More details on A/D- and D/A-converters can be found in textbooks, e.g. (van Amerongen and de Vries, 2002, p. 161-178).

2.7 Verification of the simulation model

In this section the simulation model is verified. By doing some simple simulations, the sanity of the model is checked.

2.7.1 Approach for simulation experiments

For this simulation experiments the velocity of the crosshead is used directly from the model. By means of velocity feedback the reference velocity is followed. This is done with a simple PID-controller. The end position of the reference profile can be adjusted, to be able to do a simulation for when the LSP does not hit the VSP and for the case that the LSP hits the VSP. A simple block diagram to illustrate the procedure is shown in figure 2-19.

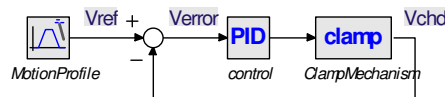


Figure 2-19 Block diagram that shows the setup for simulation experiments.

The velocity of the crosshead is taken directly from the crosshead submodel, so no delay or noise is added to this signal. The clamp mechanism block contains the model shown in figure 2-9.

2.7.2 Body orientations

The orientation of the three rotating bars changes as a function of the crosshead position. These angles are shown in figure 2-20. Here the crosshead moves from 1.62 to 0 m, from right to left. The angle of body L_2 goes from -16 via -22 to 85 degrees, the angle of body L_4 goes from 71 to 175 degrees, and the angle of body L_6 goes from 36 via 39 to -4.0 degrees. These angles are used in the coordinate transformations (Appendix C.1).

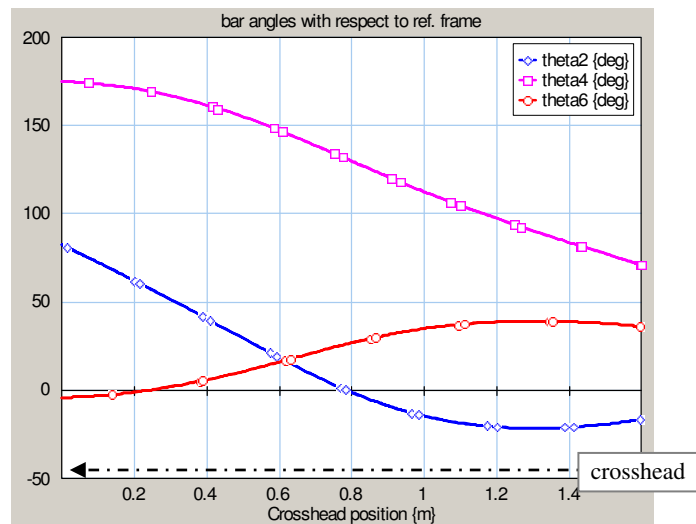


Figure 2-20 Plot of the orientation of the three rotation bodies as a function of the crosshead position. The angles are with respect to the reference frame, in this case the floor. The crosshead moves from opened to closed, in this plot from right to left.

2.7.3 Comparison between kinematic model and 2D-model

To verify the correctness of the model, the output of the model of the previous section is compared with the pure kinematic model as been used in Maple (described in Appendix B.2). The position of the LSP is shown in figure 2-21 for both methods, and the error between the two results.

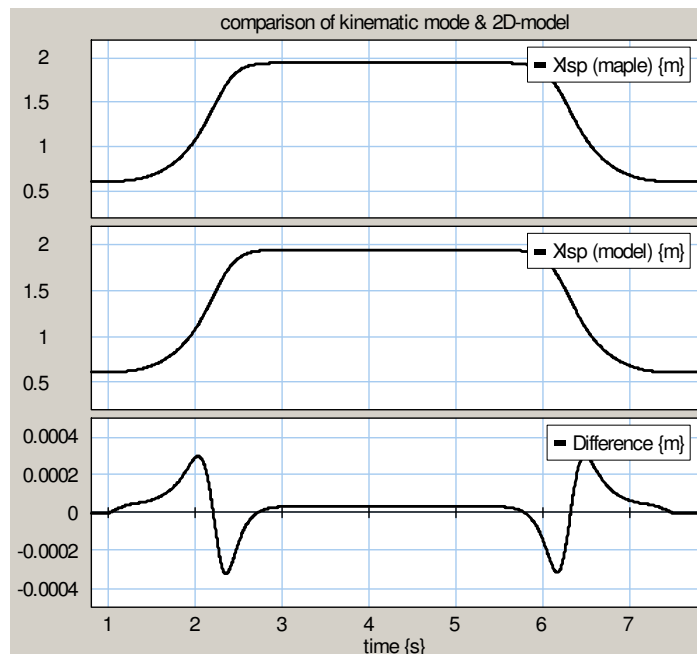


Figure 2-21 Simulation result showing the LSP position of both the kinematic model and the simulation model that includes all the dynamics. The difference is due to the numeric calculations and round-off errors.

The position of the crosshead is the same for both methods and the position of the LSP should also be almost equal. The difference is in the order of 10^{-4} and in the middle $3 \cdot 10^{-5}$. This is mainly due to round off errors in the coordinate transformations. When the simulation steps and the allowed numeric error are larger, the error will become larger too.

2.7.4 Movement and required force

The simulation result showing the reference velocity, the clamp position and the LSP position, and the force of the cylinder is shown in figure 2-22 on page 15. In this plot the LSP can move unloaded and freely without hitting the VSP. If the cylinder force is positive, the cylinder is pushing the crosshead to the right. If the force is negative, the cylinder pulls on the crosshead to move it to the left.

Another simulation plot, shown in figure 2-23, also shows the force between the LSP and the VSP, when the LSP hits the VSP and clamping force is build up. When the crosshead starts moving back after the clamping, the force of the cylinder is positive first and later becomes negative to pull the crosshead to the open-position. The force build up between the plates is pushing the LSP backwards to the APL, so when the crosshead starts moving back the crosshead will be launched if the cylinder would not give some extra support.

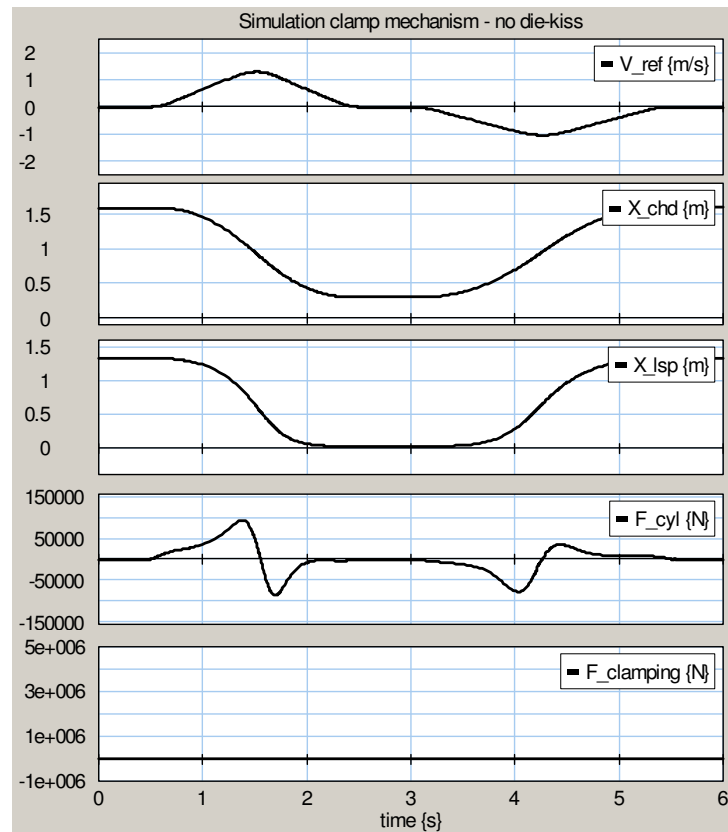


Figure 2-22 Simulation result of when a motion profile is used for moving the crosshead. The profile is a standard modified sine. When the force is positive, the crosshead is pushed towards the VSP (right) and when the force is negative, the crosshead is pulled towards the APL (left).

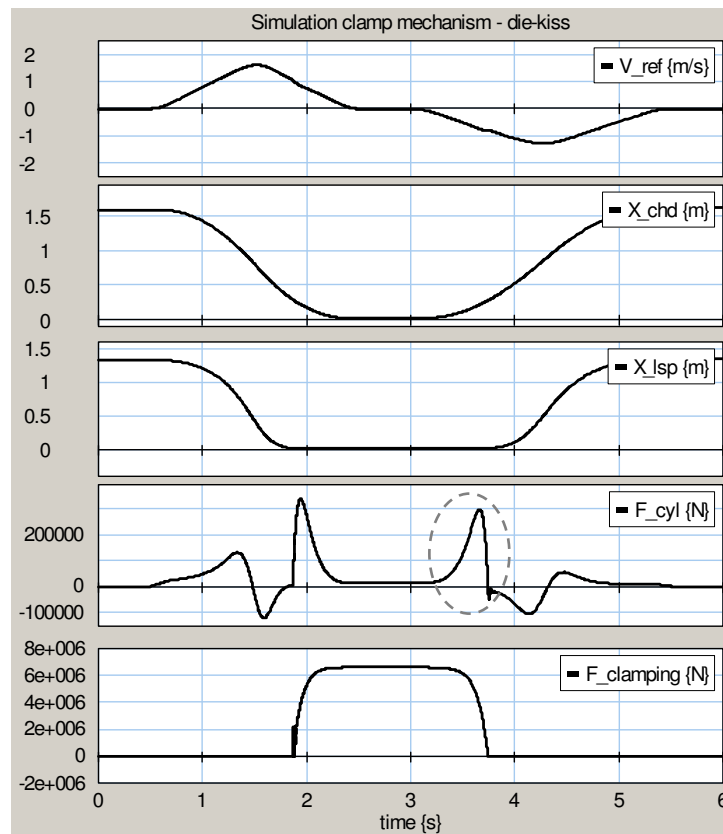


Figure 2-23 Simulation result that shows the clamping force between the LSP and the VSP when the LSP hits the VSP. With the opening after clamping at $t=3.5$ s, the cylinder has to apply a positive force first, to prevent the LSP from launching backwards.

2.7.5 Total force on the APL

The crosshead (L_1) is pushed away from, and attracted to the backside of the clamping mechanism (APL) by the cylinder. The force of the cylinder works on the APL (F_1). But when the crosshead is moved, there is also a force to the APL by the bars L_4 (F_2). The clamping force between the two mold halves also works on the APL. A simple picture that shows those forces is shown in Figure 2-24. Both translational connections to the APL can be seen in the simulation model as shown in figure 2-9.

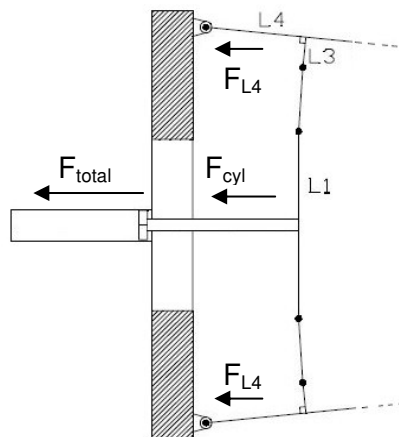


Figure 2-24 Picture of the APL with the cylinder and the bars that are connected to the APL. The total force on the APL is the sum of the two forces.

The total force on the APL is the sum of those two forces, and is given by equation 2.7.

$$F_{total_{APL}} = F_{cyl} + F_{L_4} \quad (2.7)$$

The APL is pushed backwards, away from the VSP, when the total force is positive. In the simulations the crosshead moves from 1.5939 m to 0.4 m (Figure 2-25) respectively to 0.0 m (Figure 2-26). The LSP moves from 1.3301 m to almost 0.0 m and 0.0 m.

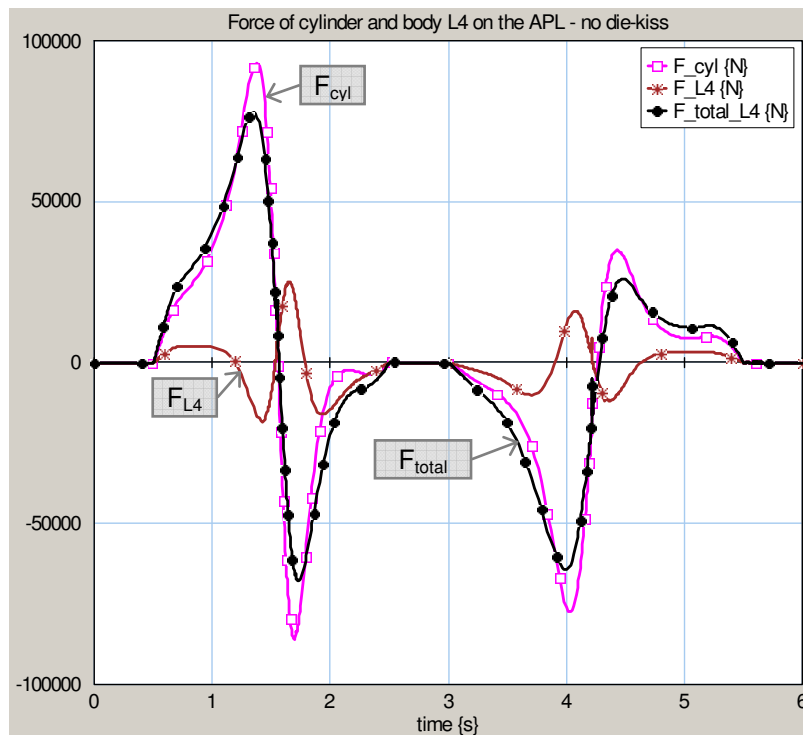


Figure 2-25 Total force on the APL, caused by the force of the cylinder and the force via body L_4 . The LSP is moved from open to closed, and back from closed to open. The LSP does not hit the VSP. The total force (dark line) is almost equal to the force caused by the cylinder.

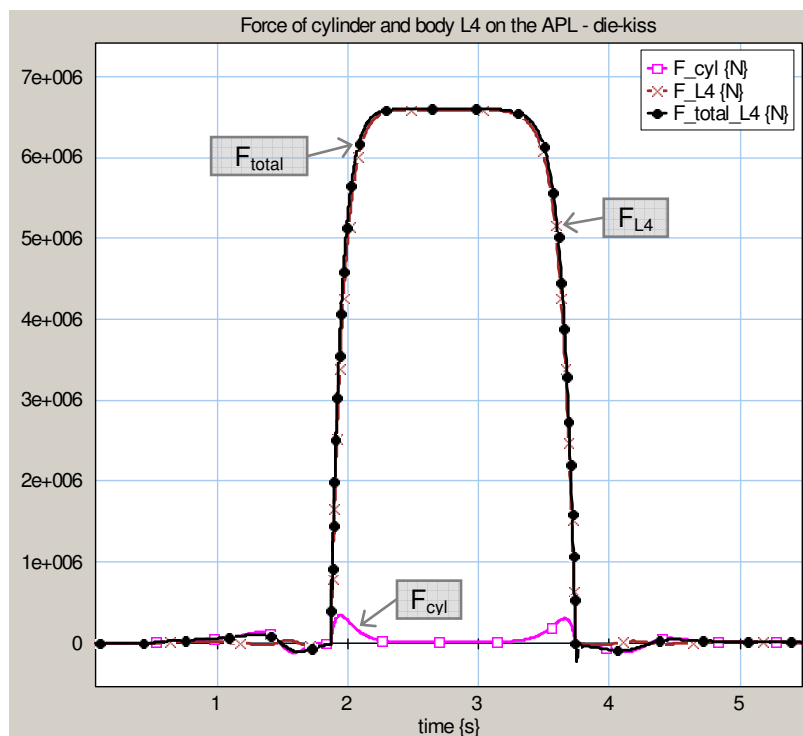


Figure 2-26 The LSP hits the VSP between $t=1.5s$ and $t=2s$ and the clamping force is build up. This force is present between the LSP and the VSP, but also between the APL and body L_4 . When the LSP hits the VSP, the total force is almost equal to the force caused by body L_4 on the APL and the force of the cylinder is negligible.

When the LSP does not make contact with the VSP, the force of body L_4 on the APL (F_2) is negligible compared to the force caused by the cylinder (F_1). But once the LSP hits the VSP it is the other way around. The clamping force works on the APL too via body L_4 . Compared to the clamping force, the force of the cylinder is negligible. This can be seen from the simulation results of figure 2-25 and figure 2-26.

2.7.6 Effect of changing friction coefficients

There are different kinds of friction. In the simulation model, only viscous friction was used. To represent the viscous friction of the LSP on the sliding bed, and the friction of the crosshead, a resistance element is added in the bond graph model. These elements can be used to fit the model with the measurement data. The friction force is based on the velocity, the normal force and the friction coefficient between the materials as shown in equation 2.8.

$$F_{\text{viscousfriction}} = v \cdot \mu_v \cdot F_N = v \cdot \mu_v \cdot m \cdot g \quad (2.8)$$

To show the effect of the viscous friction to the total force on the APL, the total force on the APL is plotted for multiple friction coefficients. In the plot of figure 2-27 the friction of the LSP on the bed is changed, and in figure 2-28 the friction of the crosshead is changed. When the transformation ratio of the clamp mechanism increases, the effect of the friction of the LSP increases. The transformation ratio is described in Appendix D.

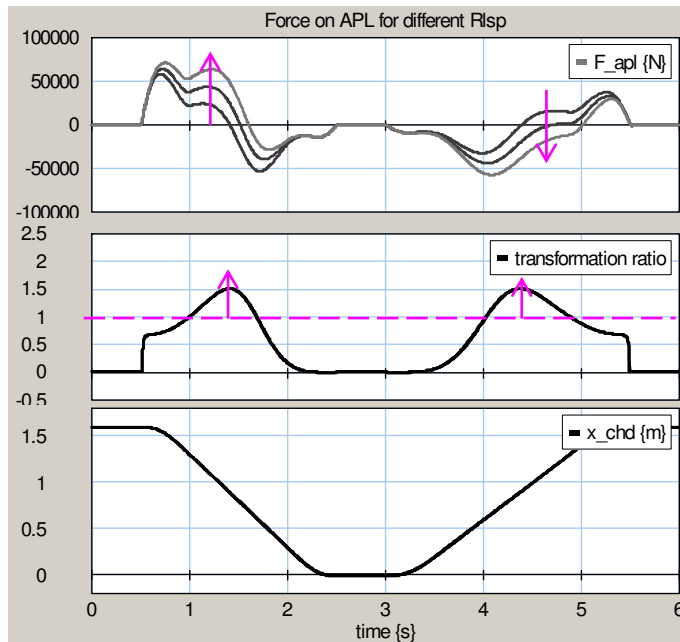


Figure 2-27 Simulation results for different friction coefficients of the LSP. Plot shows the force on the APL caused by the movement, where $\mu_{\text{CHD}}=0.0$ and μ_{LSP} is, from bottom to top in the first half, 0.0 s/m, 0.11 s/m and 0.22 s/m. The transformation ratio j , and the position of the crosshead are shown.

In the first part of the movement when the LSP is moved towards the VSP, the effect of increasing the friction can be seen. The effect of the friction of the LSP is larger when the transformation ratio becomes larger. After $t=2.5\text{s}$ the effect of the friction decreases because the transformation ratio decreases again. After $t=3.0\text{s}$ the difference between different friction coefficients can barely be seen. The inverse also occurs when the mechanism is opening again after $t=3.0\text{s}$. In the small first and last parts of the opening movement the effect of the friction is negligible. But when the transformation ratio of the clamp mechanism increases, the friction seen by the cylinder is increasing.

The effect of the friction on the crosshead is independent of the transformation ratio, because the friction is located before the clamp mechanism. When the friction increases, the whole plot is shifted up linearly; a larger force is needed for moving the crosshead with the same velocity. The distance between the lines is equal for point with a constant velocity. The first and last part of each movement are little different, due to the increasing and decreasing velocity.

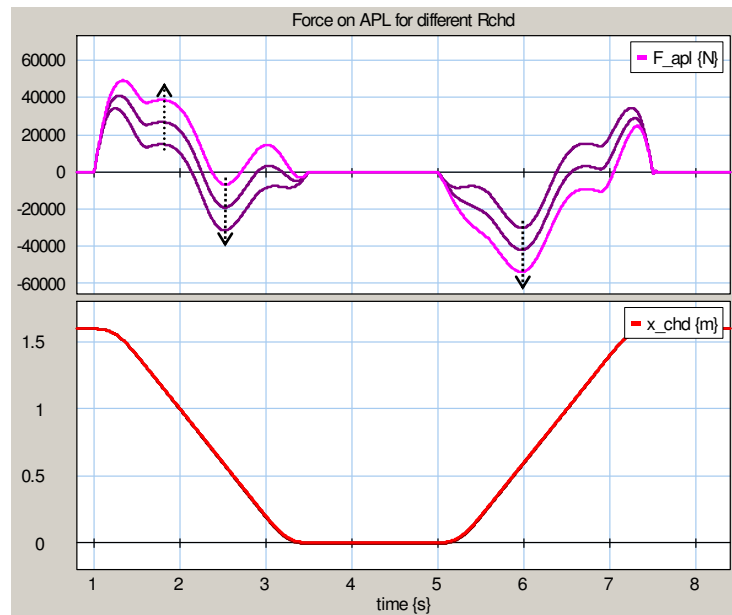


Figure 2-28 Simulation with different LSP-friction values. Plot shows the force on the APL caused by the movement, where $\mu_{LSP}=0.0$ and μ_{CHD} is, from bottom to top in the first halve, 0.0 s/m, 0.44 s/m and 0.88 s/m. The vertical arrows show that the effect of the friction of the crosshead is linear and not position dependent.

2.7.7 Effect of increasing the weight of the LSP

The clamp mechanism is tested and calibrated without anything mounted on the LSP. The dynamic behavior will change when the mass of the LSP is increased. The maximum weight for the mold is specified for each type of clamp mechanism. The part that is mounted on the LSP can be at most 2/3 of this weight. For the S-12000 or N-12000 clamp mechanisms, the maximum weight that can be mounted on the VSP is 15.000 kg. Some simulation results for four different LSP weights are shown in figure 2-29.

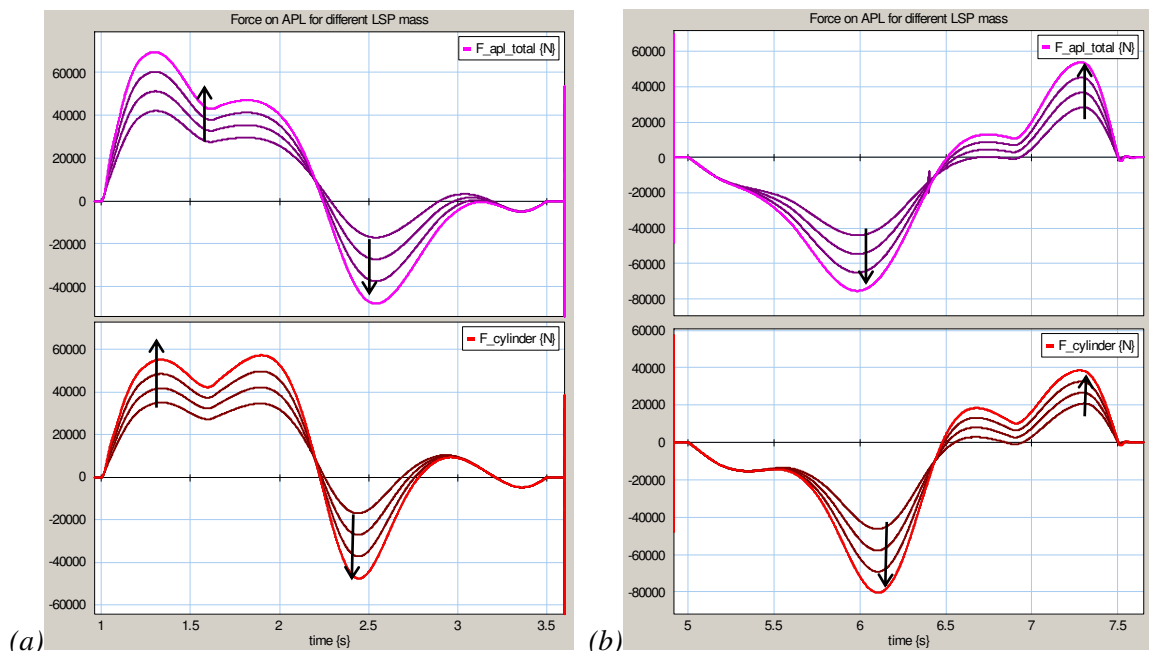


Figure 2-29 Simulation result for four different LSP weights, showing that the required force will increase when the LSP weight is increased. Weights used are 14.680 kg, 19.680 kg, 24.680 kg and 29.680 kg. (a) Force needed for closing the mechanism and (b) force required for opening the mechanism.

The required maximum force of the cylinder is almost doubled when the weight of the LSP is doubled. The effect is smaller in the beginning and in the end of the movement, due to the transformation ratio.

2.8 Concluding remarks

The simulation model is made, based on a simplified clamp mechanism. By doing some simulation experiments, the model was verified. The effect of changing the friction and mass parameters is analyzed, which is needed for fitting the model to the measurement data when validating. This is the next step, and is described in the following chapter.

3 Model validation

The model derived in the previous chapter can be validated with measurement results from the real clamping mechanism. The raw data needs to be conditioned before it can be used in the simulations. The quantization noise is filtered out, and to match the force with the acceleration, delay is added to the calculated force. The model is matched with the measurements by adjusting the friction coefficients of the crosshead and the LSP.

3.1 Measurement information

The clamp mechanism is moved according to a reference profile. The measurement data is stored in a file (figure 3-1), which can be viewed and exported with the Visiscope program from Stork. The measurements are done without a mold mounted on the LSP.

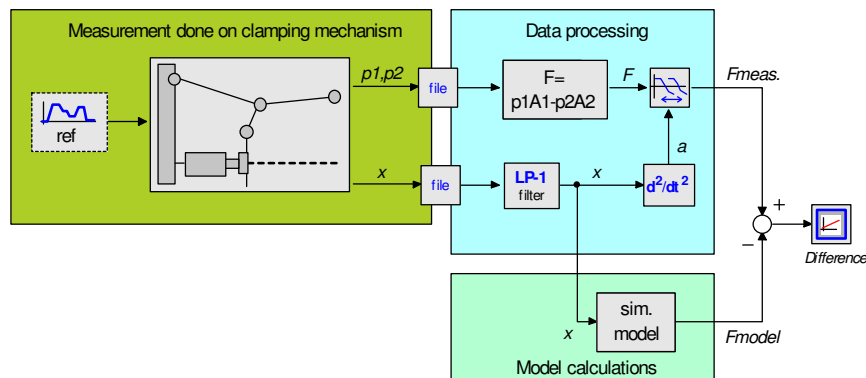


Figure 3-1 The clamp mechanism is moving according to a reference motion profile. The data is saved in a file. The position and both pressures are used to validate the force of the simulation model with the force of the measurements.

Due to the digitizing of the data, noise appears in the measured data. This can be seen in figure 3-2-a in the first 0.5 s. The frequency of this noise is 1 kHz because of the sample frequency. More details about the quantization noise can be found in subsection 2.6.2. The measured data is used as a reference signal for the simulation model and should therefore not contain too much noise. To get rid of this noise the data is filtered with a low pass filter with a cutoff frequency of 20 Hz. Based on several simulations with different cutoff frequencies this value gives the best result. When the frequency is chosen too low, the properties of the signal will get lost. A disadvantage of filtering is that phase shift is introduced, which will give delay between the measured position stored in the data, and the model reference position. This can be seen in figure 3-2-b.

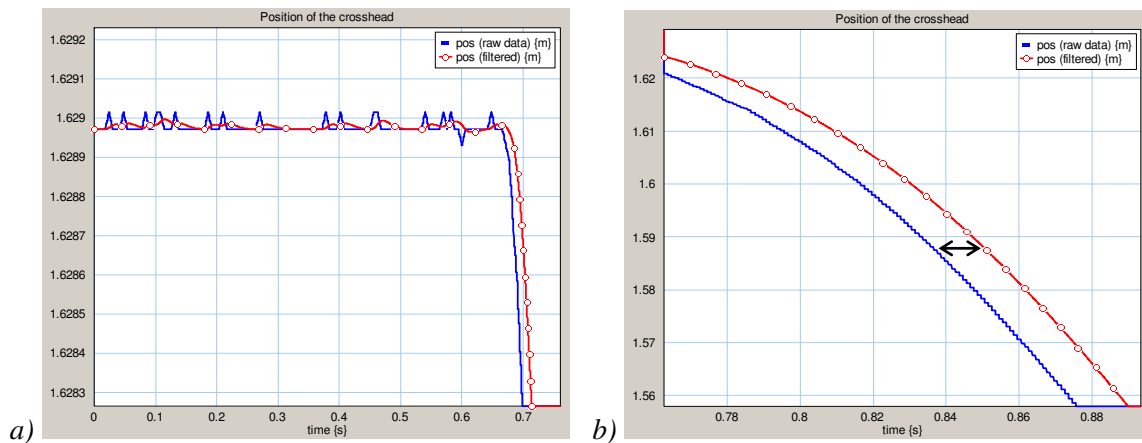


Figure 3-2 (a) The quantization noise on the raw data can be seen in the first 0.5 s. (b) The data can be cleaned-up by a low pass filter. This will introduce delay, as shown by the arrow.

After a force is applied, the mechanism will start moving. The velocity of the clamping mechanism should follow the reference velocity. The error between the actual velocity and the reference velocity is used to control the force on the crosshead.

To be able to compare the model force with the real data force, when the measured position is used as a reference position for the model, the delay between force and acceleration needs to be removed. This delay between the actuation force and the motion of the real mechanism is caused by the dynamics of the clam mechanism.

The force and the acceleration of a single moving mass are related, as shown by equation 3.1. This is only true when the mass can move freely. In case the mass is connected to a spring, it does not hold anymore. When the force applied to the mass is zero, the acceleration is also zero.

$$F = m \cdot a \quad (3.1)$$

The acceleration is derived from the measured position. When the acceleration of the measurement is compared with the force of the measurement (figure 3-3), the maximum values and the zero crossings should match. But due to the dynamics of the hydraulics and the clamp mechanism, there is a delay between the acceleration and the force. This can be seen at the arrows in figure 3-3. Figure 3-3 only shows the free movement of the clamp mechanism, before the mold halves touch each other.

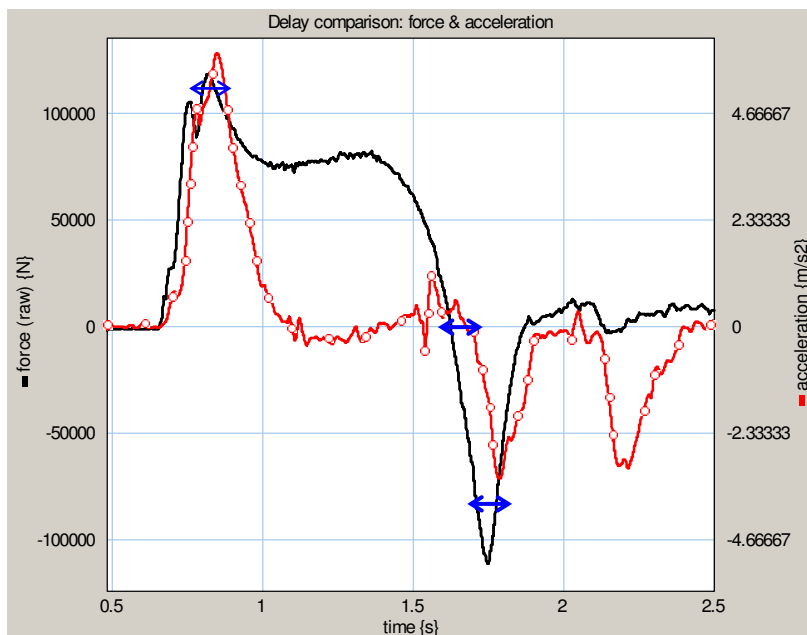


Figure 3-3 Force and acceleration of the measurement data. The acceleration is shifted in time with respect to the force. A force results in acceleration, but the system dynamics include phase shift.

This shift can be solved by adding delay to the measured force, as been done in figure 3-1. The result is shown in figure 3-4.

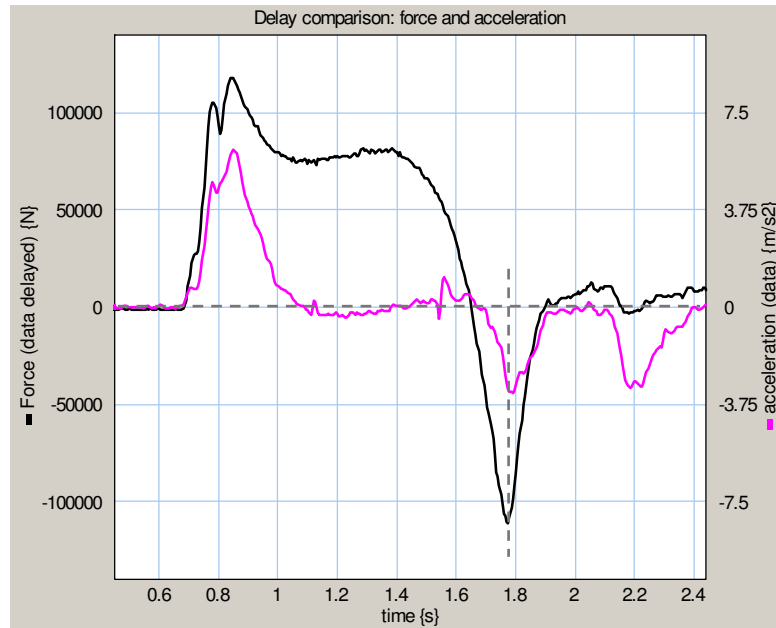


Figure 3-4 The calculated force is shifted by 25 ms to match the acceleration.

The force is compared with the acceleration as shown in figure 3-3. When the delay is 25 ms the force and acceleration start at the same time, but the other maximum values and zero crossing are not yet equal (figure 3-4). If the delay is adjusted to match the zero crossings, maximal and minimal values, the delay would be 30 ms. The delay block gives a constant delay for all frequencies, while in reality the delay is dependant for each frequency due to the dynamics.

With these results, the model can be validated with the measured data.

3.2 Validation of the model

The model is validated by comparing the force of the model with the force of the measurement, when the crosshead is moved in the same way. A simple block diagram is shown in figure 3-5, to illustrate the procedure. The measurement data is stored in a file, and the measured position of the crosshead is used as a reference for the model. The crosshead position of the model follows the reference position, by means of a PID-controller, after the position is filtered by a low pass filter. The configuration of this PID-controller has a certain influence on the result of the force of the model.

The comparison between the forces was already shown in figure 3-1. There is some delay between each stage of the block diagram, so that the total delay between the force of the model and the force of the clamp mechanism has to be cancelled by the delay block for a good comparison.

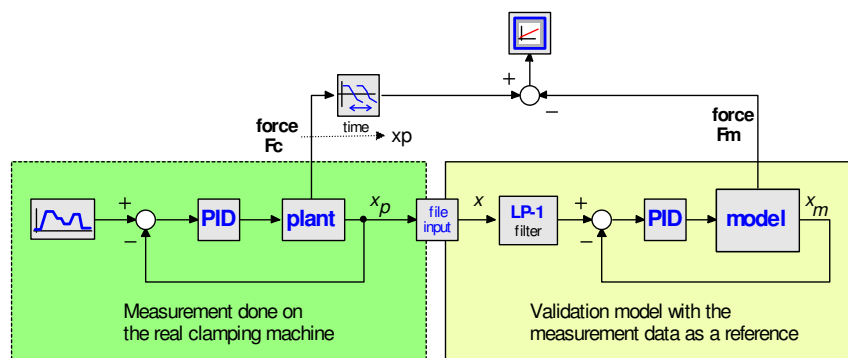


Figure 3-5 Simple block diagram shown the validation procedure. The force of the model F_m is compared with the (delayed) force of the measurement F_c .

When the derived model is correct, the force to move the crosshead in the model (F_m) should be identical with the delayed force of the measurement (F_c). This force can be calculated from the measured pressure and the area of the cylinder (equation 2.5).

The measurements are done without a mold attached to the LSP. Therefore, in the simulation no extra weight is used. The weights of the bars used in the model are estimates taken from the specification, but the real weights can be little different. The spring stiffnesses in the model are determined in section 2.4.3, based on the assumption that the maximum force gives a certain deformation in x - and y -direction.

The friction coefficients of the crosshead and the LSP are the only parameters in the model that can be adjusted to tune the force of the model. The effect of changing the friction of the crosshead and the LSP is described in subsection 2.7.6. Three simulation results are shown in figure 3-6, figure 3-7 and figure 3-8 to illustrate the difference in the force of the hydraulic cylinder, for different friction values. The measurement used here is the 100% clamping measurement (*S0212002.001*), where the clamp mechanism is closing.

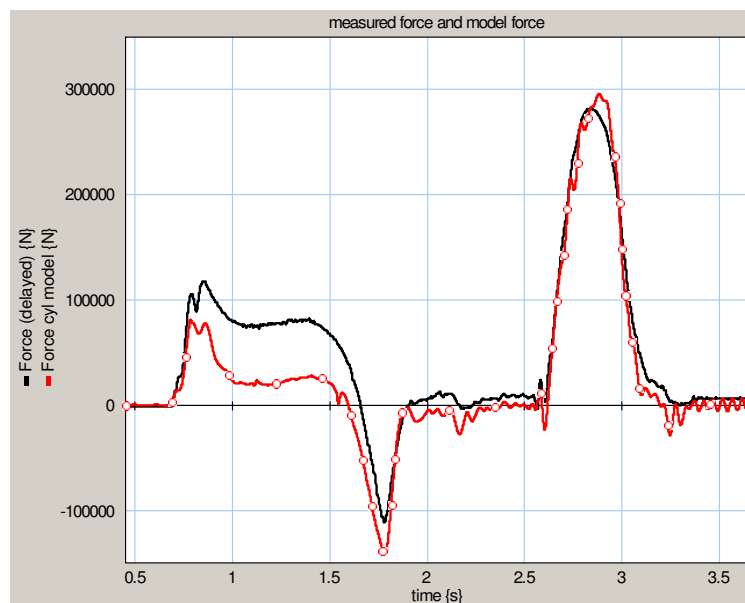


Figure 3-6 Simulation result for when no friction is used. The force of the cylinder in the model is much lower than the measured force. The LSP hits the VSP after 2.61 s.

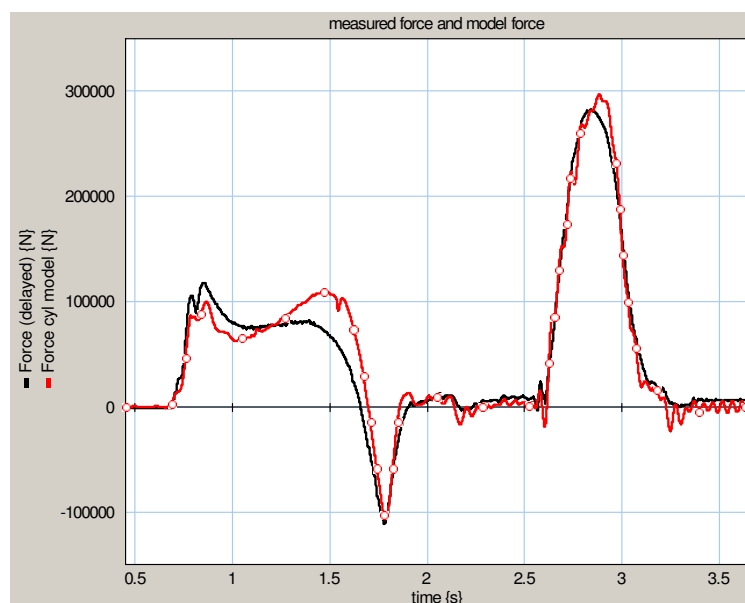


Figure 3-7 Simulation result if the wrong friction is used. Here the friction coefficient μ_{chd} is 0.5 s/m and $\mu_{lsp}=0.2$ s/m.

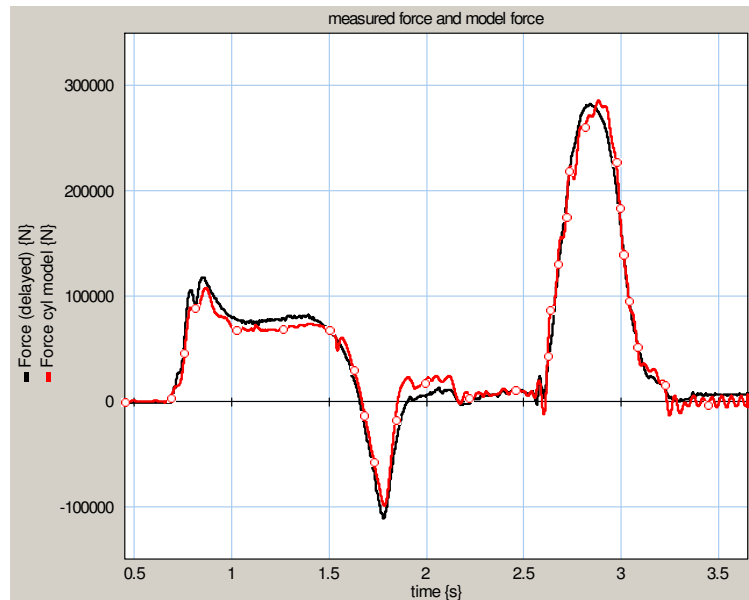


Figure 3-8 Simulation result with a good match between the measured force and the model force. Friction coefficient μ_{chd} is 1.25 s/m and μ_{lsp} is 0.01 s/m. The PID controller settings are K_p : 25, τ_i : 0.25, τ_d : 0.28, β : 0.1. The LSP hits the VSP at 2.61s.

According to figure 3-8, the model shows the same behavior as the measurements. There are minor differences in the amplitude of the force. A better match can be obtained by also increasing the mass of the crosshead and the mass of the LSP a little. Because of the increasing mass the force will also increase. A better result can be achieved when M_{CHD} is 3.850 kg and M_{LSP} is 15.800 kg. But since the exact weights of the crosshead, LSP and bars are unknown, the values as mentioned in the specifications are used.

For the closing movement, the system was at rest. When the opening movement is used for validation, knowing the initial conditions is a problem, because the system is not in rest. From the stored measurement data it is not known where exactly the die-kiss occurs, which force there is between the plates, and so on. Once the simulation is running over a longer period, the results will not be influenced by the wrong initial conditions. In figure 3-9 the real force and the model-force for the closing and opening of the clamp mechanism are shown. The same friction coefficients as in figure 3-8 have been used. The model force matched reasonably with the calculated real force.

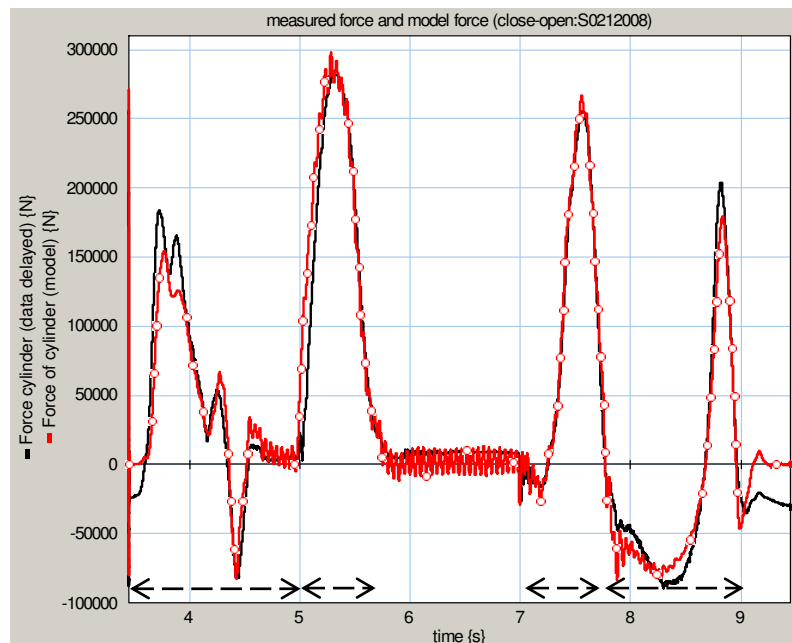


Figure 3-9 Simulation results when measurement S0212008 is used as a reference. The real force is delayed for 30 ms, and the cut-off frequency of the position filtering is 20 Hz.

The mechanism closes from $t=3.5$ to 5.0 s, clamps from $t=5.0$ to 5.8 s, eases from $t=7.0$ to 7.8 s, and opens from $t=7.8$ to 9.0 s. The noise between $t=6.0$ s and $t=7.0$ s is due to the measurement noise. The position varies constantly between 0.85 mm and 1.15 mm. If the cutoff frequency of the low pass filter is lower, this noise will reduce.

3.3 Parameters of the simulation model

After the effect of variation of the different elements is simulated and the model is validated, the final parameter values of the simulation model (see figure 3-10) are listed below in table 3-1.

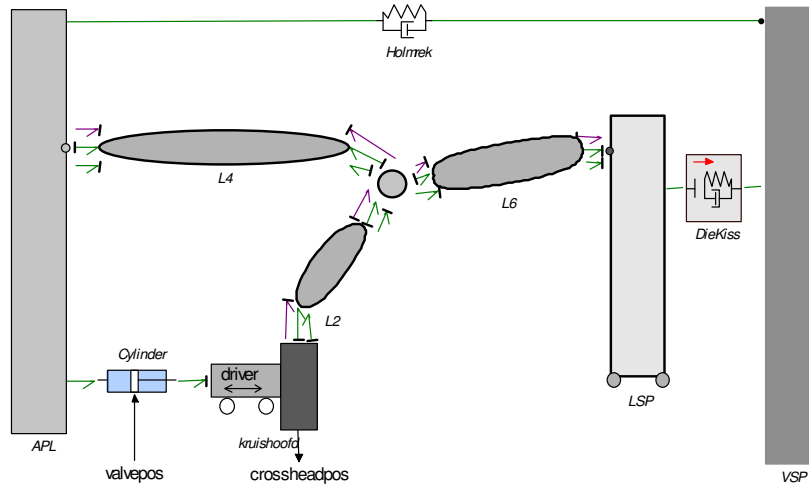


Figure 3-10 Simulation model of the clamp mechanism.

Submodel name	Parameter	Value	
Connection bars (holmrek)	Stiffness (x)	$K = 8.0 G$	N/m
	Damping	$R = 60 M$	Ns/m
APL	Stiffness (y)	$K = 500 M$	N/m
	Damping	$R = 500 k$	Ns/m
	Mass	$I = 16.940$	kg
Crosshead (CHD)	Mass	$I = 3.500$	kg
	Friction	$R = 1.25$	s/m
Bar L_2	Stiffness-x	$K = 8.0 G$	N/m
	Damping-x	$R = 1.0 M$	Ns/m
	Stiffness-y	$K = 3.5 G$	N/m
	Damping-y	$R = 10 M$	Ns/m
	Mass	$I = 420$	kg
	Inertia	$I = 6.4$	kgm^2
Bar L_4	Stiffness-x	$K = 24 G$	N/m
	Damping-x	$R = 1.0 M$	Ns/m
	Stiffness-y	$K = 8.0 G$	N/m
	Damping-y	$R = 10 M$	Ns/m
	Mass	$I = 240$	kg
	Inertia	$I = 7.5$	kgm^2
Bar L_6	Stiffness-x	$K = 24 G$	N/m
	Damping-x	$R = 1.0 M$	Ns/m
	Stiffness-y	$K = 8.0 G$	N/m
	Damping-y	$R = 10 M$	Ns/m
	Mass	$I = 970$	kg
	Inertia	$I = 51.4$	kgm^2
LSP	Mass	$I = 14.680$	kg
	Friction	$R = 0.01 s/m$	s/m
Die-kiss	Stiffness	$K = 200 M$	N/m
	Damping	$R = 1.0 k$	Ns/m

Table 3-1 Overview of the used parameter values for all the masses, springs and dampers in the clamp mechanism.

3.4 Conclusion

Based on the results of the simulations when the measured data is used as reference, the conclusion can be drawn that the model is good enough for controller analysis and design. The model shows the same behavior as the real measurement and about the same force.

To improve the result of the model, the exact bar weights and the bar stiffnesses of the real mechanism need to be known. The model can be adjusted to fit in more detail, but then better measurement results are needed.

In the designing and testing of the control system, this validated model can be used as a substitute for the real clamping machine. In the following chapter, the possible control strategies are discussed, together with the influence of the reference profile on the time duration, when using this validated model.

4 Controller design

4.1 Introduction

4.1.1 Preparation phase

The detailed model that was validated in the previous chapter can be used to test the effect of a certain motion, and the behavior of the control system, before it is implemented on the real clamp mechanism. The detailed model serves as a replacement of the physical system. To design a control system, the detailed model is too complex. A common procedure is to derive a simplified model for designing the control system (Broenink and Hilderink, 2001). The simplified model is derived in section 4.2.

When the crosshead needs to be moved, the desired motion needs to be specified. The motion of the mechanism is controlled by the controllers, which make sure that a certain reference path is followed. This reference signal is of great importance, since it determines how the clamp mechanism will move. The background of this profile was described in section 2.2.1 to 2.2.3, and the practical site is described in section 4.3.

In the model, all velocities are available for using and viewing, but in the clamp mechanism only the position of the crosshead is measured. For control purposes the velocity of the crosshead is needed, so in section 4.4 a way to obtain the velocity by estimation is described.

4.1.2 Controller design phase

The controller controls the position of the proportional valve. This valve controls the pressure in the hydraulic cylinder and thus the force on the crosshead. The movement of the crosshead is measured by a position sensor. There are several possibilities to control the motion of the clamp mechanism, namely:

- Steering
- Feedback
- Feed forward

One of the properties of steering is that no measured signal is used to adjust the signal to the actuator. The signal to the actuator can be proportional to the reference signal, or a maximum output signal can be applied for some time. The controller is not aware of the error between the velocity of the mechanism and the reference velocity, and cannot correct for that.

In a feedback controller, a measured value is used to adjust the signal to the actuator. To make sure the crosshead moves correctly, the motion is compared with a reference path. Depending on the error between the reference value and the measured value, the control signal to the actuator is adjusted. A feedback controller can consist of one or more of three actions: a proportional gain (P), an integral action (I) and a derivative action (D). Depending on the kind of system, a P-, PD-, PID-, PI- or even I-controller can be used (van Amerongen and de Vries, 2002, page 147).

When we have knowledge of the dynamics of the mechanism, we know beforehand which force is required to move the crosshead according to a reference path. We can use this knowledge to generate the valve signal so that the crosshead will follow the reference path. This is called feed forward control. The valve signal calculated by the feed forward controller is not dependent on a measured value, but only on the reference signal and the correctness of the calculations.

4.1.3 Application for time reduction

The signal from the controller to the actuator will always depend on the reference signal. The performance of the clamp mechanism will mainly depend on this reference profile. To reduce the time needed for one cycle, the reference velocity profile can be optimized. An iterative method, called cycle-to-cycle, is described in subsection 4.7.1, can be used to tune the point where the deceleration starts. Due to the performance of the hydraulics and the safety limitations, the time reduction is small. The result and comparison of using feed forward and cycle to cycle is given in section 4.8.

4.2 Model reduction

For the controller design, the model of the real mechanism is important. This complete but rather large model is described in section 2.4. By reducing the model to a simpler model, a model that can be used for control purposes is obtained.

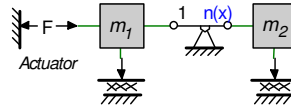


Figure 4-1 Diagram of a simplified clamp mechanism. Only the most important masses and frictions are taken into account.

The dynamics of the mechanism are mainly determined by the mass and the friction of the crosshead and the LSP (figure 4-1). If we first consider the clamp mechanism as a mechanism that exists of only two masses, connected together with a nonlinear position-dependent transformation with ratio $n(x)$, the mass seen at the actuator is given by equation 4.1.

$$m_{act}(x) = m_1 + n(x)^2 \cdot m_2 \quad (4.1)$$

When the masses are moving, mass m_{act} will change due to the position dependent transformation ratio $n(x)$. The force to move this mass m_{act} is given by equation 4.2.

$$F(t) = \frac{dp(t)}{dt} = \frac{d}{dt} m_{act}(x) \cdot v(t) = m_{act}(x) \cdot a(t) + v(t) \cdot \frac{dx}{dt} \cdot \frac{d}{dx} m_{act}(x) \quad (4.2)$$

Normally a mass is not varying in value and the position or time derivative of the mass is zero. Because mass m_{act} is position and thus time dependent, this is not true. Now the force is not only equal to m^*a , but also has a term with the derivative of the mass times the velocity.

When the clamp mechanism moves from opened to closed, the transformation ratio $n(x)$ of the clamp mechanism changes from 0.5 (opened) to 1.5 (half way) and then decreases to almost 0.0 (closed). This means that the mass seen at the actuator will vary around m_1 , with addition of 0.0 to 2.25 times m_2 . When no mold is attached to the LSP, m_2 equals 14680 kg. So the part of m_2 seen at the actuator varies from 3670 kg to 33030 kg. This has quite a large impact on the force to be delivered by the actuator.

When viscous friction is also taken into account, the friction forces of both masses are added to equation 4.2. The force calculation as shown in equation 4.3 now exists of three terms.

$$F(t) = a_{ref}(t) \cdot (m_1 + n^2(x) \cdot m_2) + v_{ref}^2(t) \cdot m_2 \cdot 2 \cdot n \cdot \frac{dn(x)}{dx} + \{ F_{CHD_viscous} + n(x) \cdot F_{LSP_viscous} \} \quad (4.3)$$

The friction force can be found from equation 2.8.

When a force is applied to the model, the position of the system will come out. In an inverse model it is the other way around. When a position is applied, the force will come out. Figure 4-2 shows the difference between a model and an inverse model.

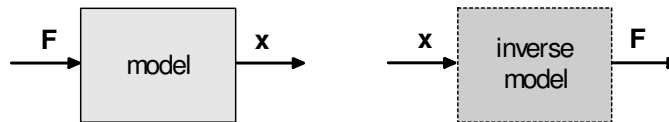


Figure 4-2 The model will give the motion of a system when a certain force is applied. An inverse model does the opposite: when a position is applied, the force will come out.

The inverse model description of equation 4.3 is a nonlinear second order model simplification of the complex clamp mechanism. The reference velocity and acceleration are used to find the force.

The reduced model is used in section 4.6 to calculate the valve position.

4.3 Reference profile

For correct and safe operation of the clamp mechanism, the crosshead has to follow a certain path. The movement of the mechanism is repetitive, so the reference path is stored in a reference profile. In general, a reference signal can be a position, velocity or acceleration. For safety reasons there are some limitations in the velocity of the crosshead on certain parts of the trajectory. Since the measured signal is a position signal, it is obvious that the reference can be a position signal too. But when the motion of the crosshead is controlled with a position reference, the velocity limitations can not be checked for. To control the velocity of the crosshead, such that it stays within the safety limitations, the reference for the controller needs to be a velocity signal. The velocity of the crosshead may not be higher than the boundary velocities as defined for the safety zones when these zones are reached.

A certain distance before the LSP hits the VSP, the velocity is limited to a lower velocity. This is the mold protection zone. The velocity needs to be less or equal then the reference velocity, which need to be held until the deceleration must begin so that just before die-kiss, the lower velocity is reached. At die-kiss the two mold halves hit each other. The reference velocity (V_{ref}), together with the mold protection (X_{mp}) and die-kiss (X_{dk}) safety positions, is shown in the simulation result of figure 4-3. The background of the current shape of the motion profile is described in subsections 2.2.2 and 2.2.3.

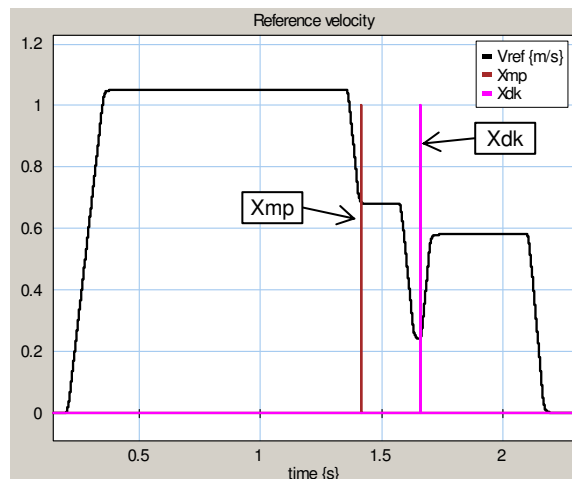


Figure 4-3 The reference velocity is plotted, with the events of when the safety zones are passed. The velocity needs to be decreased to the lower velocity before the safety zone is reached. After the plates make contact, the velocity of the crosshead can increase to build up the clamping force.

The velocities and accelerations that can be reached by the mechanism depend on the performance of the hydraulic circuit. If the oil flow can be large enough, higher velocities can be reached.

The force required for moving the crosshead in accordance with the reference velocity, depends on the position dependent transformation ratio of the clamp mechanism (described in Appendix D). Depending on this transformation ratio, the cylinder sees more or less of the mass of the LSP. The force is the lowest when the acceleration is as early as possible and when the deceleration is as late as possible, because then the transformation ratio from the clamp mechanism is the lowest.

4.4 Velocity estimation

If the crosshead is controlled with a feedback controller, the problem is that the position is measured, while the velocity is needed. Therefore, the velocity needs to be derived from the measured position. The analogue position is converted to a digital value by the A/D-converter. The signal is quantized in amplitude and time, so it fits in the available number of bits. Depending on the number of bits, the resolution will be larger or smaller. Depending on the method used for quantization, the error made by quantization is half the least significant bit (round off) or one times the least significant bit (truncate). The noise that is introduced by the quantization can be seen as white noise, with an average value of zero. This is described in literature (van Amerongen and de Vries, 2002, pages 168 and 169).

For objects with low velocities, the measured value will change very slowly. A big part of the change of content of the measured signal will be measurement noise and quantization noise. If the object is moving relatively fast the noise will have less influence, because the change in position is a lot larger than the noise. The derivative action is very sensitive to noise, because high frequencies are amplified more than low frequencies. When there is noise present in the measured signal, it will mess up the velocity signal because it will be amplified more than the information signal. A state variable filter (SVF) can be used to differentiate the measured position to obtain an estimated velocity, while rejecting noise at higher frequencies.

The derived velocity is compared with the reference velocity and based on this error the valve position is adjusted. If there is delay between the real velocity and when the velocity is known in the controller, the corresponding adjustment is based on the velocity of some time ago. Therefore, a small delay is desired. This can be achieved if the bandwidth of the SVF is chosen large enough. The required gain for this bandwidth will be high, which causes the amplification of high frequent signals. If the steps of the A/D converter are too large, the quantization noise will result in a bad result of the SVF. To solve this problem a lower bandwidth can be chosen, which results in lower gains. The SVF becomes less sensitive to noise, but at the price of a larger delay due to phase shift. Another solution is to increase the number of bits, which will decrease the step size of the amplitude of the A/D-converter and the quantization noise. In this case the result of the SVF will be better. State Variable Filters are explained in more detail in Appendix F.

4.5 Velocity feedback control

Due to safety regulations the velocity is limited in certain zones of the trajectory. To check if the velocity of the mechanism is not exceeding these limits, the velocity of the mechanism needs to be known. If position feedback is used, it is not possible to control the velocity because only the error made in the position is used. Therefore, velocity feedback control is needed for making the mechanism follow the reference velocity. A simple block diagram showing the feedback principle is shown in figure 4-4.

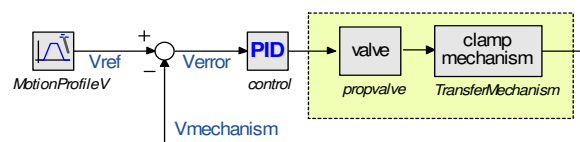


Figure 4-4 The valve opening is adjusted, based on the error between the velocity of the mechanism and the reference.

When the velocity of the mechanism would be known in the controller at the same time without any delay, and when the hydraulic circuit is not limited by a maximum force, the velocity of the crosshead can be kept equal to the reference velocity, even if the weight of the LSP is maximal. This is illustrated in figure 4-5, where the error in the velocity is at most equal to 1.4 mm/s (0.14 %) for the maximum LSP weight.

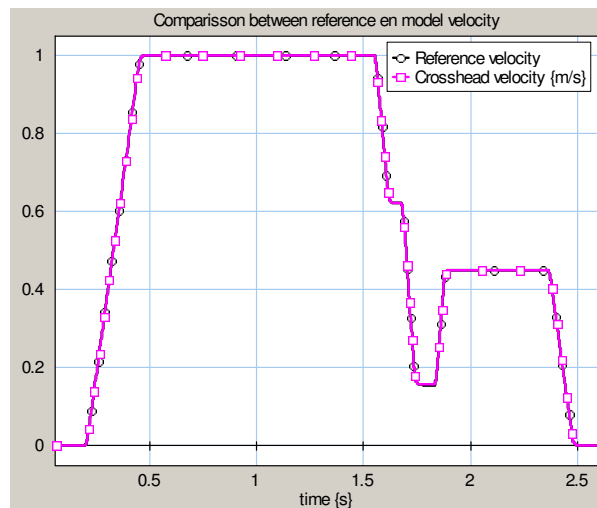


Figure 4-5 Simulation result where the clamp velocity is almost equal to the reference velocity. This can be obtained if the hydraulics is powerful enough and the real velocity is known by the controller.

But for systems with large delay times, due to the dynamics and the time for deriving the velocity, the control action is based on the error of a situation that was some time ago. Then the controller is always late with the adjustment correction. Therefore, it is harder to keep the velocity of the mechanism close to the reference velocity. For this systems with some delay, the feedback controller uses proportional (P) and integral (I) action with a little bit of derivative (D) action.

As described in the previous subsection, the delay in the SVF is added to the delay of the mechanism and the I/O. If the bandwidth of the SVF is chosen to be 100 Hz, the delay of the SVF is about 2.5 ms. But when the bandwidth is chosen to be 1 Hz, the delay becomes about 25 ms. Together with the I/O delay of two times 1.0 ms and the delay of the system itself, the results are becoming worse. This is illustrated in figure 4-6. Due to the delay the controller gain has to be lower, and this has to result that the velocity of the clamp mechanism can wander away from the reference velocity.

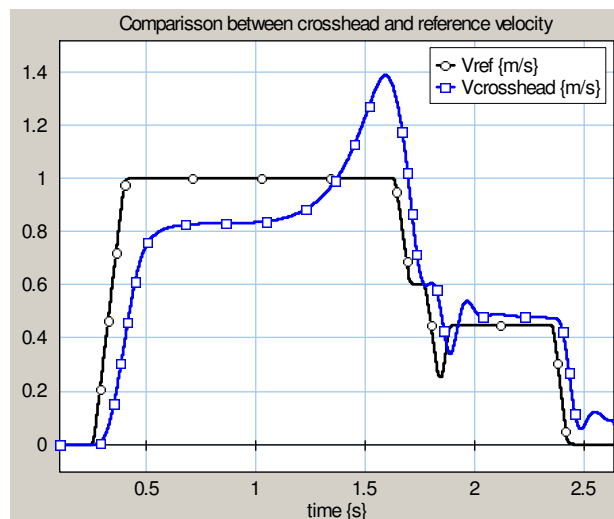


Figure 4-6 Simulation result where the bandwidth of the SVF is chosen to be 10 Hertz. The delay between the reference and the crosshead is 78 ms.

When the number of bits is chosen large enough, the digital signal is almost equal to the analog signal. The quantization noise is really small and has no influence, when the bandwidth of the SVF is 100 Hz.

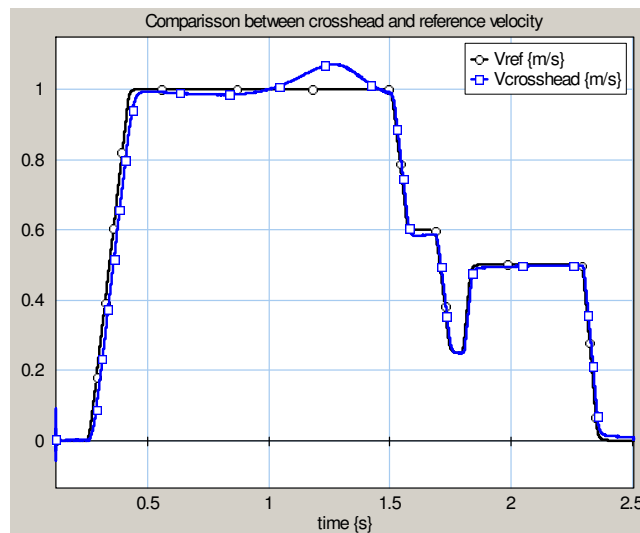


Figure 4-7 Simulation result where the A/D converter has 20 bits and the bandwidth of the SVF is chosen to be 100 Hertz. The delay between the reference and the crosshead is 16 ms.

The current position sensor has a range of 2.0 m with a resolution of 40 μm . If the resolution of the A/D converter is matched with the resolution of the position sensor, at least 16 bits are needed in the A/D converter. The quantization noise of the 16-bit A/D converter is too large for the SVF with a bandwidth of 100 Hz due to the amplification of the high frequency parts of the signal. A better SVF bandwidth for a 16-bit A/D converter is 50 Hz.

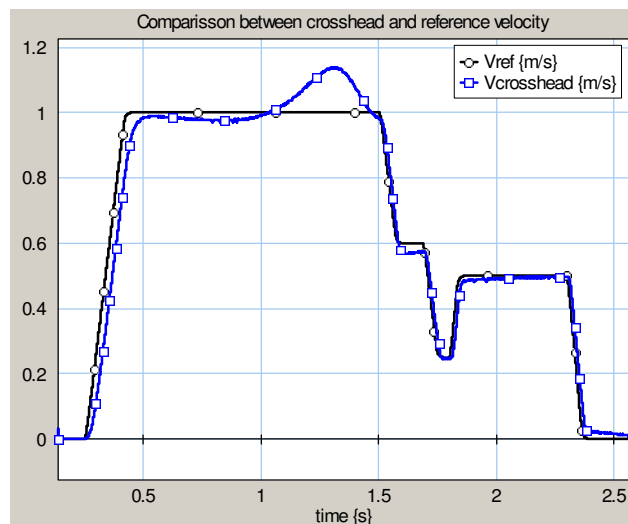


Figure 4-8 Simulation result with an A/D converter with 16 bits and a lower K_p in the controller. The bandwidth of the SVF here is 50 Hertz.

Figure 4-8 shows the simulation result for a SVF with a bandwidth of the 50 Hz. Due to the increased time needed for estimation, the proportional gain of the controller needs to be a little lower than for a SVF with a bandwidth of 100 Hz. The time difference between the reference velocity and the real velocity is 30 ms when accelerating and 12 ms when decelerating.

To keep the velocity of the crosshead of the clamp mechanism close to the velocity of the reference, it is important that the resolution of the A/D converter is small enough, but not smaller than the noise level. In that case, the measured values will contain only noise if the movement is slow. When the delay time is small, the controller can be made more stiff and the result will be better.

4.6 Feed forward

When feedback control is used, the hydraulic valve position is adjusted based on the error between the crosshead and the reference velocity. This valve will control the force delivered by the hydraulic cylinder. Since the movement is a repeating movement with the same reference velocity, the motion

of the valve will be equal for every run. The valve position can be obtained beforehand from the required force, which is based on the knowledge of the reference signal, the dynamics of the hydraulic circuit and the dynamics of the clamp mechanism.

The controller that calculates the valve position in advance, based on knowledge of the clamp mechanism and the reference signals is called a feed forward controller. If a feed forward controller is implemented, it is added in parallel to the PID-controller as shown in the block diagram of figure 4-9. To enable or disable the feed forward controller, a switch is added to the block diagram.

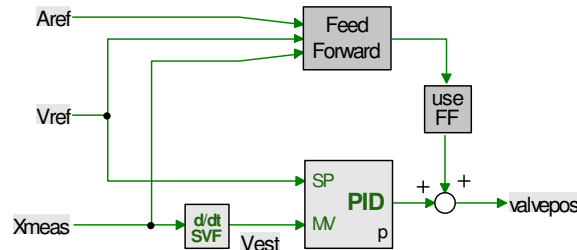


Figure 4-9 Block diagram of the controller with addition of a feedback controller. The reference velocity and acceleration are used together with the weights and friction to estimate the valve position. The error that is left will be taken care of by the PID-controller. The 'useFF' block is used to disable or enable the feed forward controller.

The required force to be delivered by the actuator depends on the weight of both masses that need to be moved and the viscous friction of the masses (equation 4.3). The content of the feed forward block is shown in the block diagram shown in figure 4-10.

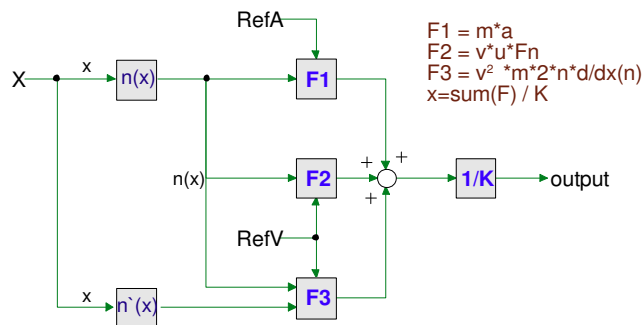


Figure 4-10 Block diagram of the feed forward controller. The content of the blocks is given by equation 4.3. The sum of the three forces is divided by the expected gain of the hydraulic cylinder to get the valve position.

The three terms of the feed forward control signal as given by equation 4.3 are shown in figure 4-11. Together they are the estimated force, calculated by the feed forward controller block of figure 4-9. The position dependent transformation ratio $n(x)$ (equations 4.2 and 4.3) and the derivative of the transformation ratio $n'(x)$ (equation 4.3) are stored in a lookup table. The acceleration and velocity used are the reference velocity and acceleration, which are known for each crosshead position.

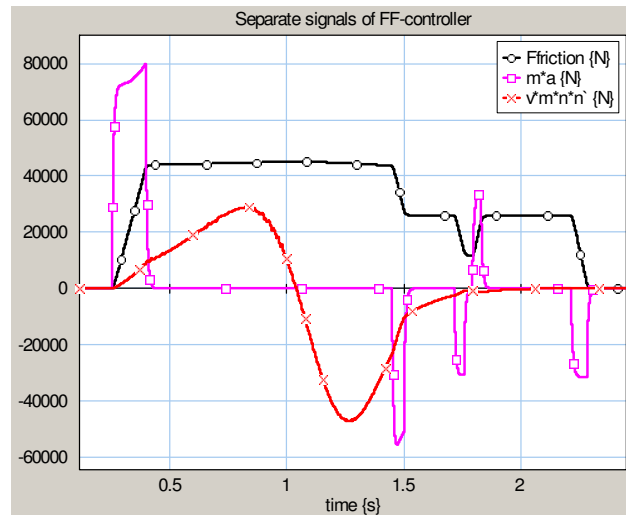


Figure 4-11 The three separate force calculations, based on the three terms of equation 4.3. Together they form the feed forward estimation of the required force that is needed to follow the reference velocity.

To get the right friction forces, the masses and the friction coefficients need to be known. If the velocity of the crosshead is multiplied by the position dependent ratio $n(x)$, the velocity of the LSP can be obtained.

The valve position can be calculated from the required force, as shown in equation 4.4.

$$valvepos = \frac{F_{feed\ forward}(x)}{cylinder - gain} \tag{4.4}$$

This is in case the cylinder is modelled as shown in figure 2-15. The hydraulic circuit is described in section 2.5. The gain can be derived by dividing the maximum force that can be delivered by the hydraulic cylinder, divided by the voltage supplied to the valve to get that force. Depending on if the differential circuit is used (see table 2-2), the gain can be 14100 or 31300.

To verify the output of the feed forward controller with the single PID-controller, the output is switched off by the *useFF* block. The result is shown in figure 4-12, where the PID-controller generates the signal to control the proportional valve. The signal calculated by the feed forward controller is matching fairly with the result of the PID-controller.

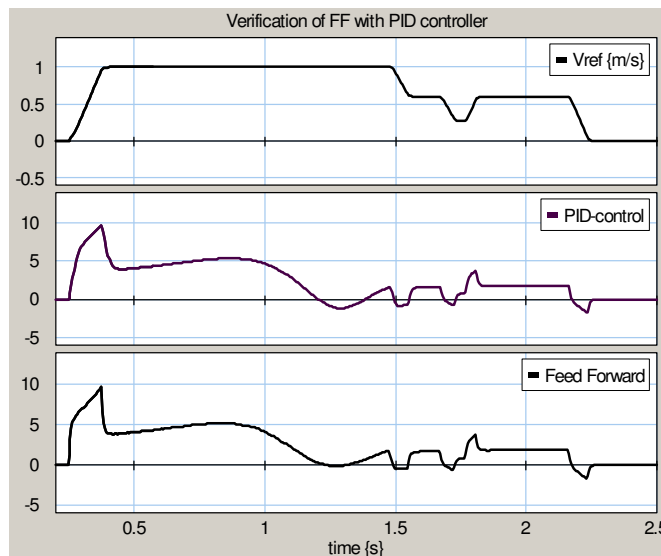


Figure 4-12 The signal of the PID-controller (based on the error between the mechanism and the reference) is shown, together with the estimation by the feed forward controller. There is only a small difference. In this case the “useFF” is not passing the feed forward signal to the valve. The PID-control output signal is used for positioning the proportional valve.

When the feed forward controller is turned on, the PID-controller only has to make small corrections. This can be seen in figure 4-13. The more correct the masses and friction coefficients are the less work the PID-controller has to do, because the calculation of the feed forward controller is more accurate.

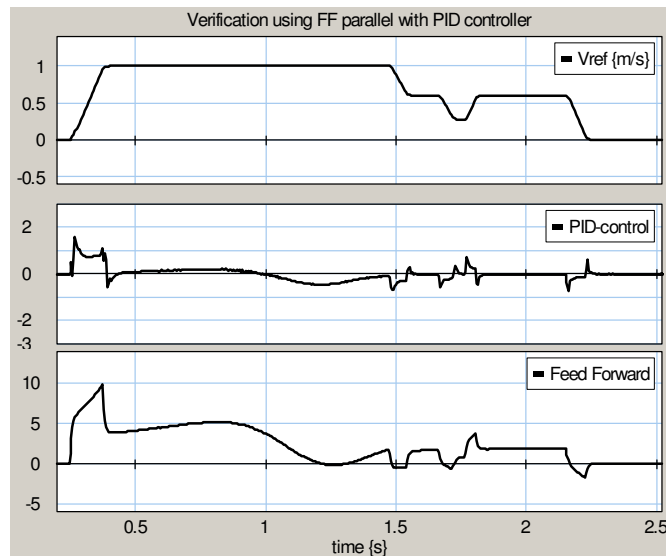


Figure 4-13 Result when the feed forward controller is turned on. The PID-controller only has to make small corrections for the remaining error.

When the feed forward controller is used, the servo behavior of the controller will improve too (figure 4-14). The feed forward controller uses the reference velocity and acceleration to generate the valve position, and does not depend on signals that suffer from delay, except for the position that is used in the transformation ratio $n(x)$. But for this ratio there is only a little difference if the delay is not too large.

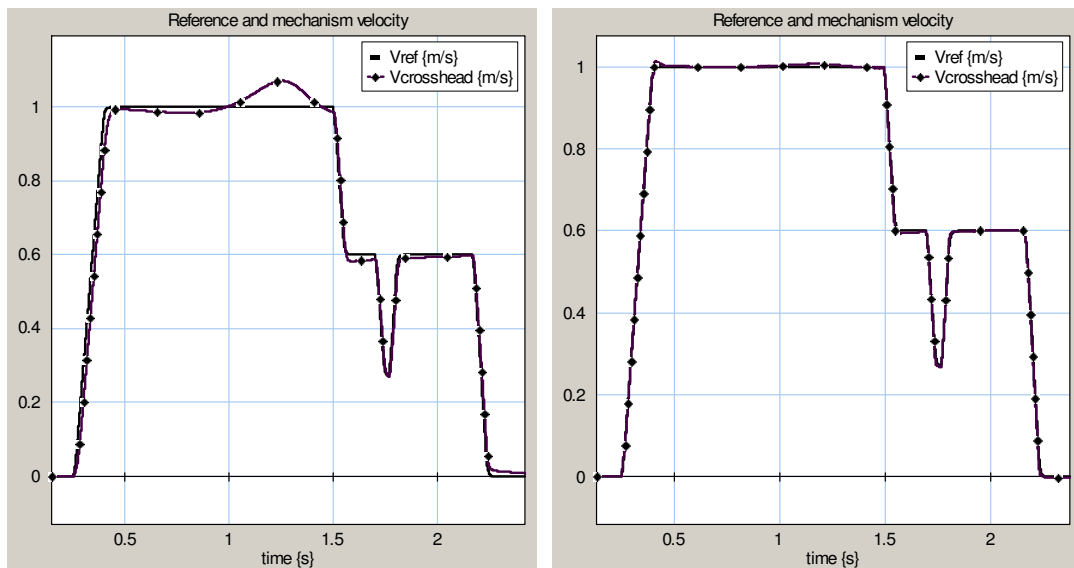


Figure 4-14 Two plots showing the difference in the use of a PID-controller (left) and a PID-controller in combination with the feed forward controller. When feed forward is used, the velocity of the crosshead matches better with the reference velocity.

If the masses and friction coefficients can be determined close to the real values, the result of the feed forward controller can be improved. If the velocity of the crosshead can be kept close to the reference velocity by the controllers, the reference velocity can be changed for faster performance.

4.7 Possible time reduction

To reduce the time that is needed for closing and opening the clamp mechanism with the current clamping mechanism, the reference velocity can be changed so that the average velocity is as high as possible, but stays within the limits. But the acceleration time (when closing) and deceleration time (when opening), depends on the performance of the hydraulic circuit. The mechanism is currently accelerating and decelerating with the maximum acceleration possible, so at this point no time reduction is possible. The velocity in the first stage of closing, and the final stage when opening, is the maximum achievable velocity, so at this point there is also no improvement possible. The only part of the reference velocity profile that is left for changing, is the middle part. If the crosshead reaches the starting position of a safety zone, the velocity has to be smaller or equal than the maximum allowed velocity for that zone.

The controller that is implemented currently is configured very robust, so that the mechanism stays safe for all possible mold weights. If the deceleration takes longer than expected, the crosshead will have some extra distance to slow down. But when the mold is lighter than the maximum allowed mold weight, the lower velocity is reached too early. Time profit can be obtained, by configuring the mechanism for the specific mold that is used.

If the reference velocity is decelerating to the lower safe velocity, it will take some time before the crosshead also reaches the lower velocity. When only a PID-controller is used, there is some more delay between the reference and the crosshead velocity (see figure 4-8) than when feed forward is used together with a PID-controller. The velocity of the crosshead is almost equal to the reference and there is almost no delay between the reference and the real velocity. It is important that the velocity of the crosshead stays within the margins, and that the velocity is lower or equal than the reference velocity when the mold protection zone is entered or when the die-kiss point is reached.

When the lower velocity is reached too far before the safety positions are reached, the deceleration was started too early. At these points it is possible to make some improvements, by optimizing the position where to start the deceleration.

4.7.1 Principle of cycle-to-cycle control

If the point where the deceleration starts can be moved, an optimal point can be chosen such that the crosshead has the specified velocity just before the safety zone is entered. Inspired by the Iterative Learning Control scheme (Verwoerd, 2005) and the Learning Feed-Forward Control scheme (Velthuis, 2000), the idea has come up to find an optimal value for this point of deceleration with an iterative approach, called cycle-to-cycle control. It is based on comparing different runs with each other, when a parameter is varied. In this case the parameters are adjusted by the human after interpreting the results. This is illustrated in figure 4-15.

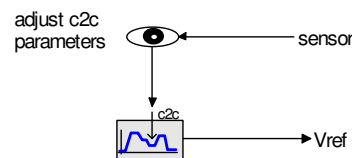


Figure 4-15 After the result is analyzed, the reference profile can be adjusted if needed.

The cycle-to-cycle approach starts with a safe position for deceleration. When the lower velocity is reached too early, this position will be decreased to a lower value so the next run the velocity is reached a little later. This process can be repeated over a few runs, until the specified velocity is reached within a safe margin before the configured start of a safety zone. Because the result of one run is compared with the result of the previous run, this optimization is called a cycle-to-cycle approach. If the higher velocity can be held over a longer period of the trajectory, the average velocity will increase.

A possible start value for the cycle to cycle controller is illustrated in the simulation results shown in figure 4-16. Here, the configured velocities are reached too early, before both zones are reached. The

crosshead moves from a position of 1.95395 m and ends just before 0.0 m. The mold protection zone begins at 0.41 m, and die-kiss occurs at 0.27 m.

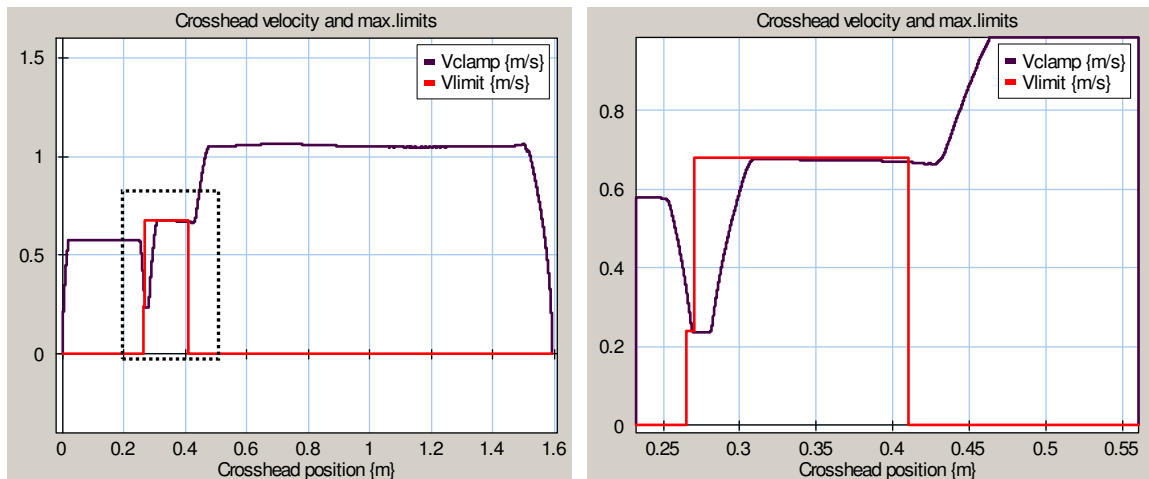


Figure 4-16 Simulation plots showing the velocity of the crosshead and the limitation. The limitation level is reached too early, so the deceleration can be started later. The crosshead moves from 1.59395 m to 0.002 m (right to left), which takes 2.179088 s. The right plot is showing the dotted part of the left plot in more detail.

Here, the maximum velocity in the mold protection zone ($0.27 \text{ m} < x < 0.41 \text{ m}$) is 680 mm/s and for the die-kiss moment ($x = 0.27 \text{ m}$) the maximum velocity is 240 mm/s.

In the simulations shown in figure 4-17 the starting position for deceleration is varied. Three different cycle to cycle parameters are used. For two of the simulations the crosshead reaches the lower velocities in time, but one of them reaches the lower safe velocity too late (most left).

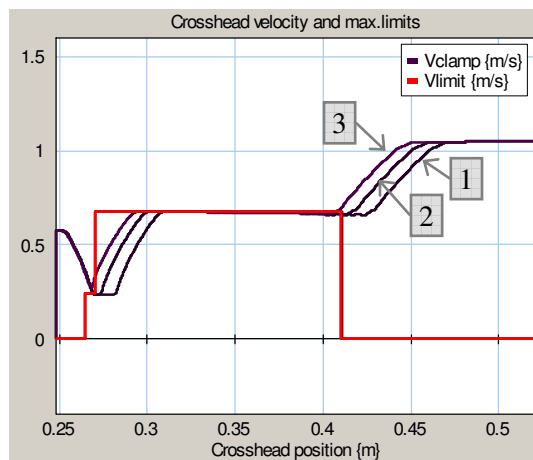


Figure 4-17 Simulation where the point of deceleration is varied. By tuning this point, the average velocity can be raised.

The time duration of the closing movement of the three simulations of figure 4-17 is shown in figure 4-18. If the deceleration starts later, the average velocity will increase and the duration to move the crosshead from 1.59395 m to 0.002 m will be shorter.

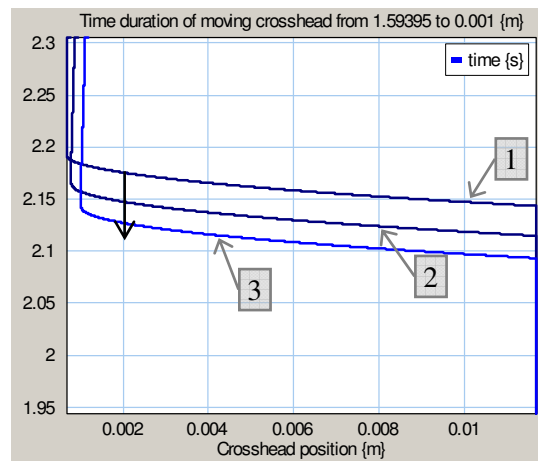


Figure 4-18 Time duration of the three simulations of figure 4-17. The later the deceleration starts, the higher the average velocity and the less time it takes to move to the end position.

The top curve (1) is the situation that the deceleration was started a little too early. The curve at the bottom (3) is the situation that the velocity was too high when the safety positions were reached because the deceleration was started too late. If we take the 2 mm position as a comparison point between the three cycles, the time durations are given in table 4-1.

Run number	Duration
1	2175.599 ms
2	2147.572 ms
3	2127.142 ms

Table 4-1 Time duration of one cycle in ms, for different starting points for deceleration.

The difference between the first two runs that were in time, is about 28 ms. The cycle time can be shortened a little by configuring the controllers for that specific mold, when a mold is used that is lighter than the maximum allowed mold weight.

For safety reasons there should always be little distance between the position where the crosshead reaches the required velocity and the position of the mold protection position and respectively the die-kiss position. When the settings of the feed forward controller differ with the practical situation, the PID-controller has to do more work, and the crosshead velocity will get more delay with respect to the reference velocity (figure 4-14).

The results and comparison with the measurements are given in the next section.

4.8 Simulation results

The improvement that is obtained by using the feed forward and cycle to cycle controller can be seen when the simulations are compared with the measurements. The complete simulation model is used. For the closing movement, the simulations are compared with two measurements, and for opening with one measurement. The measurements have been done without a mold attached to the LSP.

4.8.1 Closing movement

Measurement S0212003.001

In this measurement, the crosshead moves from 1.62245 m to 0.00283 m. The time that was needed for that movement was 2.694 s. The measurement plot is shown in figure 4-19. Similar behavior was reproduced in the simulation shown in figure 4-20.

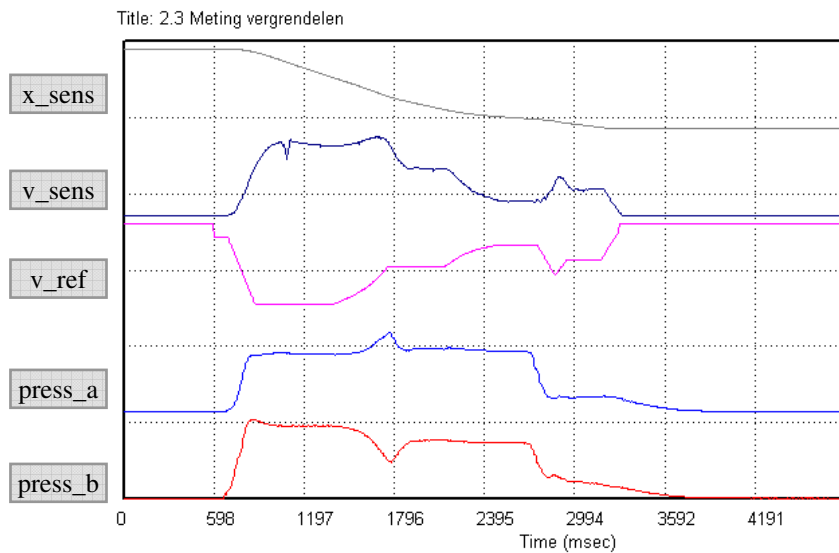


Figure 4-19 Measurement results (S0212003.001) plot from the Visiscope program. The clamp mechanism is closed, and the crosshead is moved from 1.62245 m to 0.002839 m.

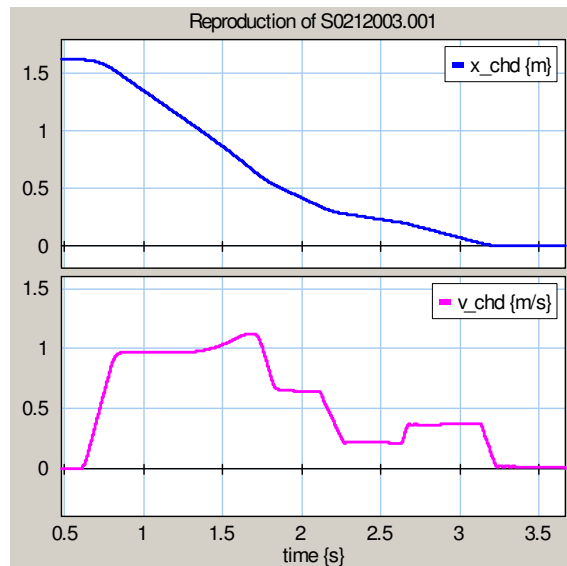


Figure 4-20 Simulation with about the same results. The time duration to move the same distance is 2.58868 s. Equal values for the velocities and acceleration of the reference profile have been used.

The velocity can not be kept stable when the transformation ratio increases (after $t=1.5$ s). The lower velocity is reached very early, before reaching the critical positions. This can be seen from the long straight lines around respectively $t=2.0$ s and $t=2.5$ s.

When the feed forward controller is used, it will be possible to keep the velocity more stable. This can be seen in the simulation results of figure 4-21. The dark line was the previous case, and the light line is the simulation with feed forward. The endpoint is reached about 46.0 ms earlier.

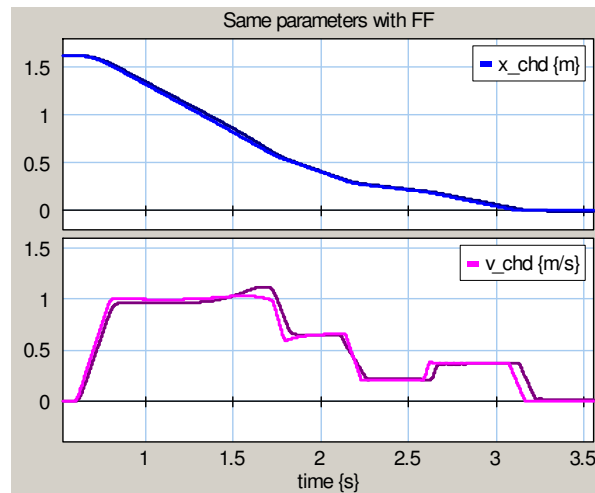


Figure 4-21 Simulation with better results, by using feed forward. The time duration to move the same distance is 2.54274 s. Equal values for the velocities and acceleration of the reference profile have been used.

If the deceleration is started at a later position, the time duration for the closing movement will become lower and the straight line parts will become shorter. In figure 4-21, the lower velocity for the mold protection is reached 120 mm too early, and for die-kiss 70 mm too early. If this is changed to respectively 30 mm and 20 mm, the duration will be 2.33681 s, which is about 252 ms shorter than the simulation of figure 4-20. The result is shown in figure 4-22 and figure 4-23.

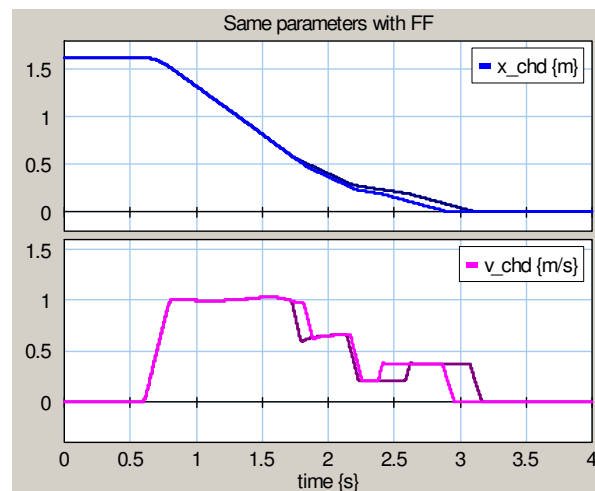


Figure 4-22 Simulation result of when the deceleration starting point is moved. The velocity can be higher for a larger period of the trajectory, so the average velocity will increase and the time duration will be shorter.

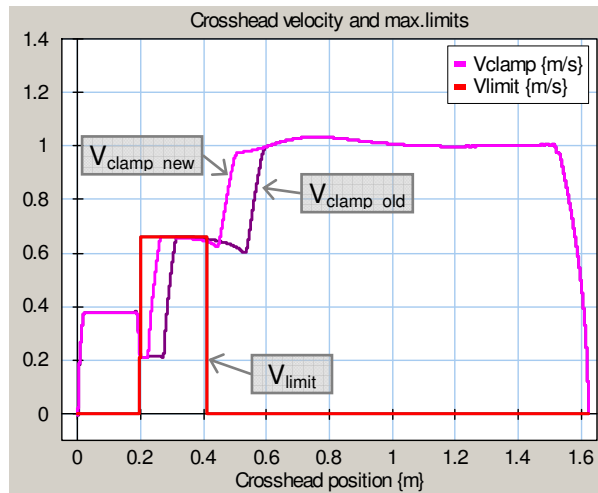


Figure 4-23 Simulation result of when the deceleration starting point is moved. The x-axis is now the position of the crosshead. The plot also shows the maximum allowed velocity. This velocity is still reached in time, but later than in the previous simulation. The average velocity will increase by this measure.

The deceleration point could be shifted more, but since the safety of the mechanism needs to be guaranteed the point is not shifted more. The results are given in table 4-2.

Situation	Duration	Profit
Figure 4-20	2.58868 s	-
Figure 4-21	2.54274 s	45.9 ms / 1.7 %
Figure 4-22	2.33681 s	252 ms / 9.7 %

Table 4-2 Time duration and profit by shifting the point of deceleration compared with measurement S0212003.001.

By shifting the point of deceleration, a large profit can be gained. With this measurement no mold was attached to the LSP. Therefore, the profit when a mold is used can be different.

Measurement S0212010.001

In this measurement the crosshead was moved from 1.7649 m to 0.00301 m, which took 2.88 s. The measurement plot is shown in figure 4-25. The same behavior was replicated in the simulation, as shown in figure 4-24 below.

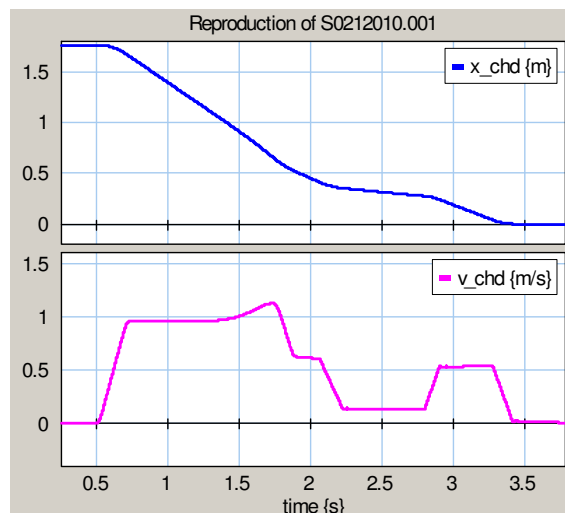


Figure 4-24 Simulation with about the same results. The time duration to move the same distance is 2.883558 s. Equal values for the velocities and acceleration of the reference profile have been used.

When feed forward is used, the behavior is better. The velocity is better under control so the reference is followed nicely, but the average velocity will become lower in this case.

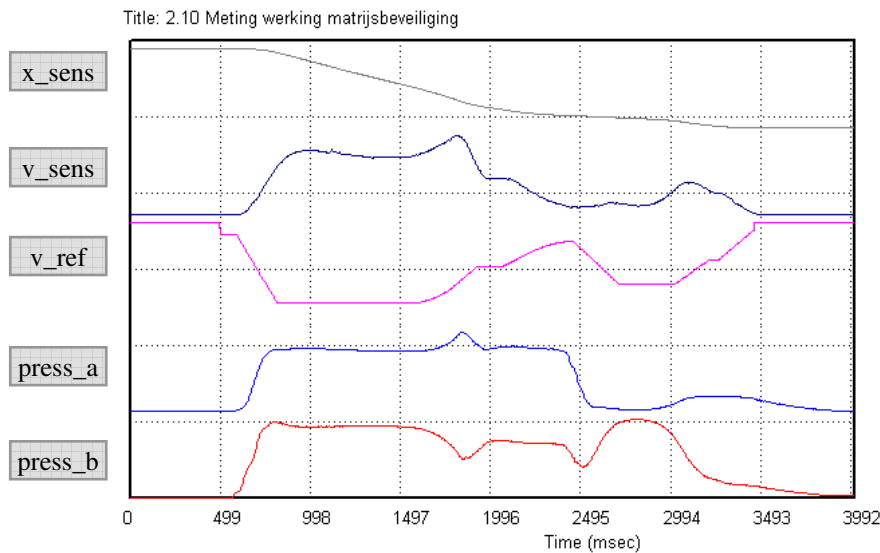


Figure 4-25 Measurement results (S0212010.001) plot from the Viscope program. The clamp mechanism is closed, and the crosshead is moved from 1.764913 m to 0.003012 m.

The lower velocities are reached respectively 130 mm and 70 mm too early. Time profit can be obtained when the point of deceleration is shifted to a later point. This simulation result, compared with the old simulation results is shown in figure 4-26. The same end point is reached more early.

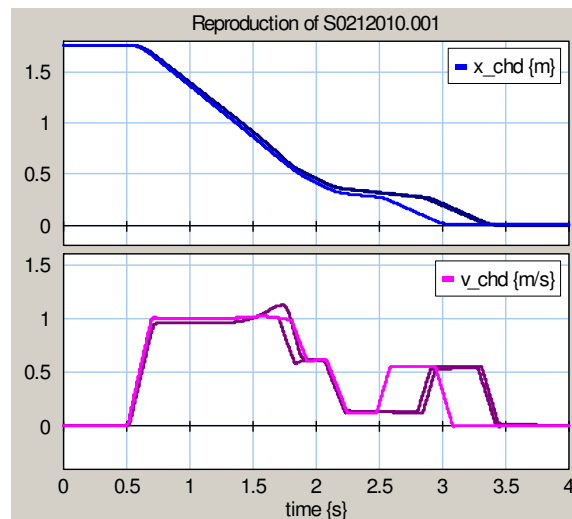


Figure 4-26 Simulation result of when the deceleration starting points are moved. The velocity is higher for a larger period of the trajectory, so the average velocity will increase and the time duration will become 2.5686 s.

The duration is now 2.568641 s. The lower velocities are reached 30 mm and 20 mm too early, which is still safe. This can be better seen when the position is used on the x -axis instead of time, shown in figure 4-27.

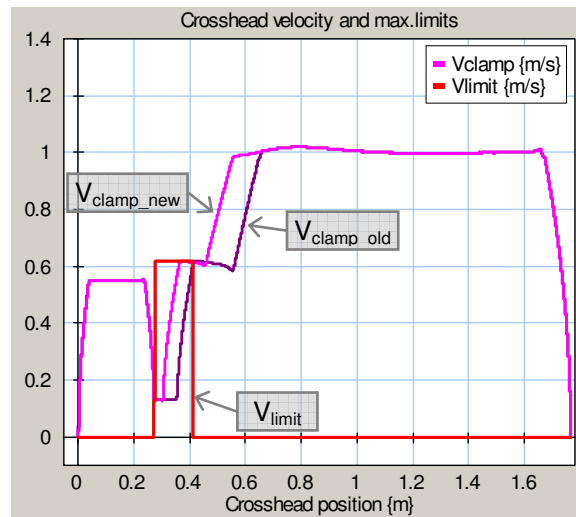


Figure 4-27 Simulation result of when the deceleration starting point is moved. The dark line is the previous result and the light line is the shifted reference. The position of the crosshead is used for the x-axis. The plot also shows the maximum allowed velocity. This velocity is still reached in time, but later than in the previous simulation.

Again, the deceleration point could be shifted a little more, but since the safety of the mechanism needs to be guaranteed the point is not shifted more. The results are given in table 4-3.

Situation	Duration	Profit
Figure 4-24	2.883558 s	-
Figure 4-26	2.568641 s	311 ms / 10.79 %

Table 4-3 Time duration and profit by shifting the point of deceleration, compared with measurement S0212010.001.

The duration of the closing movement can be made lower by moving the point of deceleration to a later position. With this measurement no mold was attached to the LSP. Therefore, the profit when a mold is used can be smaller, or even larger.

4.8.2 Opening movement

Measurement S0212005.001

To check the improvement of the controllers and the effect of moving the point of deceleration, the opening movement also needs to be compared with a measurement. In the measurement shown in figure 4-28, the crosshead moves from 0.00512 m (closed) to 1.61178 m (opened), which takes 2.43 s.

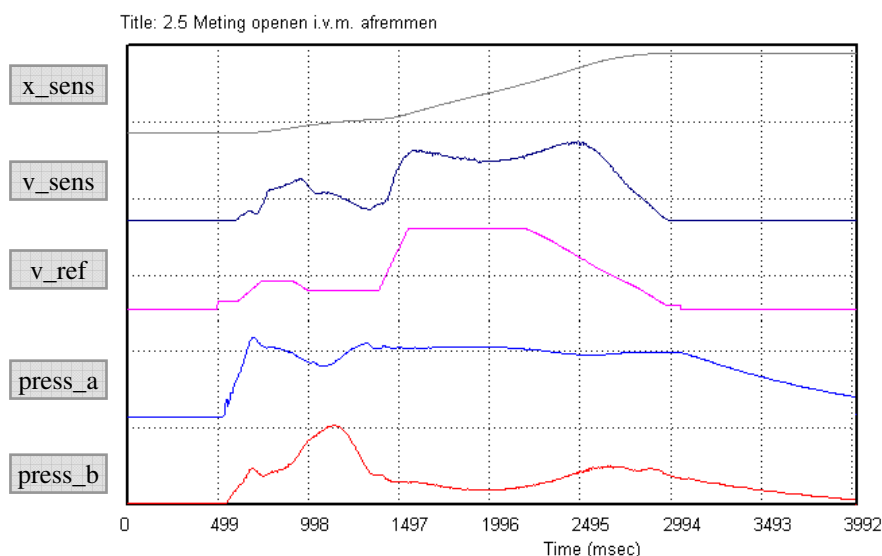


Figure 4-28 Measurement results (S0212005.001) plot from the Visiscope program. The clamp mechanism is opened, and the crosshead is moved from 0.005 m to 1.611786 m.

A simulation with identical velocities and accelerations, the same moved distance and about the same duration is shown in figure 4-29. The duration is 2.365 s, which is a little less than the measurement.

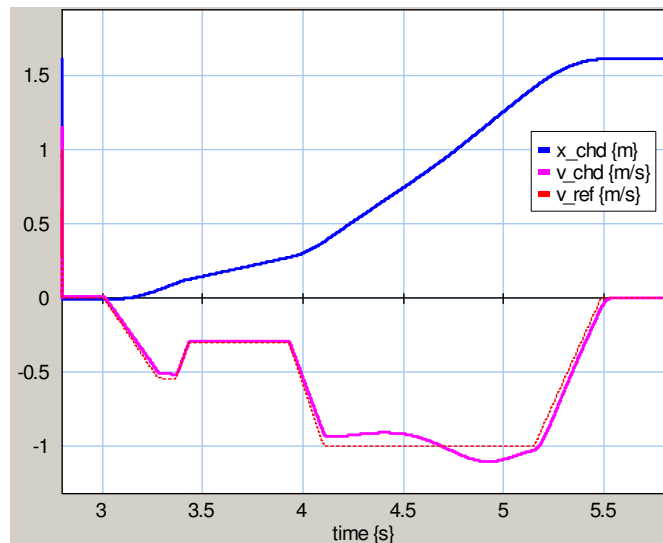


Figure 4-29 Simulation result, reasonably identical with the measurement. The time duration is 2.365 s.

The velocity of the crosshead will change with respect to the reference due to the transformation ratio of the clamp mechanism. When feed forward is used, this transformation ratio is taken into account by controlling the hydraulics. Figure 4-30 shows the same simulation, but here feed back is used. The velocity will follow the reference nicely.

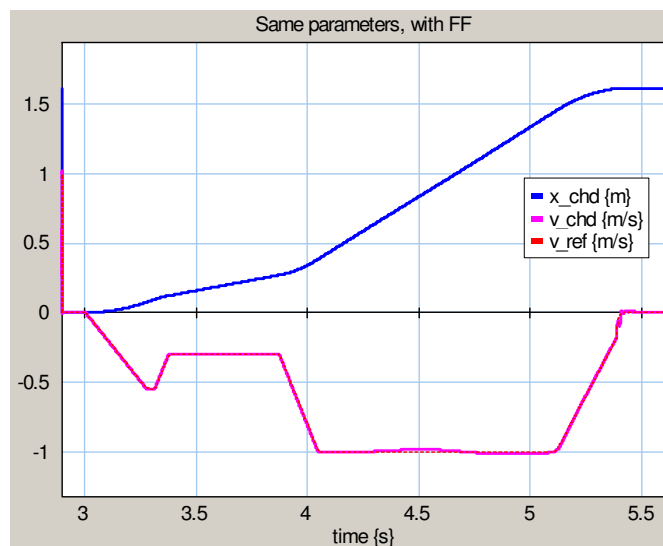


Figure 4-30 Simulation result when feed forward is used. The time duration is 2.3175 s. The crosshead velocity is plotted on top of the reference velocity, since the crosshead velocity is almost equal to the reference velocity.

There is a large part of the movement where the velocity is low, around $t=3.5$ s. The lower velocity is reached 145 mm too early, which can be seen in figure 4-32 on page 47. If the deceleration is started later, the higher velocity can be held over a longer period and the average velocity will increase. In the simulation result shown in figure 4-31, the lower velocity is still reached 45 mm too early, but this is done for extra safety. When the opening is started at 5.0 s, the end position is reached at $t=5.1669$ s instead of at $t=5.3175$ s. Both simulations are shown again in figure 4-32 with the crosshead position on the x -axis, to indicate the difference when shifting the starting point of deceleration.

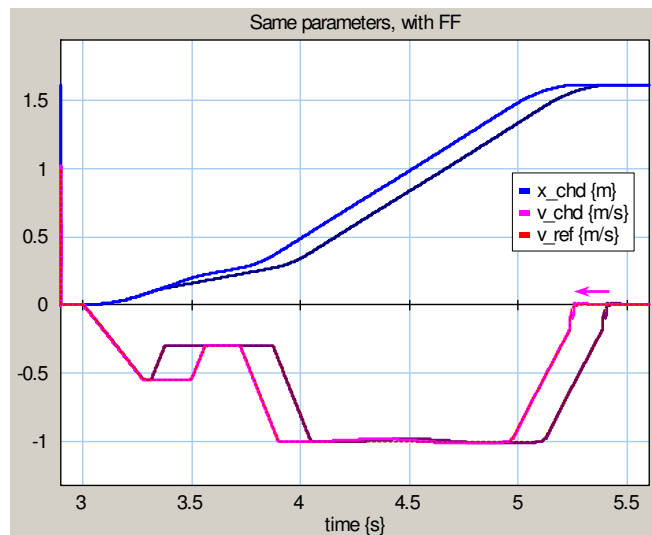


Figure 4-31 Simulation result when feed forward is used and the deceleration point is moved to a later, but still safe, point. The time duration now becomes 2.1669 s. The crosshead velocity is plotted on top of the reference velocity, since the crosshead velocity is almost equal to the reference velocity.

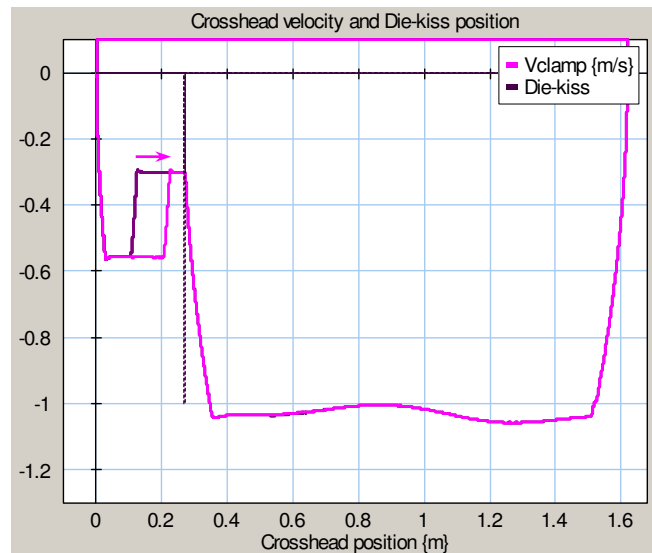


Figure 4-32 The same simulations of figure 4-31 now shown with the crosshead position on the x-axis.

The time reduction is 198 ms, but this can probably more. The maximum velocity when opening can be increased if we know that the reference velocity is followed nicely. Therefore, extra time profit can be made.

The results and improvements of using the feed forward controller and moving the point of deceleration are given in table 4-4.

Situation	Duration	Profit
Figure 4-29	2.365 s	-
Figure 4-30	2.3175 s	47 ms / 2 %
Figure 4-31	2.1669 s	198 ms / 8.3 %

Table 4-4 Time duration and profit for the opening movement by shifting the point of deceleration, compared with measurement S0212005.001.

Time reduction is also possible for the opening movement, although this is less than for the closing movement. When the maximum velocity for the opening movement is changed to a higher value, more time can be won.

5 Conclusions and recommendations

5.1 Conclusions

During this project a simulation model is created, to gain knowledge of the operation and the dynamics of the clamping mechanism of an injection molding machine. The clamp mechanism is modelled by using multi-body dynamics with bond-graphs. Also a simplified model of the hydraulic system, which actuates the clamp mechanism, was modelled. By validating and fitting the complete model with measurement data, the correctness of the model was demonstrated.

After implementing a simple feed forward controller based on a reduced model, the performance of the servo behavior is improved. To optimize the reference profile for a specific mold weight, the cycle-to-cycle method is implemented in the reference velocity profile to tune the starting point of the deceleration parts. The average velocity will increase and the time duration of the trajectory will decrease.

5.1.1 Only small time reduction possible

The realized control configuration as used with SPM is tuned robustly, to work in all cases, for all mold weights. Due to the current hardware configuration, the maximum velocity is restricted by the limitations of the hydraulic circuit. For a heavy weight mold, there is only a small part of the trajectory where potential time reduction is possible (section 2.2 and 4.7). But when a lighter mold is used, a higher maximum velocity and thus average velocity should be achievable. The potential time reduction depends on the weight of the mold.

When the position where the deceleration is started can be moved to a later point, a higher velocity can be held over a larger part of the trajectory. The average velocity will increase and running the trajectory will take less time. The best point to start decelerating can be obtained by using the cycle-to-cycle method. Different positions to start decelerating are tried sequentially, and then compared to find a fast but safe position to start decelerating. This optimization method can be used for all mold weights, to find a good starting point for decelerating.

The time duration of the closing movement can be approximately brought down by 10% and the opening movement by 8%, when the feed forward controller is implemented and the deceleration positions of the reference profile are tuned correctly. This can be concluded from the simulation experiments, see section 4.8.

5.1.2 Servo behavior better by adding feed forward

The feedback controller is dependent on the feedback signal. The servo behavior depends on the conditions of the measured signal and the performance of the differentiator. The conditioning of the measured signal will introduce delay, which influences the performance of the controller.

To improve the servo behavior, feed forward control is added parallel to the PID-controller. The velocity of the crosshead can be kept under control better, since the feed forward controller depends on the reference signals and not on the measured signal. The clamp mechanism transfer is taken into account by the calculation in the feed forward controller. Therefore, the proportional valve position can be adjusted in time according to the dynamics and the reference velocity is followed nicely. When only feedback control is used, the velocity of the crosshead will start increasing and gets out of control, due to the dynamic behavior of the clamp mechanism. Because the velocity of the crosshead follows the reference velocity nicely, the reference velocity can now be tuned for a specific mold weight.

5.2 Recommendations

5.2.1 Implementing and testing

Implement the feed forward controller

To check if the improvements shown by the simulation experiments are also feasible on the real clamp mechanism, the feed forward controller needs to be implemented and tested. By comparing the output of the feed forward controller with the PID-controller, the correctness of the parameters can be seen. When the feed forward parameters are more accurate, the error with respect to the reference becomes smaller, and the PID-controller will have to do less work. Since a reduced model is used in the calculations of the feed forward controller, the need of a PID-controller will remain.

Test for different mold weights

The model could only be validated for an empty moving clamp plate (LSP), with no extra weight attached, because there are currently only measurements of an empty LSP. When more measurements are available, the model can be validated for more situations. The simulations are especially important to test the behavior when heavy weight molds are used, but the conclusions are less reliable when the model is only validated for an empty LSP with no extra weight. More measurements for a variety of weights attached to the LSP need to be done, so the model can be validated and become more reliable for different mold weights.

Testing of cycle-to-cycle control

The reference velocity profile can be optimized when a mold with a weight lower than the maximum allowed mold weight is used. After the cycle-to-cycle control scheme optimization is implemented, the result can be verified. Due to the safety demands, it is really important that the velocity is not larger than the limited velocity. When the velocity at die-kiss is too high, the mold will get damaged.

5.2.2 Improve model and software

Differentiation by means of State Variable Filter

For velocity feedback control, the derivative of the measured position is needed. A recommended alternative for deriving the velocity from the measured position is by means of the State Variable Filter (SVF). The SVF is less sensitive to noise, easy to implement and will result in a smaller delay between the real velocity and the estimated velocity for certain frequencies. The theory of the SVF is included in Appendix F.

Analyze the hydraulic circuit

The restricting factor for larger time reduction is the hydraulic circuit. For large mold weights, the maximum acceleration and velocity are currently used. To make the clamp mechanism move faster, the hydraulic circuit needs to be analyzed thoroughly. If a more detailed model of the hydraulic circuit including the differential circuit is made, the effect of the behavior can be analyzed and optimized.

The differential circuit probably has a large impact on the behavior of the acceleration in the first part of the closing motion. This differential circuit is used to save oil when the clamp mechanism is closing, at the price of halving the available force delivered by the hydraulic cylinder. The advantages and disadvantages of this solution to the required large oil flow should be analyzed and considered.

5.2.3 Analyze clamp mechanism transfer

The knee-lever structure is a common way to make a clamp mechanism. The lengths of all the levers are based on standard formulae. Because of the transformation ratio of this mechanism, it is favorable to accelerate and decelerate when the ratio is low. When the ratio increases, the required force will increase also, because the weight of the LSP seen at the cylinder is the transformation ratio squared times the weight of the mass of the LSP. The ratio might effect the possible time duration, since the force delivered by the cylinder determines the (average) velocity of the mechanism. If the best result is wanted, the transformation ratio should be studied to see what the effect is of changing the different parameters. The force that is required for clamping should stay the same.

Appendix A Specifications of the clamp mechanism

This chapter contains a brief enumeration of specific important numbers and issues. The construction of the clamp mechanism is shown in Figure A-1-a and -b.

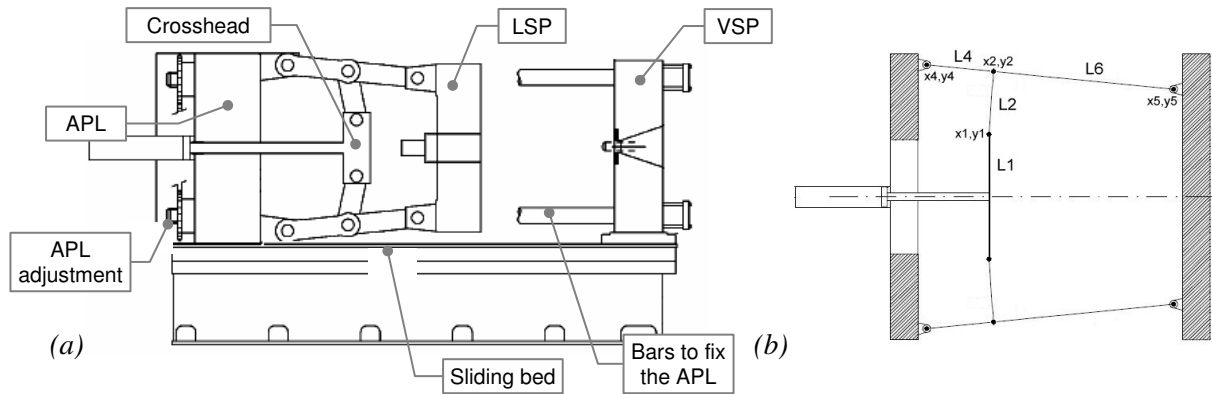


Figure A-1 Clamping mechanism, part of the injection molding machine.

The clearance of the APL adjustment mechanism is 2 mm.

When the clamping force is maximal (12000 kN):

- The bars L_4 and L_6 of the knee-lever mechanism become 1.5 mm shorter
- The bars that keep the APL in place become 1.5 mm longer
- The bearings at the APL that keep bar L_4 will be pressed about 5 mm apart in vertical direction.

These are assumptions based on practice.

The maximum total mold weight is 22500 kg. The part that is mounted to the LSP can be at most $\frac{2}{3}$ of this weight, which is 15000 kg.

The sample frequency of the I/O is 1 kHz and the I/O delay is 1 ms.

The ADC and the DAC are 12 bit-converters.

The resolution of the position sensor is 40 μm .

Appendix B Mathematic models

B.1 Position definitions

For accurate positioning of the moving plate (LSP), the position needs to be known. Due to limitations in the construction, it is not possible to measure the position of the LSP. Therefore, the position of the crosshead is measured and by means of a look-up table, the position of the LSP is determined.

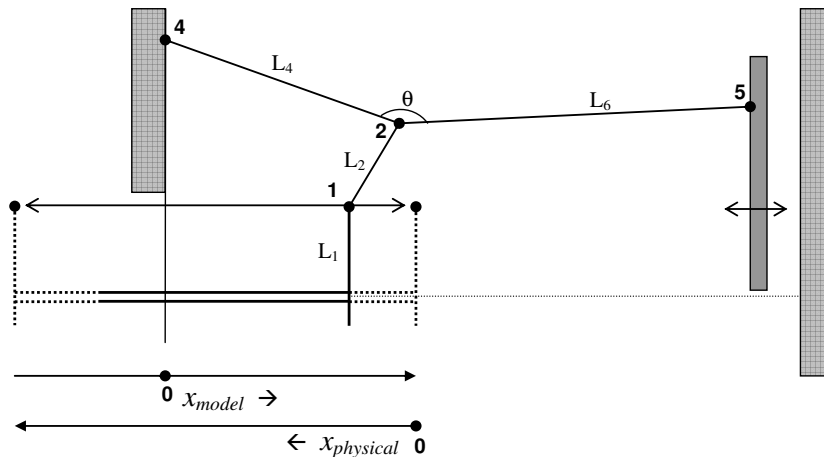


Figure B-1 Top half of clamp mechanism to simplify modelling. Two ways of defining the crosshead position are shown: x_{model} and $x_{physical}$.

The physical distance between the LSP and the VSP is measured. The position of the crosshead ($x_{physical}$) is defined to be zero when the angle between the bars L_4 and L_6 is just below 180 degrees. If the angle θ would get beyond 180 degrees, it is difficult to move the LSP back again.

Using this position definition, the mathematics of the model done with kinematic relations is a lot more complex. To cope with this, a different way of defining the position is used. The orientation of the x -axis is opposite and an offset is added, as shown in equation B.1.

$$x_{model} = x_{offset} - x_{physical} \quad (B.1)$$

The offset value x_{offset} is the physical distance between the backside of the mechanism (APL) and the position of the fixed plate (VSP).

The initial values for the mechanism, like angles and positions, are calculated with the mathematical formulae in Maple based on the *model* position of equation B.1. Both ways of describing the position are illustrated in Figure B-1. The current software uses the first way of describing the position with the model position. Therefore equation B.1 is used in the software for calculating the physical position when needed.

In the following sections, the position will be described in the mathematical way (x_{model}) because it makes it easier to compare the results with the mathematical results, although it is not necessary when bond graphs are used.

B.2 Mathematical model

The mathematical model is an equation model with the kinematic relations, and can be used in MathCAD or in Maple. From the crosshead to the LSP all the positions of the connection points are

calculated. The position of the LSP is given as a function that depends on the constant bar lengths and on the varying position of the crosshead (x_{model}). To be able to calculate point '2' an extra fictitious line is added. Together with the two angles α and β , as shown in Figure B-2, the position of point '5' can be calculated.

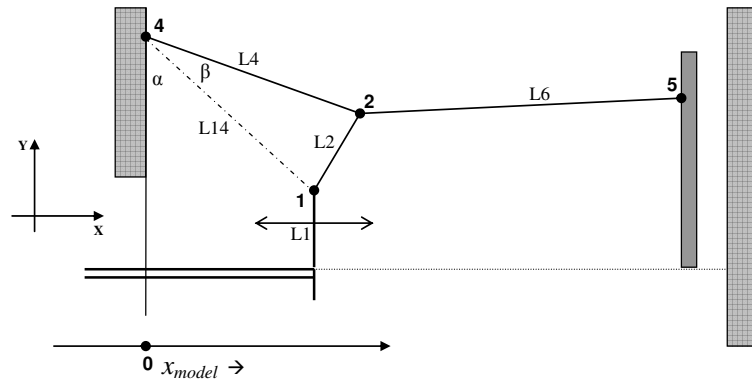


Figure B-2 Top half of clamp mechanism to simplify modelling

First a fictitious line L_{14} is adopted so the two angles α and β that are created can be calculated, and with these angles the x - and y -coordinates of point 2 can be found. From this together with the bar lengths the x -position of point 5 (LSP) can be calculated. The complete formulae are shown in equations B.2 to B.5.

$$L_{14}(X_1) = \sqrt{X_1^2 + (Y_4 - L_1)^2} \quad (B.2)$$

$$\alpha(X_1) = \arctan\left(\frac{X_1}{Y_4 - L_1}\right) \quad (B.3)$$

$$\beta(X_1) = \arccos\left(\frac{L_4^2 + L_{14}(X_1)^2 - L_2^2}{2 \cdot L_4 \cdot L_{14}(X_1)}\right)$$

$$X_2(X_1) = L_4 \cdot \sin(\alpha(X_1) + \beta(X_1)) \quad (B.4)$$

$$Y_2(X_1) = Y_4 - L_4 \cdot \cos(\alpha(X_1) + \beta(X_1))$$

$$X_5(X_1) = X_2(X_1) + L_6 \cdot \cos\left(\arcsin\left(\frac{Y_2(X_1) - Y_5}{L_6}\right)\right) \quad (B.5)$$

An example of how the movement of the LSP (X_5) looks when the crosshead moves linearly, is shown in Figure B-3. This relation is nonlinear. In the last part, the crosshead still moves while the LSP is almost not moving anymore.

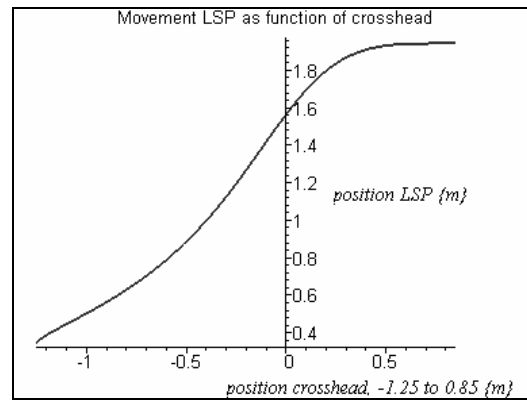


Figure B-3 Position of the LSP $\{y\}$ as a function of the position of the crosshead position $\{x\}$.

B.3 Elaboration of mathematical model

Bond graphs can also be used to model the kinematic relations from the previous section. A bond graph model uses velocities and forces. When the position-dependent relations from the mathematical model are differentiated, the result is a velocity-based kinematic, mathematical model.

The kinematic structure of the model does not contain any dynamics, like the bar weights or stiffnesses. Eventually a mass element for the crosshead and the LSP can be added to the model, but the bar masses need not be included.

Identical steps compared to the mathematical model are made. The length of fictitious line L_{14} is calculated first. The angular velocities of angles α and β are calculated from the velocity of the crosshead. From these angular velocities, the length of fictitious line L_{14} and the velocity of the crosshead, the velocities of point 2 in x - and y -direction are calculated. From these velocities the velocity of the LSP in x -direction is calculated. The model containing the calculations is shown in Figure B-4.

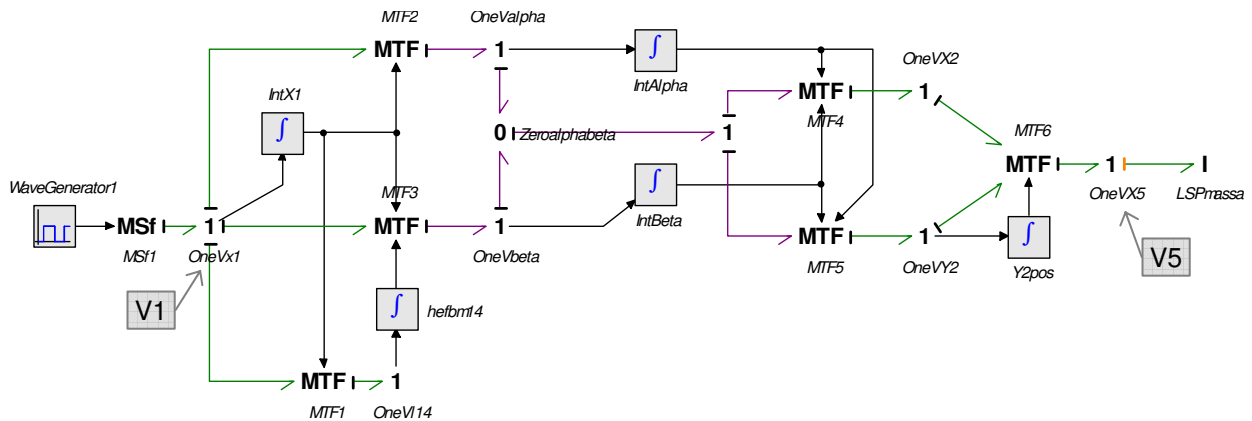


Figure B-4 Bond graph model of the clamp mechanism. The velocity relations can be represented in a bond graph. The velocity of point 2 is calculated from the velocity of point 1 (left part) and the velocity of point 5 from point 2 (right part).

The simulation results are equal to the position-based model, but the slight difference is due to some numerical errors caused by integration.

Appendix C Modelling of 2D rigid bodies

A rigid body can be modeled with a 2D rigid body bond graph model. These bodies are interconnected by joints and hinges. Using these standard models, the complete clamp mechanism can be constructed. In this appendix, the background of this modelling method is described. The theory of multibody dynamics with bond graphs can be found in (Bos, 1986) and the theory of bond graph modelling is described in (Breedveld and Amerongen, 1996).

C.1 A single moving body

The construction of a bond graph model for a single body that can move in space freely is described in this section. A list of bond graph elements is given in Table E-1 in Appendix E. A two-dimensional model is derived by simplifying the three-dimensional model. The two-dimensional model is adequate for modelling the clamping mechanism, because the motions can be described in two dimensions.

Each body has a body-fixed frame. The frame can be placed in each point on the body, but the best choices are often to place the frame in a hinge point or in the centre of mass, because calculations will get more simple. When the body moves in rotational or translational direction, the body-fixed frame moves fixed with the body. The body-fixed frame can be described with respect to the inertial frame, which is a non-moving frame. For example, earth or some other reference point. This is illustrated in Figure C-1.

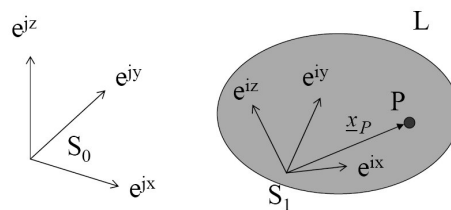


Figure C-1 Body L with respect to both the body-fixed frame (base S_1) and the inertial frame (base S_0). Point P is a point on the body.

The velocity of each point on the body can be described with respect to the body fixed frame, but also with respect to the inertial frame. If the point on a rotating body is fixed on the body, the location of the point with respect to the body-fixed frame will always be the same, while the location of the point with respect to the inertial frame does change. To get the velocity of point P with respect to the inertial frame, equation C.6 needs to be used.

$$\vec{v}_P^{S_1, S_0} = \vec{v}_{S_1}^{S_1, S_0} + \vec{v}_P^{S_1, S_1} + \vec{\omega}^{S_1, S_0} \otimes \vec{x}_P^{S_1, S_0} \quad (C.6)$$

The velocity with respect to the inertial frame is the sum of the velocity of the body-fixed frame (base S_1) with respect to the inertial frame (base S_0), the velocity of the point P with respect to the body-fixed frame (S_1) and the results of the cross product. This cross product is taken between the rotation of the body-fixed frame S_1 with respect to the inertial frame S_0 , and the position of point P with respect to the body-fixed frame S_1 . The position is a vector that contains the distances from the point to the body-fixed frame, and the velocity is a vector, containing the velocities in x-, y-, and z-direction.

The first superscript index S_i is an indication that the values are described in coordinates of S_i . The second superscript index S_j indicates with respect to which base the coordinates are described. Equation C.6 gives the velocity of point P with respect to base S_0 , described in coordinates of base S_1 .

When the cross product is worked out, the result is shown in equation C.7.

$$\bar{\omega}^{S_1, S_0} \otimes \bar{x}_P^{S_1, S_0} = \begin{bmatrix} \omega_x \\ \omega_y \\ \omega_z \end{bmatrix} \otimes \begin{bmatrix} x_P \\ y_P \\ z_P \end{bmatrix} = \begin{bmatrix} \omega_y z_P - \omega_z y_P \\ \omega_z x_P - \omega_x z_P \\ \omega_x z_P - \omega_y x_P \end{bmatrix} \quad (C.7)$$

An alternative way of describing the cross product is by using the tilde operator. The cross product then becomes a matrix-vector multiplication. This is shown in equation C.8, which yield the same result.

$$\bar{\omega}^{S_1, S_0} \otimes \bar{x}_P^{S_1, S_0} = \tilde{x}_P \bar{\omega}^{S_1, S_0} = \begin{bmatrix} 0 & z_P & -y_P \\ -z_P & 0 & x_P \\ y_P & -x_P & 0 \end{bmatrix} \cdot \begin{bmatrix} \omega_x \\ \omega_y \\ \omega_z \end{bmatrix} \quad (C.8)$$

If the body is modelled in only two dimensions, for example in the x,y -plane, then z_P , ω_x and ω_y will be zero. Equation C.6 can than be simplified to equation C.9.

$$\begin{bmatrix} v_x \\ v_y \end{bmatrix}_P^{S_1, S_0} = \begin{bmatrix} v_x \\ v_y \end{bmatrix}_{S_1}^{S_1, S_0} + \begin{bmatrix} v_x \\ v_y \end{bmatrix}_P^{S_1, S_1} + \begin{bmatrix} -y_P \\ x_P \end{bmatrix}_P^{S_1, S_0} \omega_z^{S_1, S_0} \quad (C.9)$$

These equations can be implemented in bond graphs, as shown in Figure C-3. A one-junction represents the velocity of a point. There the sum of all forces equals zero. In a zero-junction, it is the other way around: it represents the force in a point and the sum of all velocities is zero. The MTF is a modulated transformer. The multiplication factor of the transformer depends on the input signal. Here the MTF is used for taking the cross product, by means of the tilde operator. The signal is a constant matrix, as shown in equation C.8.

To connect the body, each body needs inputs and outputs to implement the rotational and translational motions. This is shown in Figure C-2.

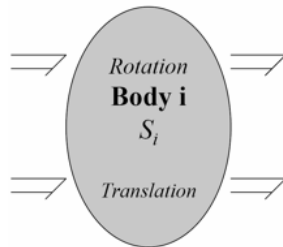


Figure C-2 Rigid body with separate inputs and outputs for rotational and translational motion. The body-fixed frame is put in point P instead at the center of mass (c.o.m.).

The bond graph model of Figure C-2 is shown in Figure C-3, where there are bond graphs pointing towards and from the middle. The velocity of the body-fixed frame is indicated by V_{I1} , and the velocities of points I (origin) and P are indicated by V_I and V_P .

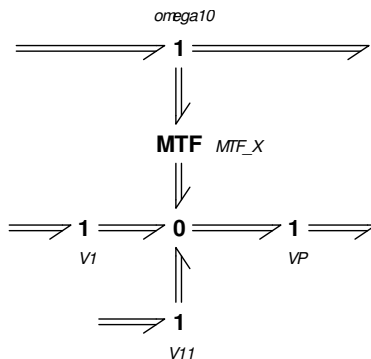


Figure C-3 Bond graph that describes the velocity of a point P with respect to the inertial frame, base 0, in coordinates of base 1.

The body-fixed frame is often put in the center of mass (c.o.m.). If this is done, the forces (translation) and torques (rotation) will be decoupled. A 2-dimensional kinematic junction structure without dynamic elements is shown in Figure C-4. The body is modelled with single bonds.

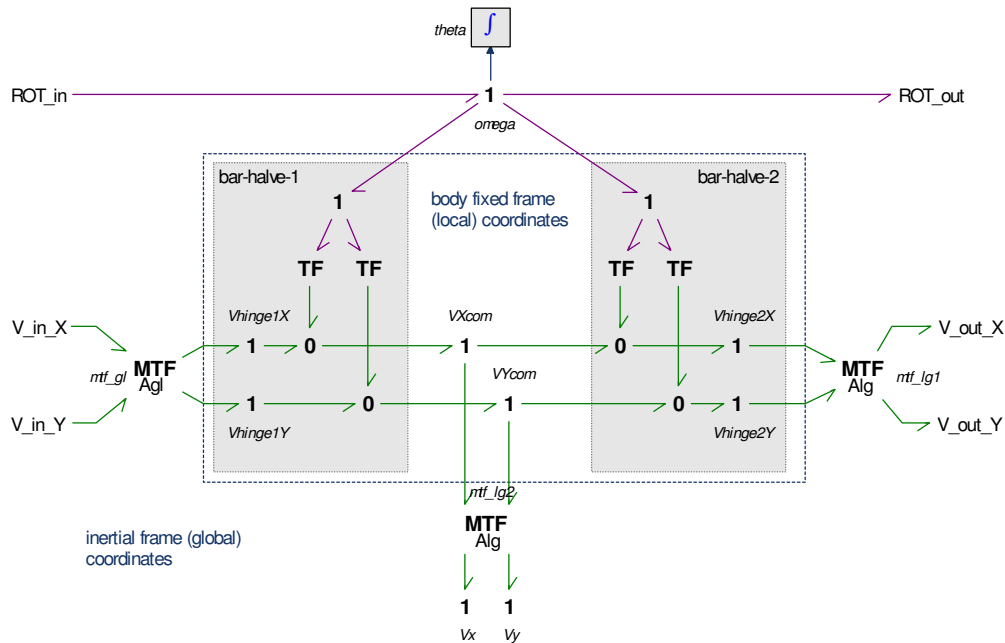


Figure C-4 Kinematic junction structure of a bar. Each bar can be described with this structure. The bar exists of two halve bars mutually connected in the center of mass.

The model of a two-dimensional body is made out of multiple different elements. To describe the interaction of the model with the other bars, the velocity of the hinge points must be known with respect to the inertial frame. This way all the bodies can be connected to each other, based on coordinates of the inertial frame. By means of a coordinate transformation, each point in the body-fixed frame can be translated to a point in the inertial frame. The required coordinate transformation can be done by multiplying the coordinates of a point with a rotation matrix. The angle, θ , of the body-fixed frame with respect to the inertial frame is the only parameter that is needed. The coordinate transformations are given in equation C.10.

$$A^{0,1} = \begin{bmatrix} \cos \theta & -\sin \theta \\ \sin \theta & \cos \theta \end{bmatrix} \quad A^{1,0} = \begin{bmatrix} \cos \theta & \sin \theta \\ -\sin \theta & \cos \theta \end{bmatrix} \quad (C.10)$$

By multiplying with matrix $A^{1,0}$ coordinates are transformed from the inertial frame to the body-fixed frame. Matrix $A^{0,1}$ does the opposite. The variable θ is the angle of the body with respect to the inertial frame.

The transformer (TF) elements are multiplications used for the cross product. The multiplication factor in each TF element is the distance from the hinge point to the center of mass. If one of the hinge points is chosen exactly on the x- or y-axis, one of the distances equals zero and equation C.7 can be simplified. If the hinge points are located on the y-axis, the transformer of the translation in y-direction can be omitted, since the multiplication factor (x) is zero.

When the dynamic elements, like compliances, inertias and masses, are added to the model, the body becomes more like a real physical object. A physical model is shown in Figure C-5. The body (rectangle) exists of two halves (ellipses); each body half contains compliance in x-direction and in y-direction. By placing the compliance in each bar-half, the compliance is equally divided over the bar. The center of mass is located in the middle.

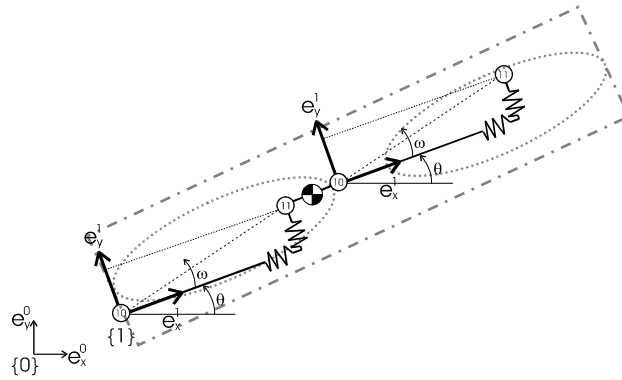


Figure C-5 IPM of a rigid bar with compliance in both x- and y-direction. The mass is added in the center of mass.

The bond graph model with the dynamic elements is shown in Figure C-6. The model consists of coordinate transformations, two bar-halves with compliance, the mass in translational directions and a rotational inertia. The masses and the inertia are connected to the center of mass.

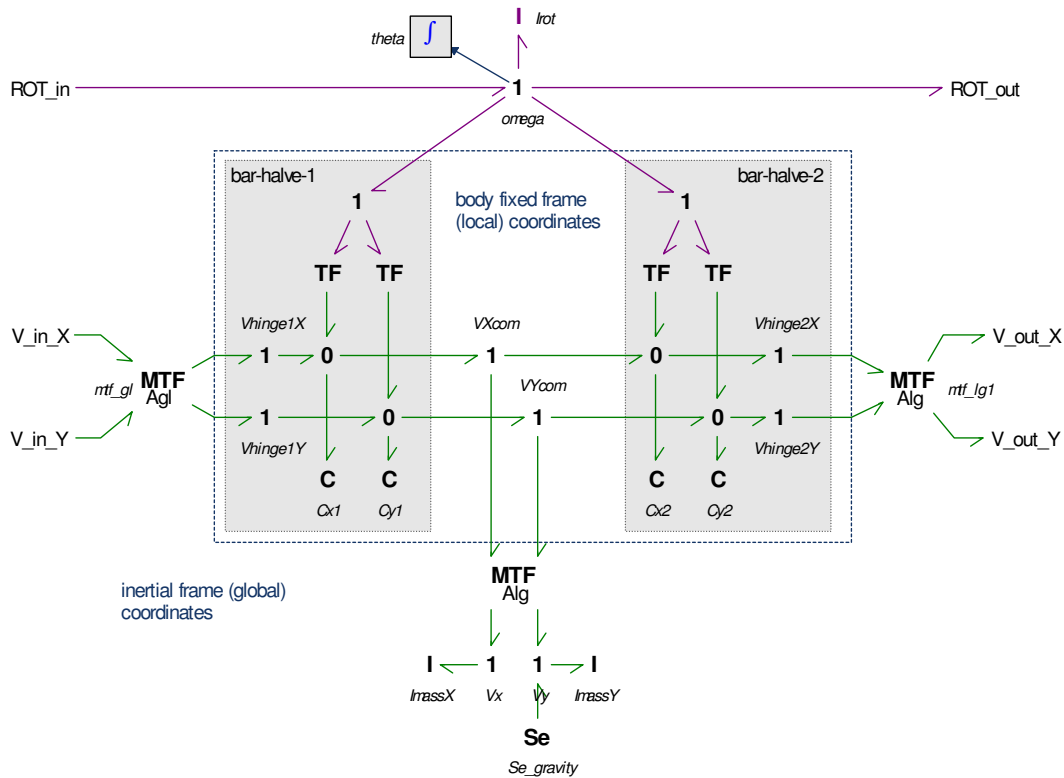


Figure C-6 Junction structure with dynamics added. Gravity works on the center of mass of the bar, in y-direction. Angle θ is used for calculation of the coordinate transformation.

The compliance also contains damping, which is not shown in Figure C-6. If no damping is added to the simulation model, the vibrations will not be damped. This is not possible in a physical system.

The model can now be interconnected to make a chain of bodies. This will be described in the next section.

C.2 Connecting multiple bodies

Bodies can be interconnected with other bodies, or with fixed objects. Possible connections are hinge and joints connections, actuated or non-actuated.

A *joint* is a connection between two or more bodies. Depending on the constraints, the bodies can rotate with respect to each other. A body can be connected to a fixed object with a *hinge* connection. The movement of the body is constraint, which means that the velocities in *x*- and *y*-direction are equal to the velocities of the fixed object.

In a joint, the bodies can rotate with respect to each other. The torque between the bodies is equal to zero, which leaves one degree of freedom. When there is a rotational actuator between the bodies, or when there is friction, it can be added to the rotational domain of the joint. The velocities in *x*- and *y*-direction are equal, which can be seen from the 1-junctions for the translational domain. The bond graphs of a joint and hinge connection are shown in Figure C-7.

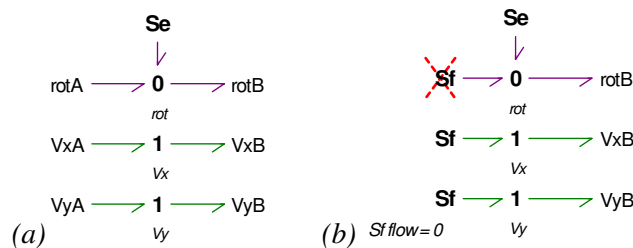


Figure C-7 Bond graphs of (a) joint connection and (b) hinge connection. The torque source (Se) has a zero value, so that the A and B site can rotate freely. The flow sources (Sf) all have zero values, to keep the position fixed. The flow source on top can be removed because it does not contribute to the working.

The joint of Figure C-7-a can be used to connect to bodies together. When a body is connected to earth, and is able to rotate, the hinge connection of Figure C-7-b can be used. Instead of connecting a body to one of the connections (A), the fixed object can be modelled by connection an effort or flow source to the connection point (A). A flow source constraints the velocity, and an effort source constraints the force or torque.

There are actuated and a non-actuated hinge points. For a non-actuated connection, the effort source has a value of zero, but for an actuated hinge point, the effort source can be given a value. If needed, also friction can be added to the hinge point model.

A combination of bodies, hinges and a joint can be made. This example model is shown in Figure C-8.

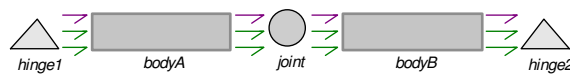


Figure C-8 Example model of 2 bodies, connected to a hinge and to a joint.

More about modelling of rigid bodies can be found in e.g. (van der Zwaag, 1998) and (Bos, 1986).

Appendix D Clamp mechanism transfer

To be able to get a high clamping force with a smaller force source, the mechanism is designed such that the transfer is optimal for building up a high clamping force. The relation between the velocity of the crosshead and the LSP is position-dependent, and is shown in Figure D-1.

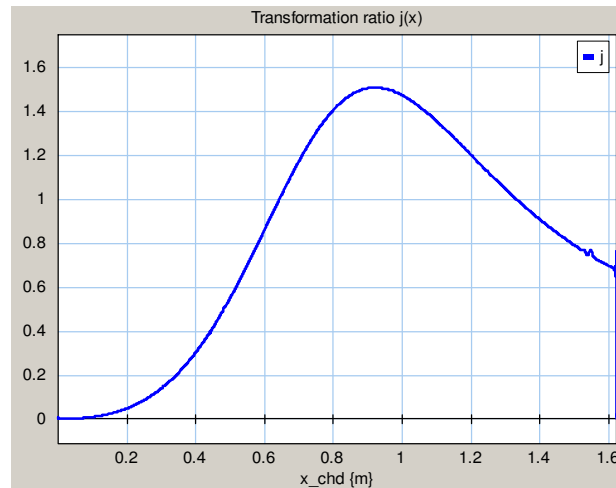


Figure D-1 Position-dependent transformation ratio j

The transformation ratio of the clamp mechanism is given by equation D.1. If the crosshead moves from opened to closed (from right to left in Figure D-1) with a velocity of 1.0 m/s, the velocity of the LSP will be equal to the transformation ratio j .

$$j(x_{crosshead}) = \frac{v_{lsp}(x_{crosshead})}{v_{crosshead}} \quad (D.1)$$

The ratio j describes the transfer from the crosshead to the LSP. This ratio is nonlinear and position-dependent, but is chosen such that a linear movement of the cylinder gives the optimal LSP movement. The velocity and the position of the crosshead determine the velocity of the LSP. For a different position of the crosshead, the velocity of the LSP will be different.

When j is smaller than 1, the velocity of the LSP (v_{lsp}) is lower than the velocity of the crosshead ($v_{crosshead}$). At the begin point and the end point the transformation ratio is smaller than 1, which is needed for accelerating the heavy LSP from stand still. Once the LSP is moving it can speed up, and the ratio will become larger than 1.0. When the LSP is about to hit the VSP, the LSP needs to decelerate. The velocity of the LSP then becomes almost equal to zero ($j \downarrow 0$) while the crosshead is still moving. Some values of the crosshead position and the corresponding ratio are shown in Table D-1.

$x\text{-chd (m)}$	j
1.59	0.68
1.304	1
0.89	1.51
0.6136	1
0.4529	0.5
0.005	0.001

Table D-1 Values of the mechanism transformation ratio j

Appendix E Description of bond graph elements

To better understand the bond graph described in the report, a small explanation is given for most of the bond graph elements.

In Table E-1 all bond graph elements are described. The causality stroke in the most right figure indicates the fixed or preferred causality of the element.

Element	Purpose	Equation	Bond Graph model
C	stores q variable	$e = \frac{1}{C}q$ $q = \int f dt + q(0)$	
I	stores p variable	$f = \frac{1}{I}p$ $p = \int e dt + p(0)$	
R	dissipates free energy	$e = Rf$ $f = \frac{1}{R}e$	
Se	effort source	$e = b_b$	
Sf	flow source	$f = f_b$	
(M)TF	transforms effort to effort and flow to flow, depending on n	$f_2 = nf_1, e_1 = ne_2$ $f_1 = \frac{f_2}{n}, e_2 = \frac{e_1}{n}$	
0	junction, $\Sigma f=0$	$e_1 = e_3, e_2 = e_3$ $f_3 = f_1 - f_2$	
1	junction, $\Sigma e=0$	$f_1 = f_3, f_2 = f_3$ $e_3 = e_1 - e_2$	

Table E-1 Bond graph elements

The symbol “e” stands for “effort”, which can be used for force, torque, voltage or pressure, depending on the domain where the source is used. The symbol “f” stands for “flow”, which is used for velocity, angular velocity, current or (fluid) flow depending on the domain. The symbols p and q stand for momentum and displacement.

A C-element represents a spring or compliance, an I-element represents an inertia and a R-element represents a resistive element, like a damper. In the electrical domain, these elements represent a capacitor, a coil and a resistor.

The (M)TF is the transformer element, which has a constant or modulated transformation ratio *n*. A (M)TF can be a representation of two coupled coils, a gearbox or a lever mechanism.

Appendix F State Variable Filter

The SVF is a state estimator, and can be used in the continuous and discrete domain. When the output of the system is known (position) but a system state (velocity) needs to be known, one way of deriving the state (velocity) is by differentiating the system output (position).

Because of the dynamic behavior of a differentiator, high frequency signals will be amplified. This means that for example measurement noise will be enlarged. A practical way to differentiate, without amplification of high frequency signals, is to use a state variable filter (SVF).

In this section a first and second order discrete SVF is described, and a comparison with another method is shown.

F.1 First order SVF

The first order SVF amplifies the system output by a constant gain factor K . The error signal is integrated and again amplified. The error between those two signals will become equal to the state of the system, if K is chosen large enough. The block diagram of the first order SVF is shown in Figure F-1.

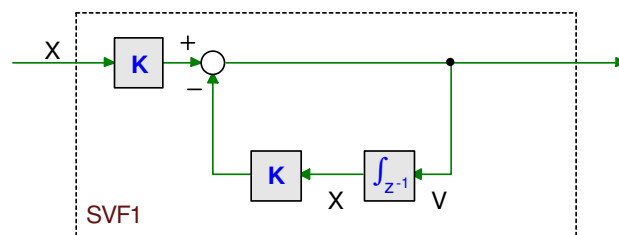


Figure F-1 Discrete first order State Variable Filter. By choosing gain factor K large enough, the integrator input will be an estimate of the state of the system.

The frequency behavior of the first order SVF is represented by a Bode plot, which is shown in Figure F-2. Three different gain values are shown, to illustrate the influence of the K -factor. To have a good differentiator, a phase shift of 90 degrees is wanted for high frequencies. This can be done by choosing K large enough. The gain factor K equals the cut-off frequency as shown in equation F.1.

$$K = \omega_{SVF} \quad (F.1)$$

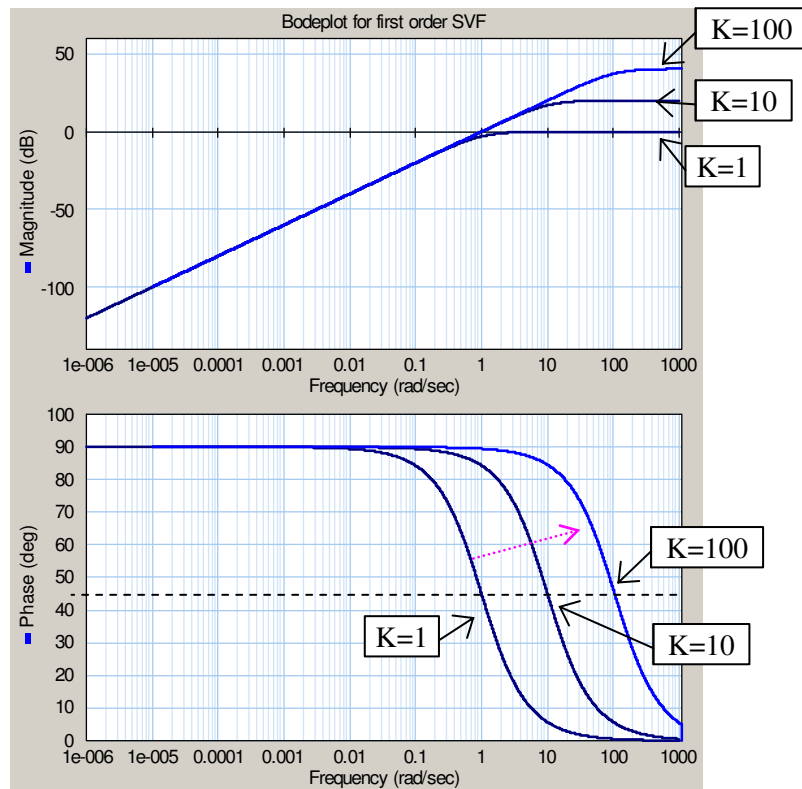


Figure F-2 Bode plot of first order SVF for different gains: $K=1, 10$ and 100 rad/s. If K is larger, the phase shift will move to higher frequencies and there will be 90 degrees phase shift for higher frequencies.

The disadvantage of a high K -factor is that for high frequencies the gain will become larger, and the high frequent parts of the input signal will be amplified. This effect can be reduced by using a second order SVF.

The continuous transfer function of a first order SVF is given by equation F.2. To transform from the continuous to the discrete domain with the Forward Euler approximation, s is replaced by F.3. The different approximations and how to convert a system from continuous to discrete are described in (van Amerongen and de Vries, 2002, pages 178-181).

$$H(s) = \frac{K \cdot s}{s + K} \tag{F.2}$$

$$s \Rightarrow \frac{z-1}{\tau_{sample}} \tag{F.3}$$

The discrete domain transfer function can be found by substituting equation F.3 in equation F.2, which results in equation F.4.

$$H(z) = \frac{K(z-1)}{z - (1 - K \cdot \tau_{sample})} \tag{F.4}$$

By increasing the gain factor K of the SVF the point where the phase shifts from +90 degrees to 0 degrees can be shifted to higher frequencies. But this can only be done if the high-frequent unwanted signals are very small compared to the amplitude of the signal.

F.2 Second order SVF

For higher order systems the result of the SVF estimator will be better if the order is also increased. When a second order SVF is used the results are much better, especially the reduction of the effect of amplification of high-frequent unwanted signals.

The block diagram of the second order SVF is shown in Figure F-3. There are three gain factors, with two of them having the same value.

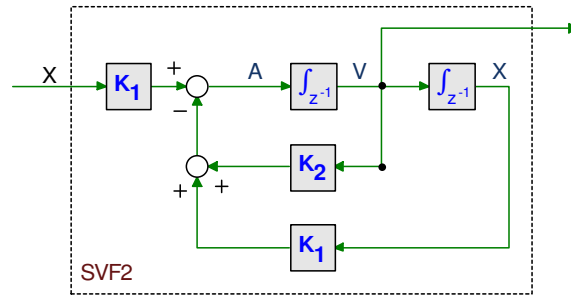


Figure F-3 Second order State Variable Filter. By choosing gain K_1 and K_2 large enough, the integrator inputs will be estimates of the states of the second order system. The velocity and acceleration can be estimated, and the position signal will have less noise than the position input signal.

The continuous transfer function $H(s)$ from input X to output V is given by equation F.5.

$$H(s) = \frac{K_1 \cdot s}{s^2 + K_2 \cdot s + K_1} \quad (\text{F.5})$$

The discrete transfer can be found by substituting F.3 in equation F.5, which gives equation F.6.

$$H(z) = \frac{(z-1) K_1 \cdot \tau_{\text{sample}}}{z^2 + z(K_2 \cdot \tau_{\text{sample}} - 2) - K_2 \cdot \tau_{\text{sample}} + K_1 \cdot \tau_{\text{sample}}^2} \quad (\text{F.6})$$

To find the right parameters, the bandwidth of the SVF is chosen ten times the bandwidth of the system. From this bandwidth, ω_{SVF} , and the required damping factor ξ the gain factors K_1 and K_2 can be found as shown in equations F.7.

$$\begin{aligned} K_1 &= \omega_{\text{SVF}}^2 \\ K_2 &= 2 \cdot \xi \cdot \omega_{\text{SVF}} \end{aligned} \quad (\text{F.7})$$

For a normalized low pass filter the poles and zeros can be found by the Butterworth polynomials. For a second order filter the poles are located at the unit circle, at $-0.7071 \pm 0.7071j$ for ω_n equal to one. The bandwidth of the clamp mechanism is about 5 Hz, so the bandwidth of the SVF is chosen ten times the system bandwidth, $\omega_{\text{SVF}} = 2\pi \cdot 50 \text{ Hz} = 314,16 \text{ rad/s}$.

The Bode plot of the second order SVF is show in Figure F-4, for a bandwidth ω_{SVF} of 1256.6 rad/s (200 Hz) and damping factors ξ of 0.4, 0.6, 0.8 and 1.0.

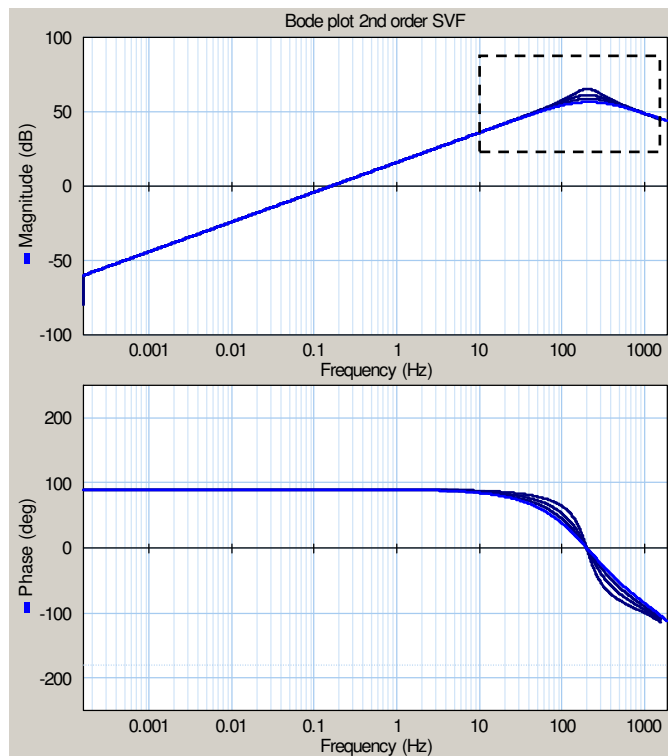


Figure F-4 Bode plot of the second order SVF. The different values for the damping factor used are 0.4, 0.6, 0.8 and 1.0.

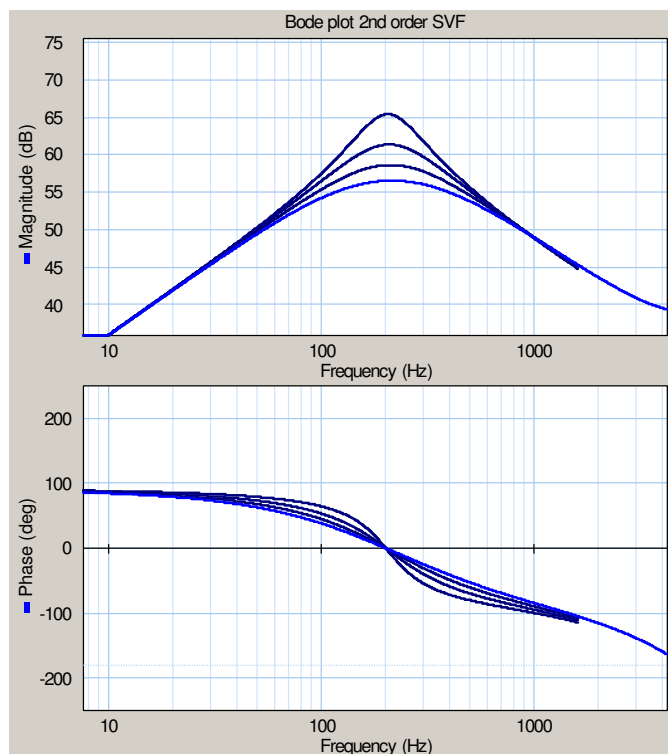


Figure F-5 The same Bode plot as Figure F-4, zoomed in on the cut-off frequency. When the damping is larger, the peak (magnitude) and the steepness (phase) will become lower.

The steepness of the phase shift from +90 to -90 degrees is determined by the damping factor ξ and thus by K_2 . The phase will be steeper (around 200 Hz) if K_2 is chosen smaller. The frequency where the phase tilts from +90 to -90 degrees is determined by the constant gain K_1 , the frequency squared. If K_1 is larger, the tilting-point shifts to the right. If K_1 is chosen smaller, it will shift to the left and will also become less steep. This can also be seen from equation F.7.

F.3 Software differentiation

A method to differentiate used in software, without amplifying the high frequent signals, is described in this section. It is compared with the first and second order SVF in section F.4.

To filter out the measurement noise, the position measurement data is filtered with a first order Bessel low pass filter. After that a moving average filter is combined with the differentiating function. Then the velocity obtained is filtered again with a low pass filter. The block diagram is shown in Figure F-6.

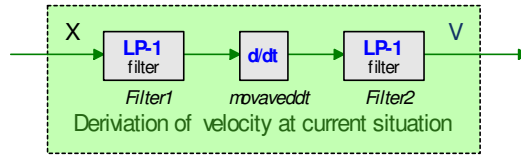


Figure F-6 Block diagram of differentiation in software with noise suppression by low pass filtering.

The simplest way of differentiation is shown in equation F.8. If this way is combined with a moving average filter, the differentiation shown in equation F.9 is obtained.

$$v = \frac{x_k - x_{k-1}}{\tau_{sample}} \quad (\text{F.8})$$

$$v = \frac{(x_k - x_{k-3}) + (x_{k-1} - x_{k-4}) + (x_{k-2} - x_{k-5})}{(3 \cdot \tau_{sample})} \quad (\text{F.9})$$

Six samples are stored and the derivative is determined three times, between an input sample and an input of three samples before that sample. The effective sample time is thus three times the actual system sampling time. That is why the numerator shows three times the sampling time.

F.4 Comparison between methods

To compare the differentiation methods the three bode plots are given. The system bandwidth is expected to be 5.0 Hz. The first order SVF cutoff frequency is 25 Hz (157.08 rad/s) and the second order SVF cutoff frequency is 50 Hz (314.16 rad/s). The gain parameters are as follows:

$$\begin{aligned} K_{svf1} &= (25 \cdot 2\pi) &= 157.08 \\ K1_{svf2} &= (2\pi \cdot 50)^2 &= 98696 \\ K2_{svf2} &= (2\pi \cdot 50) \cdot 2 \cdot 0.7 &= 439.82 \end{aligned}$$

The damping ξ used is equal to 0.7. To get a correct derivative, the phase shift needs to be +90 deg. A plot with the three Bode plots for comparison is shown in Figure F-7 on page 67. The sampling frequency used is 500 Hz.

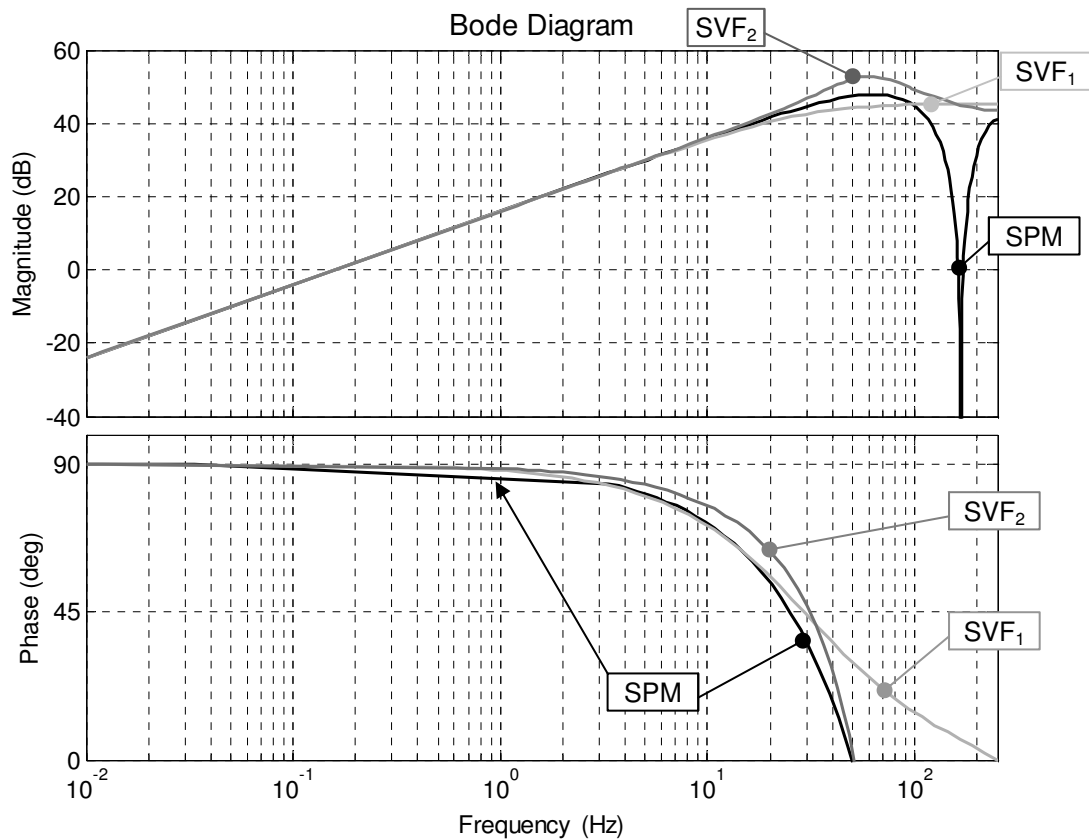


Figure F-7 Bode plot for comparing of the software differentiation method, the first order SVF and the second order SVF.

The disadvantage of the Stork (SPM) method is that the phase shift starts decreasing below 90 degrees at a lower frequency. This means that the derivative will be worse for frequencies between 0.1 and 3 Hz. Another disadvantage of the SPM method, which also holds for the first order SVF, is that the gain (magnitude in Figure F-7) stays large for higher frequencies, so that noise will be amplified more than for the second order SVF. The gain of the second order SVF starts decreasing above the cutoff frequency, which is an advantage.

References

- van Amerongen, J. and P.C. Breedveld (2002), Modelling of Physical Systems for the Design and Control of Mechatronics Systems, *IFAC Professional Briefs, published in relation to the 15th triennial IFAC World Congress* (<http://ifac-control.org>), pp. 1-56.
- van Amerongen, J. and T.J.A. de Vries (2002), *Digitale Regeltechniek*, Enschede.
- Bos, A.M. (1986), *Modelling Multibody Systems in Terms of Multibond Graphs with Application to a Motorcycle*, PhD-Thesis, Control Engineering, University of Twente, Enschede, pp. 226, ISBN: 90-90001442-X.
- Breedveld, P.C. and J.v. Amerongen (1996), *Dynamische Systemen: modelvorming en simulatie met bondgrafen*, Enschede, ISBN: 90-358-1302-2.
- Broenink, J.F. and G.H. Hilderink (2001), A structured approach to embedded control systems implementation, in: *2001 IEEE International Conference on Control Applications*, M. W. Spong, D. Repperger and J. M. I. Zannatha (Eds.), IEEE, México City, México, pp. 761-766, ISBN: 0-7803-6735-9.
- van der Zwaag, J.A. (1998), *Towards Dynamic Tolerance Analysis Using Bond Graphs*, MSc Thesis, no PT-620, Design, Production and Management (Eng Tech), University of Twente, Enschede.
- Velthuis, W.J.R. (2000), *Learning feed-forward control - theory, design and applications -*, PhD thesis, Faculty of Electrical Engineering, University of Twente, Enschede, Netherlands, ISBN: 90-36514126.
- Verwoerd, M.H.A. (2005), *Iterative Learning Control: A Critical Review*, PhD-thesis, Faculty of Electrical Engineering, University of Twente, Enschede, pp. 159, ISBN: 90-365-2133-5.